Concurrent TMS-fMRI for causal network perturbation and proof of target engagement

Bergmann, Til Ole; Varatheeswaran, Rathiga; Hanlon, Colleen A; Madsen, Kristoffer H; Thielscher, Axel; Siebner, Hartwig Roman

Published in:
NeuroImage

Link to article, DOI:
10.1016/j.neuroimage.2021.118093

Publication date:
2021

Document Version
Publisher's PDF, also known as Version of record

NeuroImage 237 (2021) 118093

Contents lists available at ScienceDirect

NeuroImage

journal homepage: www.elsevier.com/locate/neuroimage

Concurrent TMS-fMRI for causal network perturbation and proof of target engagement

Til Ole Bergmann[a,b,*], Rathiga Varatheeswaran[a,b], Colleen A. Hanlon[c], Kristoffer H. Madsen[d,e], Axel Thielscher[d,f], Hartwig Roman Siebner[d,g,h]

[a] Neuroimaging Center (NIC), Focus Program Translational Neuroscience (FTN), Johannes Gutenberg University Medical Center, Langenbeckstr. 1, 55131, Mainz, Germany
[b] Leibniz Institute for Resilience Research, Wallstraße 7-9, 55122, Mainz, Germany
[c] Department of Cancer Biology, Wake Forest School of Medicine, 1 Medical Center Blvd., Winston-Salem, NC 27157, USA
[d] Danish Research Centre for Magnetic Resonance, Centre for Functional and Diagnostic Imaging and Research, Copenhagen University Hospital Hvidovre, Kettegård Allé 30, 2650, Hvidovre, Denmark
[e] Department of Applied Mathematics and Computer Science, Technical University of Denmark, Kgs. Lyngby, Denmark
[f] Department of Electrical Engineering, Technical University of Denmark, Kgs. Lyngby, Denmark
[g] Department of Neurology, Copenhagen University Hospital Bispebjerg, Bispebjerg Bakke 23, 2400 København NV, Denmark
[h] Department of Clinical Medicine, University of Copenhagen, Blegdamsvej 3B, 2200 Copenhagen N, Denmark

ARTICLE INFO

Keywords:
Transcranial magnetic stimulation (TMS)
Functional magnetic resonance imaging (fMRI)
Concurrent
Interleaved
Simultaneous
Review

ABSTRACT

The experimental manipulation of neural activity by neurostimulation techniques overcomes the inherent limitations of correlative recordings, enabling the researcher to investigate causal brain-behavior relationships. But only when stimulation and recordings are combined, the direct impact of the stimulation on neural activity can be evaluated. In humans, this can be achieved non-invasively through the concurrent combination of transcranial magnetic stimulation (TMS) with functional magnetic resonance imaging (fMRI). Concurrent TMS-fMRI allows the assessment of the neurovascular responses evoked by TMS with excellent spatial resolution and full-brain coverage. This enables the functional mapping of both local and remote network effects of TMS in cortical as well as deep subcortical structures, offering unique opportunities for basic research and clinical applications. The purpose of this review is to introduce the reader to this powerful tool. We will introduce the technical challenges and state-of-the art solutions and provide a comprehensive overview of the existing literature and the available experimental approaches. We will highlight the unique insights that can be gained from concurrent TMS-fMRI, including the state-dependent assessment of neural responsiveness and inter-regional effective connectivity, the demonstration of functional target engagement, and the systematic evaluation of stimulation parameters. We will also discuss how concurrent TMS-fMRI during a behavioral task can help to link behavioral TMS effects to changes in neural network activity and to identify peripheral co-stimulation confounds. Finally, we will review the use of concurrent TMS-fMRI for developing TMS treatments of psychiatric and neurological disorders and suggest future improvements for further advancing the application of concurrent TMS-fMRI.

1. Introduction

The experimental manipulation of brain function via neurostimulation tools has become a main pillar of the empirical neurosciences, as it allows researchers to overcome the limitations of merely correlative recordings of neural activity and to investigate causal brain-behavior relationships. While being a driving force in animal research, the experimental use of invasive electric, optogenetic, or chemogenetic stimulation, is not (yet) practicable in healthy humans. Yet, transcranial brain stimulation techniques have been established to stimulate the human brain in a non-invasive manner via the induction of electric fields in the brain tissue through the intact skull. Transcranial magnetic stimulation (TMS) and transcranial electric stimulation (TES) enable neuroscientists and clinicians to causally manipulate regional neuronal activity and thereby to investigate and modulate brain function in healthy volunteers as well as patient populations. Note that TMS does not excite neurons via its time-varying magnetic field but via the accompanying induced time-varying electrical field (i.e., via “inductive” electrical neural stimulation). To investigate the immediate response of the brain to the stimulation (‘online effects’) as well as the longer lasting changes in neural

* Corresponding author.
E-mail address: tobergmann@uni-mainz.de (T.O. Bergmann).

https://doi.org/10.1016/j.neuroimage.2021.118093.
Received 11 January 2021; Received in revised form 6 April 2021; Accepted 14 April 2021
Available online 30 April 2021.

activity based on synaptic plasticity ('offline effects'), transcranial brain stimulation can be combined, concurrently or sequentially, with non-invasive recording techniques, such as functional magnetic resonance imaging (fMRI) and electroencephalography (EEG). A particularly challenging combination, which, however, provides unique insights into the brain-wide response to local network perturbation and facilitates proof of target engagement, is the concurrent application of TMS and fMRI. Because TMS pulses are technically interleaved with MR slice acquisition, the technique is also referred to as "interleaved TMS-fMRI". However, since the blood oxygen level dependent (BOLD) signal is slow and delayed relative to the neural activity it reflects, and the acquisition gaps for TMS application are very brief, BOLD response sampling is not considerably interrupted by TMS. Given the conceptually concurrent (as opposed to consecutive) application of the techniques, we have adopted the more commonly used term "concurrent TMS-fMRI" throughout this paper. The technique has been pioneered 20 years ago, its use has long been limited to a small number of research groups, partially due to the particular challenges of implementation and data acquisition. Only recently, it began to experience a renaissance, thanks to new technical developments. In this paper, we review the current state of the art of concurrent TMS-fMRI, including the technical challenges and solutions as well as the unique discoveries it can provide for basic, translational, and clinical research in humans.

1.1. A primer on transcranial magnetic stimulation (TMS)

TMS uses the principle of electromagnetic induction to induce an electrical current in the targeted cortical area. The time-varying magnetic field, generated by a transient current flow in the TMS coil positioned over the scalp, penetrates the intact human skull and in turn induces a respective electric field (E-field) in the underlying brain tissue, which eventually depolarizes the membrane of neural elements to a degree that results in the firing of action potentials. While the strength and extent of the induced E-field depends on several physical factors such as coil design and stimulation intensity, it usually reaches suprathreshold currents in a relatively focal cortical volume (few cubic millimeters to centimeters), evoking a local response of synchronized neuronal firing. However, this local activation then causes a transsynaptic spread of action potentials to connected brain regions, thereby engaging entire networks instead of isolated brain regions. The most obvious demonstration of polysynaptic engagement by single-pulse TMS is the motor evoked potential (MEP). When TMS is delivered, for example, to the hand area of primary motor cortex (M1), a muscle contraction in the contralateral hand muscles can be observed (note that MEPs can be recorded also from other muscles depending upon which part of the M1 is targeted by TMS), not only demonstrating that the TMS pulse depolarized the corticospinal pyramidal cells of M1, which descend down the spinal cord, but that action potentials were also transmitted along the peripheral nerve descending to the hand muscles, ultimately resulting in depolarization at the neuromuscular junction and an electric muscle potential, the MEP, recordable with surface electromyography (EMG). This TMS-evoked MEP was first displayed by Anthony Barker (Barker et al., 1985) and remains one of the most common dependent measures in TMS research today, as it allows the indexing of motor cortical and corticospinal excitability as well as effective connectivity within the corticospinal tract.

The ability to non-invasively cause immediate neuronal firing in both local cortical targets and connected remote regions, and thereby to probe the excitability of those regions and the effective connectivity within entire brain networks, puts TMS in a unique position compared to other existing brain stimulation techniques, which do not provide such a 'perturb-and-measure' approach. Deep brain stimulation (DBS), for example, is also capable of fully depolarizing the neurons' membrane potential and triggering action potentials, but is invasive, hardly reversible, and associated with risks and side-effects that limit its neuroscientific use to patient populations (Horn and Fox, 2020). High-intensity TES (Merton and Morton, 1980), while non-invasive and allowing suprathreshold stimulation, is not only spatially less precise but also painful, and therefore hardly used in healthy subjects either. Low-intensity TES, a widely used non-invasive technique, comprising transcranial direct (TDCS) (Nitsche and Paulus, 2000) and alternating current stimulation (TACS) (Antal et al., 2008), is of lower spatial and temporal precision compared to TMS, and only causes subthreshold modulation of membrane polarization without immediately evoking action potentials. Similarly, transcranial static magnetic field stimulation (Oliviero et al., 2011) can produce transient excitability changes, but given the lack of temporal dynamics in the magnetic field, unlike TMS, it does not immediately trigger action potentials. Finally, transcranial ultrasound stimulation (TUS), yet another emerging technique for non-invasive neuromodulation, has superior spatial precision and can selectively target deep brain regions, but also produces only temporally delayed subthreshold neuromodulation in humans (Fomenko et al., 2018; Pasquinelli et al., 2019).

TMS is therefore currently the only non-invasive technique that produces an immediate ('online') suprathreshold neuronal response in the human brain, associated with a transsynaptic spread of activation, and directly observable behavioral effects (i.e., the MEP following TMS of M1). Moreover, while both repetitive TMS (rTMS) protocols and low-intensity TES can produce transient, synaptic plasticity-dependent changes in neuronal excitability and functional connectivity that outlast the stimulation protocol ('offline' or 'after-effects') (Huang et al., 2017), and also TUS has demonstrated respective effects in non-human primates (Verhagen et al., 2019), rTMS is the non-invasive brain stimulation technique with the strongest evidence for effectivity in treating psychiatric and neurological disorders (Lefaucheur et al., 2019; Lefaucheur et al., 2014). TMS is thus currently the method of choice for many applications in basic systems and cognitive neuroscience research as well as diagnostic or therapeutic clinical applications.

1.2. Combining TMS with neuroimaging

TMS has been combined with a variety of neuroimaging methods, sensitive to different aspects of neuronal activity, and with different spatial and temporal resolution. A detailed review of TMS with other neuroimaging techniques is beyond the scope of this paper (for respective reviews see Bergmann et al., 2016; Bestmann and Feredoes, 2013; Reithler et al., 2011; Siebner et al., 2009), but it should be noted that concurrent TMS-EEG in particular complements many of the strengths and weaknesses of concurrent TMS-fMRI while also sharing many of the principal technical challenges. Functional MRI exploits neurovascular coupling and can non-invasively map TMS-evoked neuronal activity with high spatial resolution and whole-brain coverage. In contrast, electro- and magnetoencephalography (EEG and MEG) directly measure the electric and magnetic fields associated with post-synaptic neuronal activity – though only EEG can be combined concurrently with TMS to assess its immediate online effects. EEG has excellent temporal resolution and is a superior fit for the temporal precision of TMS, but it has lower spatial resolution and limited sensitivity for deep brain regions. Concurrent TMS-fMRI and TMS-EEG are thus complementary methods with opposite strength regarding spatial and temporal resolution, each one being optimally suited to answer a particular type of question. TMS-EEG has become an established method to assess the brain's response to TMS and is often used to assess cortical excitability, connectivity, and brain state-dependent changes in response complexity (Bortoletto et al., 2015; Ferreri and Rossini, 2013; Sarasso et al., 2014), and TMS-fMRI is principally able to assess similar features – but on different temporal and spatial scales. Both concurrent TMS-EEG and TMS-fMRI also share some common challenges, namely the control for peripheral sensory co-stimulation induced neuronal responses (section 4.2), while each one of them also has its own technical caveats. A concurrent combination of all three techniques (TMS-EEG-fMRI) is technically feasible in principle

but has so far only been achieved in an alternating fashion, i.e., using pre-TMS EEG but post-TMS fMRI data (Peters et al., 2020; Peters et al., 2013). The addition of EEG recordings does not cause particular problems with respect to TMS-related artifacts in the BOLD fMRI signal, but the EEG cap simply adds to the scalp-cortex distance, further reducing the efficacy of MR-compatible TMS coils (section 2.1.1). In contrast, conducting concurrent TMS-EEG in the presence of the strong B_0 field of the MR augments many of the TMS-related artifacts in the EEG signal, which originate from the interaction of current induction in the electrode leads, coil vibration, cranial muscle responses, electrode movements, and associated motion artifacts (Ilmoniemi and Kicic, 2010; Rogasch et al., 2017; Vernet and Thut, 2014). In particular the inevitable TMS-related EEG electrode movements produce nonlinear EEG-artifacts in the post-TMS period that are of considerable amplitude and large inter-trial variability and thus very difficult to remove. The EEG signal preceding TMS onset, however, does not differ considerably from that of simultaneous EEG-fMRI recordings in the absence of TMS and can be recovered by removal of MR-gradient and cardio-ballistic artifacts (Ritter and Villringer, 2006).

Importantly, there are a few general caveats to consider when interpreting BOLD fMRI and EEG signal changes (not only in response to TMS). Both signals are related to local field potentials and reflect the net result of synaptic activity (i.e., peri- and postsynaptic processes) rather than firing rate (i.e., action potentials) in the neuron populations where the signals originate, and neither technique can distinguish between the specific contribution of excitatory vs. inhibitory circuits to the measured signal (Buzsaki et al., 2012; Cohen, 2017; Logothetis, 2008; Logothetis et al., 2001). In fact, spontaneous BOLD signal increases may also be observed for balanced proportional changes of both excitatory and inhibitory contributions, e.g. as a result of neuromodulatory input (Logothetis, 2008). Thus, both EEG and BOLD fMRI rather represent compound measures of the net responsiveness of the targeted neuron population to TMS, and some caution is warranted when interpreting local BOLD response amplitude as an immediate index of neuronal excitability (see section 3.1 for a more detailed discussion).

While concurrent TMS-fMRI is technically challenging, it allows the experimenter to address some of the most pressing questions in the field of human neurostimulation. By assessing the immediate neurovascular response to TMS with whole brain coverage (including deep subcortical structures), it enables the detailed mapping of both local and remote effects of the stimulation and the evaluation of both regional excitability and effective connectivity between brain regions. Concurrent TMS-fMRI can thus be used to perturb and measure entire brain networks and to provide direct proof of engagement for both superficial and deep brain targets. By systematically varying the stimulus parameters (i.e., extrinsic variables) or the brain state during stimulation (i.e., intrinsic variables), the experimenter can delineate dose-response relationships and characterize response profiles for the targeted brain networks. Such brain-wide mapping of TMS-evoked BOLD signal changes also helps to identify the anatomical origin of TMS-related changes in behavioral task performance (indexing cognitive function) and to exclude or expose confounding influences resulting from non-target activations and peripheral co-stimulation (Bergmann and Hartwigsen, 2021).

1.3. A brief history and synopsis of existing concurrent TMS-fMRI studies

While the TMS-evoked MEP was first demonstrated in 1984, the direct effects of TMS on brain activity were not visualized for another 15 years. In 1998/99, Daryl Bohning and colleagues performed first intrepid experiments wherein they applied single pulses of TMS over M1 inside the bore of an MRI scanner while acquiring T2*-weighted images of the BOLD signal before and after the TMS pulses (Bohning et al., 1999; Bohning et al., 1998). They demonstrated a TMS-evoked BOLD signal increase following the TMS pulse in areas in the vicinity of the TMS coil, but not directly beneath the coil. The ten years that followed these initial investigations brought further insights and methodological refinement from several other groups (e.g., Baudewig et al., 2001; Bestmann et al., 2003a; Bestmann et al., 2003b; Li et al., 2004b; Nahas et al., 2001). Specifically, in 2004 both Bestmann et al. (2004) and Li et al. (2004b) demonstrated that TMS of the left M1 not only induced BOLD-responses changes in cortical areas close to the TMS coil (for suprathreshold intensities), but also in connected remote sites, including subcortical ones such as the basal ganglia (even for subthreshold intensities). These findings were later supported by Denslow et al. (2005) and extended by Hanakawa et al. (2009). The first (and still most) concurrent-TMS-fMRI studies have targeted the hand representation of the human M1. As the technique quickly matured, groups soon started applying TMS also to frontal and parietal cortices (e.g., de Vries et al., 2009; Nahas et al., 2001; Ruff et al., 2008; Ruff et al., 2006; Sack et al., 2007). Also, one of the first references to the state-dependent effects of TMS was demonstrated in an early study by Bestmann et al. (2008c). In that study, they demonstrated that TMS to the dorsal premotor cortex induced a larger BOLD response when the participant was squeezing their hand compared to rest. In the following ten years, the number of concurrent TMS-fMRI studies kept growing steadily but slowly, targeting an increasing variety of research questions in basic neuroscience (e.g., de Graaf et al., 2018; Hawco et al., 2018; Heinen et al., 2014; Heinen et al., 2011; Hermiller et al., 2020; Leitao et al., 2015; Leitao et al., 2012; Moisa et al., 2012; Vink et al., 2018) as well as clinical research (e.g., Eshel et al., 2020; Fonzo et al., 2017; Guller et al., 2012; Hanlon et al., 2017; Hanlon et al., 2016; Kearney-Ramos et al., 2018; Webler et al., 2020). By now, this powerful technique has come of age, and accompanied by recent technical developments, such as novel TMS-compatible MR-receiving coil arrays (Navarro de Lara et al., 2017; Navarro de Lara et al., 2015), more concurrent TMS-fMRI studies should be expected in the near future.

To synthesize the existing literature, we conducted a systematic literature search on PubMed (last updated on September 11th 2020) with the search term *concurrent OR interleaved OR simultaneous AND "transcranial magnetic stimulation" AND fmri.* The resulting publications (initially 215 items) were examined to include only those studies in which TMS was conducted concurrently with fMRI, i.e., *online* (and not merely subsequently, i.e. *offline*) and in which human participants were investigated (and not merely MR-phantoms). In addition, these papers were searched for references to further concurrent-TMS-fMRI studies that were not found during the initial PubMed search, and one additional study was added during the revision of this paper. This procedure eventually revealed a total number of 69 concurrent TMS-fMRI studies in human subjects, published in 71 peer-reviewed journal articles. Table 1 provides a complete list of these publications together with extracted information about general study design and objectives as well as TMS and fMRI parameters and equipment, whereas Table 2 provides descriptive summary statistics for some of the key parameters. We hope that this synopsis will provide a useful resource for researchers planning concurrent TMS-fMRI studies. Of the 68 studies, 57 were conducted in healthy participants and 12 in clinical populations (3x major depressive disorder, MDD, 1x posttraumatic stress disorder, PTSD, 3x cocaine addiction, 2x schizophrenia, 1x dystonia, 1x stroke, 1x limb amputation). The majority of superficial cortical targets were the primary motor cortex (29x), followed by subregions of the parietal cortex (18), the dorsolateral prefrontal cortex (dlPFC) (15x) and the dorsal premotor cortex (dPMC) (5), (anterior) medial prefrontal cortex (mPFC) (4x), frontal eye fields (FEF) (3x), primary visual cortex (V1) (3x), as well as occasional examples of sensorimotor cortex (SMC), pre-supplementary motor area (preSMA), Wernicke's area, and vertex (note that sometimes multiple targets were included within the same study). While several studies report remote activations in deep targets, only 8 published studies explicitly aimed to indirectly stimulate a priori defined deep targets, including anterior cingulate cortex (ACC), subgenual ACC (sgACC), ventromedial prefrontal cortex (vmPFC), amygdala, caudate nucleus, thalamus, and hippocampus, via connected superficial cortical targets (Dowdle et al., 2018; Fonzo et al., 2017; Hanlon et al., 2013; Hanlon et al., 2015;

Table 1
Comprehensive list of concurrent TMS-fMRI studies, published until September 11th, 2020.

	Study design & objectives				TMS parameters & equipment								fMRI parameters & equipment			
Study	Objective	N	TMS protocol /fMRI design	Local Acti-vation[*3]	Intensity (% RMT[*1])	Frequency of train/burst or SOA of SP/ burst (ER design)	# pulses (duration in s) per burst/train	# trials/blocks (pulses) per condition	Comparisons, Controls, and Sham conditions	Surface Target [MNI or 10/20 coordinates] (Deep Target)	Method for determining target site	Method for verifying coil position relative to MRI	TMS device and coil[*2]	TR/TE in ms	Flip angle	#Slices (slice thickness / gap in mm)	RF-coil type
Studies in healthy subjects																	
Bohning et al., 1998	Demonstrating feasibility of TMS-fMRI	3	train/block	Y	110 %	0.83 Hz	20(24 s)	6(120)	rest	L M1	visual MHS	fiducials	DT	infinite/27	90°	11 (4.5/1.51)	?
Bohning et al., 1999	Assessing dose-response relationship for M1	7	train/block	Y	110 %, 80 %	1 Hz	36(36 s)	8 (288)	rest	L M1	visual MHS	fiducials	DT	infinite/40	90°	12 (5/1.5)	?
Bohning et al., 2000b	Demonstrating feasibility of TMS-fMRI with single trial-TMS	5	SP/ER	Y	120 %	12 s		15(1)		L M1	MHS	fiducials	DT	600/40	40°	5 (5/1.5)	?
Bohning et al., 2000a	Comparison of BOLD response for TMS-evoked and voluntary movements	5	train/block	Y	110 %	1 Hz		8(21)	voluntary thumb movement triggered by TMS at 50 % RMT	L M1	MHS	fiducials	DT	3000/40	90°	12 (5/1.5)	?
Nahas et al., 2001	Proof of target engagement of the PFC	7	train/block	Y	80 %, 100 %, 120 %	1 Hz	21(21s)	7(147)	rest	L PFC	5 cm rule[*4]	fiducials	DT	3000/40		12 (5/1.5)	?
Baudewig et al., 2001	Mapping the effects of rTMS on M1	6	burst/ER	Y	110 %, 90 %	10 Hz, 16 s	10(1 s)	23(230)	sequential finger opposition triggered by TMS at 25 % RMT	L M1 and L lPMC	MHS		MS	2000/53	70°	16 (6/?)	"standard head coil"[*6]
Bestmann et al., 2003a	Minimizing EPI artifacts induced by TMS	1	SP/ER	Y	100 %, 45 % AMT	20 s		8(10)	finger-tapping task	L M1	MHS	MEP	MSR	2000/54	70°	? (?/?)	"standard head coil" (1 chan)[*6]
Bestmann et al., 2003b	Mapping (remote) effects of sub- and suprathreshold rTMS	9	train/block	Y	110 %, 110 % AMT, 90 %	4 Hz	40 (10 s)	8 (320)	finger-tapping task, rest	L M1	visual MHS	fiducials	MSR	2000/53	70°	? (4/?)	birdcage (1 chan)
Bohning et al., 2003b	Measure BOLD response in M1 and auditory cortex as a function of train length	6	train/block	Y	120 %	1 Hz	1, 2, 4, 8, 16 (1, 2, 4, 8, 16 s) and 1, 2, 4, 8, 16, 24 (1, 2, 4, 8, 16, 24 s)	5(155) 4(220)		L M1	visual MHS	fiducials	DT	1000/40 3000/40	72° 88°	? (5/15)	?
McConnell et al., 2003	Study age-related effects of TMS in cortex vs. periphery	11	train/block	NR	110 %	1 Hz	21(21 s)	8(168)	voluntary thumb movement triggered by TMS at 20 % MSO, rest	L M1	MHS	fiducials	DT	3000/40	90°	12 (5/1.5)	?
Bestmann et al., 2004	Mapping (remote) effects of sub- and suprathreshold rTMS	12	train/block	Y	110 %, 90 %	3.125 Hz	30 (9.96 s)	8(240)	rest, voluntary finger movement	L M1	MHS	MEP	MSR	3320/36	70°	20 (4,?)	birdcage (1 chan)
Denslow et al., 2004	Comparison of variation in location and intensity of BOLD response for TMS-evoked vs. voluntary movements	9	train/block	Y	110 %	1 Hz	21(21 s)	7(147)	rest, thumb movement triggered by TMS at 20 % RMT	L M1	visual MHS	calibrated coil holder	DT	3000/40	88°	15 (6/1)	birdcage (1 chan)
Li et al., 2004b	Measuring the impact of lamotrigine on TMS-evoked BOLD response	10	train/block	Y NR	120 %, 100 %				rest	L M1 dlPFC	MHS 5 cm rule[*4]	calibrated coil holder	DT	3000/40	90°	15 (7/1)	?
Denslow et al., 2005a	Comparing image-guided vs. function-guided coil placement	11	train/block	Y	110 % (image-guided vs. function-guided coil placement)	1 Hz	21 (21 s)	7(147)	rest, voluntary thumb movement triggered by TMS at 20 % RMT	L M1	visual MHS	MEP vs. calibrated coil holder	DT	3000/40	88°	15 (6/1)	?
Denslow et al., 2005b	Mapping effects of 1 Hz rTMS on motor circuitry	11	train/block	Y	110 %	1 Hz	21 (21 s)	7(147)	rest, voluntary thumb movement triggered by TMS at 20 % RMT	L M1	visual MHS	calibrated coil holder	DT	3000/40	88°	15 (6/1)	?

(*continued on next page*)

Table 1 (*continued*)

Study	Study design & objectives Objective	N	TMS protocol /fMRI design	Local Activation[*3]	TMS parameters & equipment Intensity (% RMT[*1])	Frequency of train/burst or SOA of SP/burst (ER design)	# pulses (duration in s) per burst/train	# trials/blocks (pulses) per condition	Comparisons, Controls, and Sham conditions	Surface Target [MNI or 10/20 coordinates] (Deep Target)	Method for determining target site	Method for verifying coil position relative to MRI	TMS device and coil[*2]	fMRI parameters & equipment TR/TE in ms	Flip angle	#Slices (slice thickness / gap in mm)	RF-coil type
Ruff et al., 2006	Probing state-dependent top-down impact of FEF on retinotopic activity in visual cortex	4	burst/block	NR	85 %, 70 %, 55 %, 40 % total output	9 Hz	5 (555 ms) (3 bursts per block)	48(720)	vertex, control blocks w/o TMS w/o presence of visual stimuli	R FEF [MNI 33, 1, 62]	individual brain anatomy	neuronavigation + fiducials	MSR	3000/50		27 (2.5/1.25)	visual surface coil (1 chan)[*6]
Sack et al., 2007	Mapping (remote) effects of TMS-related disruption of parietal activity during visuospatial judgment	8	burst/block	Y	100 % MSO	13.3 Hz	5(375 ms) (10 bursts per block)	80(400) * 2 runs	task without TMS, only TMS	R PC	1 cm posterior to P4 and P4	fiducials	MSR	2000/36	70°	16 (4/?)	Tx/Rx
Blankenburg et al., 2008	Mapping state-dependent interhemispheric modulation of sensory processing by right parietal cortex TMS	5	burst/block	NR	110 %, 50 %	10 Hz	5(500 ms) (3 bursts per block)	11(165) * 4 conditions	behavioral experiment	R PC	2-4 cm posterior to MHS, avoiding muscle contractions		MSR	2880/50		39 (2/1)	standard circular polarized receive- head and body-transmit coil
Ruff et al., 2008	Probing state-dependent top-down modulation of visual processing by right IPS	4	burst/block	NR	85 %, 70 %, 55 %, 40 % total output	9 Hz	5 (500 ms) (3 bursts per block)	48(720)	control blocks w/o TMS and w/o presence of visual stimuli	R IPS [MNI 36, -52, 48]	individual brain anatomy	neuronavigation + fiducials	MSR	3000/50		27 (2.5/1.25)	visual surface coil (1 chan)[*6]
Bestmann et al., 2008c	Mapping state-dependent top-down modulation of motor areas by dPMC during motor task	12	burst/ER	Y	110 %, 70 % AMT	11 Hz, 16.11 s	5(454 ms)	80(400)	trials w/o TMS	L dPMC	2 cm anterior and 1 cm medial to MHS on scalp		MSR	1800/50	90°	20 (2.5/1.25)	receive circular polarized head array (1 chan)
Ruff et al., 2009a	Mapping hemispheric differences in state-dependent modulation of visual processing by FEF and IPS	4	burst/block	NR	85 %, 70 %, 55 %, 40 % total output	9 Hz	5 (555 ms) (3 bursts per block)	48(720) per TMS site	vertex TMS	L IPS [-36, -48, 45] and L FEF [-27, -1, 57]	MNI coordinates from literature[*5]	neuronavigation + fiducials	MSR	3000/50		27 (2.5/1.25)	visual surface coil (1 chan)[*6]
Hanakawa et al., 2009	Assessing dose-response relationship for M1 with single-pulse TMS and MEP measurements	16	SP/ER	Y	N = 12: 30 % - 95 % in 5 % steps; N = 7: 30 % - < 80 % in 10 % steps 80 % - 110 % in 5 % steps	5.4 or 8.1 s		16-21 runs(320-420)		L M1	MHS	MEP	MSR	2700/30	90°	30 (?/?)	circular polarization head coil
(Moisa et al., 2009)	Development of new coil placement method	5	train/block	Y	110 %	5 Hz	10(2 s)	50(500)	voluntary movement triggered by TMS at 50 % RMT	L M1	MHS	neuronavigation + calibrated coil holder	MVX	2410/30	?	24 (?/0.5)	Tx/Rx (1 chan)
de Vries et al., 2009	Mapping state-dependent effect of left parietal cortex on motor control circuits during movement preparation and motor imagery	10	train/block	NR	115 %	1 Hz	10(10 s)	15(150)	rest	L sPC [MNI -24, -60, 68]	MNI coordinates from literature[*5]	neuronavigation + calibrated coil holder	MSR	2300/?		23 (3.5/?	surface coil (1 chan)[*6]
Li et al., 2010; Li et al., 2011	Measuring the impact of lamotrigine and valproic acid on TMS-evoked BOLD response	30	train/block	Y	100 %, 120 %	1 Hz	5(5 s)	17(85) * 2 conditions	voluntary thumb movement triggered by light	L M1 and L PFC	5 cm rule[*4]	calibrated coil holder	MSSR	2300/32	90°	23 (3.5/0.5)	SENSE (8 chan)
Blankenburg et al., 2010	Mapping state-dependent top-down parietal to visual cortex modulation during visuospatial attention	6	burst/block	Y	75 %	10 Hz	5(500 ms) (9 burst per block)	4(20) x 6 conditions	TMS at 35 % RMT	R pPC [MNI 22, -60, 60]	MNI coordinates from literature[*5]	neuronavigation + fiducials	MSR	3000/50	90°	27 (2/1)	visual surface coil (1 chan)[*6]
Moisa et al., 2010	Demonstrating feasibility of TMS with continuous arterial spin labelling (CASL)	10	train/block	Y	100 %, 110 %, 120 %	2 Hz or 10 Hz	2(24 s) 16(2 s), 32(4), 96(12 s)	16(768) per intensity 2(32, 64, 192)	voluntary movement triggered by TMS at 50 % RMT	L M1	MHS	neuronavigation + calibrated coil holder	MVX	4000/20		8 (?/0.5)	Tx/Rx (1 chan)

(*continued on next page*)

Table 1 (*continued*)

Study	Study design & objectives Objective	N	TMS protocol /fMRI design	Local Activation[*3]	TMS parameters & equipment Intensity (% RMT[*1])	Frequency of train/burst or SOA of SP/ burst (ER design)	# pulses (duration in s) per burst/train	# trials/blocks (pulses) per condition	Comparisons, Controls, and Sham conditions	Surface Target [MNI or 10/20 coordinates] (Deep Target)	Method for determining target site	Method for verifying coil position relative to MRI	TMS device and coil[*2]	fMRI parameters & equipment TR/TE in ms	Flip angle	#Slices (slice thickness / gap in mm)	RF-coil type
Caparelli et al., 2010	Mapping the neuronal corelate of phosphene perception	12	train/block	Y	100 % PT (or 40 % MSO)	0.25 Hz	8(28 s)	3(24)	rest	V1	PHS	phosphene	MS	2000/20	90°	33 (4/1)	standard quadrature head resonator
(Heinen et al., 2011)	Mapping state-dependent top-down modulation by FEF during visuospatial attention	12	burst/ER	Y	110 %	11 Hz, 7.3-9.7 s	3(270 ms)	48(432)	vertex TMS, TMS at 40 % RMT	R AG [MNI 40, -73, 44]	dorsolateral termination of STS	neuronavigation + fiducials	MSR	2430/42	90°	27 (2.5/1.25)	receive head array (1 chan)
Shitara et al., 2011; Shitara et al., 2013	Assessing dose-response relationship for M1, trying to disentangle primary activation from sensory feedback	36	SP/ER	Y	120 %, 90 %	7.98-13.97 s		1(42)	cued voluntary movement, MNS	L M1	MHS	MEP	MSSR	998/25	60°	12 (?/?)	circular polarization head coil
Ricci et al., 2012	Mapping neuronal correlates of visuospatial neglect-like effects for right parietal TMS	3	SP/ER	NR	115 %	?		18(18) per TMS sites	vertex	R pPC	9 cm dorsal and 6 cm lateral to the inion	fiducials	MSSR	2300/35	90°	23 (3.5/0.5)	SENSE head coil (8 chan)
Moisa et al., 2012	Mapping state-dependent role of left dPMC for action selection based on visuomotor mapping using CASL	9	train/block	NR	110 %	10 Hz	5(500 ms) (15 bursts per 60 s train)	3(225) * 2 conditions	70 % RMT	L dPMC	2 cm anterior and 1 cm medial to MHS	neuronavigation + calibrated coil holder	MVX	4000/20	?	16 (?/0.5)	Tx/Rx (1 chan)
Leitao et al., 2012	Mapping state-dependent top-down modulation of visual and auditory cortex by right IPS	12	train/block	NR	100 %	1.9 Hz	37(20 s)	10(370) * 18 conditions	pseudo-TMS clicks, vertex TMS, TMS at 60 % RMT	R IPS [38, -44, 46] Talairach	MNI coordinates from literature[*5]	neuronavigation + fiducials	MVX	3210/40	90°	36 (2.6/0.4)	?
Chen et al., 2013	Testing causal modulation of default mode network (DMN) by stimulation of central executive network (CEN) and salience network (SN)	22	train/block	NR	120 %	0.4 Hz	7(16.8 s)	10(70) * 2 conditions		pMFGand aMFG	ICA of rs-fMRI from independent sample	neuronavigation	MSR[2]	2000/30	85°	29 (4/?)	?
Hanlon et al., 2013	Mapping lateral and medial prefrontal cortical-subcortical circuits	17	SP/ER	Y	100 %	10.18 s		2(12)	TMS of V1	dlPFC [F3] and mPFC [FP1]	10-20 EEG system	fiducials	MSSR	2520/23	90°	? (?/?)	RAPID Biomedical head coil (12 chan)
Peters et al., 2013	Demonstrating feasibility of concurrent TMS-EEG-fMRI	1 1	SP/ER	Y	80 % MSO ?	11.25-15.75 s ?	?	?	?	R PMC and R IPS	2 cm anterior and 1 cm medial to MHS; MNI coordinates from literature[*5]	MEP + neuonavigation	MS D70	2250/30 2320/30	78°	21 (?/?) 17 (?/?)	2x flex (8 chan)
Yau et al., 2013	Developing new method for visualizing coil position and identifying cortical target location	8	train/block	Y	90 %	1 Hz	10(10 s)	5(50) * 2 intensities	voluntary finger tapping cued by TMS at 50 % RMT	L M1	MHS	fiducials	MS	1000/30	61°	15 (6/0)	array surface coil (6 chan)
Heinen et al., 2014	Mapping state-dependent top-down modulation of feature attention by FEF	16	burst/ER	Y	110 %	11 Hz, 8.91±1.49 s	3(270 ms)	72(216) * 4 runs	TMS at 40 % RMT	R FEF [31, 1, 58]	MNI coordinates from literature[*5]	neuronavigation + fiducials	MSSR	2970/42	?	33 (?/50%)	receive head array (1 chan)
de Weijer et al., 2014	Developing new setup with flexible MR-RF coils	6 (M1) 3(dSMG)	SP/ER	Y	110 % vs. 70 %	10 s		23 * 2 conditions		L M1 and L dSMG [-47, -39, 52]	MHS and MNI coordinates from literature[*5]	neuronavigation + fiducials	MS	2000/23	70°	30 (3.6/0.4)	2x flex (8 chan)
Mason et al., 2014	Mapping compensatory response of language network for language comprehension during pSTG disruption	26	train/block	decreased activation	110 %	1 Hz	300(5 min)	1(300)	contralateral homolog	Wernicke's area [CP5]	10-20 EEG system		MSR[2] model 3812-00	1000/30	60°	14 (5/1)	Tx/Rx circular polarized coil
Leitao et al., 2015	Mapping state-dependent top-down modulation of target detection and sustained spatial attention by IPS	10	burst/block	Y	125 %	10 Hz	4 pulses (400 ms) (12 bursts per block)	84(336) * 8 runs	sham: 2 cm thick plastic plates	R aIPS [42.3, -50.3, 64.4]	MNI coordinates from literature[*5]	neuronavigation + fiducials	MVX (MRI-B88)	3290/35	90°	40 (3/0.3)	Tx/Rx (1 chan)

(*continued on next page*)

Table 1 (*continued*)

Study	Study design & objectives Objective	N	TMS protocol /fMRI design	Local Activation[*3]	TMS parameters & equipment Intensity (% RMT[*1])	Frequency of train/burst or SOA of SP/burst (ER design)	# pulses (duration in s) per burst/train	# trials/blocks (pulses) per condition	Comparisons, Controls, and Sham conditions	Surface Target [MNI or 10/20 coordinates] (Deep Target)	Method for determining target site	Method for verifying coil position relative to MRI	TMS device and coil[*2]	fMRI parameters & equipment TR/TE in ms	Flip angle	#Slices (slice thickness / gap in mm)	RF-coil type
Navarro de Lara et al., 2015	Development of a new ultrathin 7-channel MR RF coil- array	1	train/block	Y	110 % AMT	10 Hz	8(800 ms) * 10 trains per block	3(240)		L M1	MHS	MEP	MVX (MRI-B91)	2000/33	60°	10 (3/?)	Rx only surface coil array (7 chan)
Jung et al., 2016	Mapping the effects of vertex stimulation at different coil orientations	32	train/block	NR	120 %	1 Hz	12(12 s)	18(216)		Vertex [Cz] and L M1	10-20 EEG system	MEP	MSR[2]	2000/35	90°	30 (?/?)	Nova-medical Head Coil (6 chan)
Xu et al., 2016	Mapping state-dependent modulation of response inhibition by preSMA	17	SP/ER	Y	80, 120 %	9.2 –13.8 s	30(<6 min)	4(120)	TMS at 40 % RMT	R preSMA	MHS	fiducials	MSSR	2000/25	90°	34 (4/?)	2 x matrix (12 chan)
Navarro de Lara et al., 2017	Demonstrating superiority of Development of new 7-channel RF coil- array and assess dose-response relationship for M1	7	train/block	Y	80, 90, 100, 110 % AMT	1 Hz	10(10 s)	5(50) * 4 conditions	rest	L M1	finger-tapping task	fiducials	MVX(MRI-B91)	1000/33	60°	14 (3/?)	Rx only surface coil array (7 chan)
(Leitao et al., 2017b)	Mapping neuronal correlates of neglect-like effects on visual perception by TMS of IPS and occipital cortex	8	burst/block	Y	125 %	10 Hz	4 pulses (400 ms) (12 bursts per block)	84(336) * 8 runs	sham: 2 cm thick plastic plates	R Occ [19.42, -102.35, 13.4] and R aIPS [42.3, -50.3, 64.4]	MNI coordinates from literature[*5], pilot study	neuronavigation + fiducials	MVX (MRI-B88)	3290/35	90°	40 (3/0.3)	Tx/Rx (1 chan)
Leitao et al., 2017a	Mapping state-dependent modulation of perceptual decision making by IPS	7	burst/block	Y	125 %	10 Hz	4 pulses (400 ms) (12 bursts per block)	84(336) * 4 runs (actually 8 runs, but only 4 reported)	sham: 2 cm thick plastic plates	R aIPS [42.3, -50.3, 64.4]	MNI coordinates from literature[*5]	neuronavigation + fiducials	MVX (MRI-B88)	3290/35	90°	40 (3/0.3)	Tx/Rx (1 chan)
Hawco et al., 2017	Mapping remote effects of TMS to dlPFC onset during associative memory encoding	17	burst/ER	Y	100 %	10 Hz, 4.4-11.2 s	3(300 ms)	30(90) * 3 conditions	no TMS condition	L dlPFC [F3]	10-20 EEG system		MSR[2]	3000/30	?	30 (?/?)	matrix (12 chan)
Dowdle et al., 2018	Developing sham control and assessing dose-response relationship for dlPFC	20	SP/ER	Y	90-120 % (10 % steps)	10-15 s		2(40) * 2 conditions	sham (3 cm of firmly compressed open-cell foam)	L dlPFC [F3] (aCC, caudate, Th)	10-20 EEG system		MS	1000/23	60°	16 (?/?)	(12 chan)
Vink et al., 2018	Mapping remote effects in sgACC following TMS to left DLFPC	9	SP/ER	Y	115 % vs 60 %	10-16 s		?	L M1	L dlPFC	border between BA46 and BA9	fiducials	MSR[2]	2000/23	70°	30 (3.6/0.4)	2 x ?
Hawco et al., 2018	Mapping remote effects of TMS to left dlPFC	22	SP/ER	Y	100 %	8.5-14.5 s		2(50) * 2 conditions	TMS at 40 % RMT	L dlPFC [mid-point of F3 and F5]	10-20 EEG system	fiducials	MSR[2]	2100/60	?	35 (?/?)	(12 chan)
de Graaf et al., 2018	Mapping the neuronal corelate of phosphene perception	3 / 1	SP/ER		80/90, 100, 110/120 % PT	16.5 s		4(12) for sub- and supra-PT, 4(48) for PT; 10(60) for sub- and supra-PT, 10(120) for PT		V1	PHS	phosphene	MVX (MRI-B90 II)	1500/30	?	44 (?/0)	2x flex (8 chan)
Oh et al., 2019	Developing point spread function correction for TMS-related EPI artifacts	1	train/block	Y	40 %, 50 % MSO	16 Hz	3(187.5 ms) * 3	10(90)	finger tapping task	L SMC	MHS	fiducials	MSR[2]	3000/30	86°	46 (?/?)	Posterior part of 12-chan head coil (6 chan) + flex coil (6 chan)
Jung et al., 2020	Mapping neuronal correlates of bodily self-consciousness resulting from multisensory experience of TMS to M1	36	train/block	Y	100 %	1 Hz	11(11 s)	9(99) * 4 conditions	rest, TMS of vertex at 120 % RMT	M1	MHS	MEP	MSR[2]	2000/35	90°	30 (?/?)	(6 chan)
Peters et al., 2020	Demonstrating feasibility of assessing state-dependent oscillatory modulation of motor system by concurrent TMS-EEG-fMRI	4	burst/ER	Y	55 % MSO	15 Hz, 13.5±2.25 s	3(200 ms)	120-125(360-375)	rest	R PMd	finger tapping task	neuronavigation + fiducials	MVX (MRI-B88)	2250/30	78°	21 (?/?)	2x flex (8 chan)

(*continued on next page*)

Table 1 (*continued*)

Study	Study design & objectives Objective	N	TMS protocol /fMRI design	Local Activation[*3]	TMS parameters & equipment Intensity (% RMT[*1])	Frequency of train/burst or SOA of SP/ burst (ER design)	# pulses (duration in s) per burst/train	# trials/blocks (pulses) per condition	Comparisons, Controls, and Sham conditions	Surface Target [MNI or 10/20 coordinates] (Deep Target)	Method for determining target site	Method for verifying coil position relative to MRI	TMS device and coil[*2]	fMRI parameters & equipment TR/TE in ms	Flip angle	#Slices (slice thickness / gap in mm)	RF-coil type
Hermiller et al., 2020	Providing evidence for successful state-dependent, frequency-specific, and target-specific modulation of hippocampal activity during memory encoding	16	burst/ER	NR	80 %	50 Hz triplets at 5 Hz vs. 12.5 Hz bursts every 11-19.5 s	30(2000 ms) vs 30(2400 ms)	72 (2160) vs 72 (2160)	Memory encoding vs. numerical task	L PC (hippocampus)	coordinates from functional connectivity analysis	neuronavigation + fiducials	MVX(MRI-B91)	2230/20 vs. 2440/20	90°	22 (3/?) vs. 30 (3/?)	Tx/RX coil (1 chan)
Oathes et al., 2021	Connectivity-based targeting of the sgACC and the amygdala via the dlPFC	14	train/block		120%	~0.42 Hz	~7 pulses (16.8 s); some pulses omitted as catch trials	72	Multiple target sites per subject	Left dlPFC	coordinates from functional connectivity analysis	Neuronavigation	MVX(MRI-B91	2400/30	75°	32 (4/?)	RAPID quad T/R single channel
Studies in patients																	
Li et al., 2003	Mapping local brain diffusion in MDD to test for TMS-related pathologic changes or leakage of the blood-brain barrier	14	train/block	NR	100 %	1 Hz	21(21 s)	7(147)		L PFC	5 cm rule[*4]	calibrated coil holder	DT	4491/116	?	15 (6/1)	?
Li et al., 2004a	Proof of target engagement of limbic regions following TMS of left dlPFC in MDD	14	train/block	Y	100 %	1 Hz	21 (21 s)	7(147)	rest	L PFC	5 cm rule[*4]	calibrated coil holder	DT	3000/?	90°	15 (7/1.5)	?
Bestmann et al., 2006	Mapping the neural correlates of phantom sense of movement in a limb amputee	1	SP/ER	Y	83 %, 78 %, 73 %, 68 % MSO	5 and 14 s		20, 40, 40, 20 trials per intensity		L M1	Motor mapping of reported phantom movement	fiducials	MSR	2000/36	70°	20 (4/1)	Tx/Rx
Bestmann et al., 2010	Mapping the interhemispheric impact of TMS to contralesional M1 in stroke	12	burst/ER	Y	110 %, 70 % AMT	11 Hz, 11-21 s	5(454 ms)	20(100) * 4 conditions	trials w/o TMS, rest	contralesional PMd	2 cm anterior and 1 cm medial to MHS	fiducials	MSR	1800/42	90°	20 (2.5/1.25)	standard circular polarized receive head and body transmit coil
Guller et al., 2012	Probing integrity of cortico-thalamic and cortico-cortical circuits in schizophrenia	28	SP/ER	Y	110 %	16-24 s		2(20) * 2 conditions	sham (4cm hollow plastic block); noise masking; button pressing task	L PCG (ROIs: Th, mSFG, insula)	Part of PCG where no visible motor response was evoked	neuronavigation + fiducials	MSR[2]	2000/25	60°	35 (3/0.6)	quadrature head coil
de Vries et al., 2012	Mapping of compensatory mechanisms in cervical dystonia	17	train/block	NR	115%	1 Hz	10(10 s)			L sPC [-24, -60, 68]	MNI coordinates from literature[*5]	neuronavigation + fiducials	MSR	2300/?		23 (3.5/?)	Nova Medical
Hanlon et al., 2015; Hanlon et al., 2017	Mapping the offline effect of cTBS to left frontal pole on front-striatal connectivity in alcohol and cocaine addiction	11 (preliminary) 49 (final25+24)	SP/ER	Y	110 %	10.18 s		20 * 4 conditions	sham cTBS outside the scanner in between TMS-fMRI sessions	L mPFC [Fp1]	10-20 EEG system		MSSR	2500/23	90°	? (?/?)	RAPID (12 chan)

(*continued on next page*)

Table 1 (*continued*)

Study	Study design & objectives Objective	N	TMS protocol /fMRI design	Local Activation[*3]	TMS parameters & equipment Intensity (% RMT[*1])	Frequency of train/burst or SOA of SP/ burst (ER design)	# pulses (duration in s) per burst/train	# trials/blocks (pulses) per condition	Comparisons, Controls, and Sham conditions	Surface Target [MNI or 10/20 coordinates] (Deep Target)	Method for determining target site	Method for verifying coil position relative to MRI	TMS device and coil[*2]	fMRI parameters & equipment TR/TE in ms	Flip angle	#Slices (slice thickness / gap in mm)	RF-coil type
Hanlon et al., 2016	Mapping differential remote effects of dlPFC and mPFC TMS in cocaine-addiction	36	SP/ER	NR Y	110 %	12 s		12 * 2 conditions	healthy controls	F3 (dlPFC) Fp1 (vmPFC)	10-20 EEG system	fiducials	MSSR	6700/87	?	50 (3/0)	array (12 chan)
Fonzo et al., 2017	Linking the effect of rTMS treatment in PTSD to indirect amygdala activation via TMS	17	train/block	NR	120 %	0.4 Hz	7(16.8 s)	10(70) * 2 conditions	no-TMS group	R pMFGand R aMFG	ICA of rs-fMRI from independent sample	neuronavigation	MSR^2	2000/30	85°	31 (4/0.5)	?
Kearney-Ramos et al., 2018	Evaluate the contribution of white matter integrity and gray matter volume to frontal pole TMS-induced striatal activity in cocaine-addiction	49	SP/ER	N	100 %	10-12 s		? total #pulses not reported		Fp1 (vmPFC)	10-20 EEG system		MSSR	2500/23	90°	43 (?/?)	(12 chan)
Eshel et al., 2020	Mapping effective connectivity between dlPFC and amygdala in MDD	41	train/block	NR	120 %	0.4 Hz	7(16.8 s)	10(70)* 2 stimulation sites		dlPFC part in FPCN and dlPFC part in VAN	ICA of rs-fMRI from independent sample	neuronavigation	MSR^2	2000/30	80°	? (?/?)	(8 chan)
Webler et al., 2020	Probing prefrontal hyperexcitability and reduced interhemispheric connectivity in schizophrenia	19	burst/ER	Y	0, 80, 100, 120 %	10 Hz, 8 or 10 s	3(300 ms)	5(105)	healthy controls	BA9	MNI coordinates from literature[*5]	neuronavigation + calibrated coil holder	MS	2000/35	90°	32 (?/?)	surface (1 chan)[*6]

Abbreviations: aCC = anterior cingulate cortex, AG = angular gyrus, APB = abductor pollicis brevis, AMT = active motor threshold, cTBS = continuous theta burst stimulation, DT = Dantec MagPro, dlPFC = dorsolateral prefrontal cortex, dSMG = dorsal supramarginal gyrus, DWI = diffusion-weighted imaging, EEG = electroencephalography, EMG = electromyography, ER = event-related design, FC = frontal cortex, FEF = frontal eye field, FPCN = frontoparietal control network, IPS = intraparietal sulcus L = left, l = lateral, M1 = primary motor cortex, MS = MagStim, MDD = major depressive disorder, MFG = middle frontal gyrus, MNS = median nerve stimulation, mPFC = medial prefrontal cortex, MSR = MagStim Rapid, MSR^2 = MagStim Rapid^2, mSFG = medial superior frontal gyrus, MSH = motor hot spot, MSO = maximum stimulator output, MSSR = MagStim SuperRapid, N = no, NR = not reported, p = posterior, PC = parietal cortex, PCG = precentral gyrus, PFC = prefrontal cortex, PHS = phosphene hotspot, PMC = premotor cortex, PT = phosphene threshold, R = right, RMT = resting motor threshold, RSC = resting state connectivity, S1 = primary sensory cortex, s = superior, SMC = sensorimotor cortex, SOA = stimulus onset asynchrony, STS = superior temporal sulcus, SP = single pulse, Tx/Rx = transmit/receive head coil, MVX = MagVenture MagPro X100, Th = thalamus, V1 = primary visual cortex, VAN = ventral attention network, vmPFC = ventromedial prefrontal cortex, Y = yes; ? = information could not be extracted from publication.

[*1] Intensity reported in % RMT unless specified otherwise;

[*2] If the coil model was not further specified, only the stimulator model is mentioned;

[*3] Most of the studies did not look into local activation explicitly, therefore remarked as *not reported*, which does not implicate that there was no local activation;

[*4] Location 5 cm rostral and in parasagittal plane from the site of max APB stimulation;

[*5] MNI coordinates from the literature were transformed into native space;

[*6] Assumed number of channels as not mentioned in the article;

Table 2
Summary statistics for selected study parameters based on Table 1.

	N
Total number of studies in humans	69
Healthy participants	57
Patients	12
TMS protocol	
Single-pulse	18
Burst	18
Train	33
fMRI design	
Block	42
Event-related (ER)	27
Superficial Targets	
Primary visual cortex (V1)	3
Primary motor cortex (M1)	29
Sensorimotor cortex (SMC)	1
Dorsal premotor cortex (dPMC)	5
Pre-supplementary motor area (preSMA)	1
Parietal cortex (PC), thereof…	18
"Superior"/"Posterior" PC	9
Intraparietal sulcus (IPS)	7
Supramarginal gyrus (SMG)	1
Angular gyrus (AG)	1
Frontal eye field (FEF)	3
Dorsolateral Prefrontal Cortex (dlPFC)	15
Medial prefrontal cortex (mPFC)	4
Wernicke's area	1
Vertex	1
Deep targets	
Anterior cingulate cortex (aCC)	1
Subgenual anterior cingulate cortex (sgACC)	2
Ventromedial prefrontal cortex (vmPFC)	1
Thalamus	1
Caudate Nucleus	1
Hippocampus	1
Amygdala	1
Stimulator	
MagVenture/Dantec	26
MagStim	43
Method for determining the target site	
Functional MEP hotspot search	22
Functional phosphene hotspot search	2
Positioning rule in cm relative to motor hotspot	11
Scalp anatomy (10-20 EEG system or skull landmarks)	10
MNI coordinates from literature converted to native space	12
MNI coordinates from own pilots/analyses	4
Landmarks from individual brain anatomy	4
Native coordinates from individual localizer tasks	5
Method for verifying the coil position relative to MR	
Functional (MEPs)	9
Coil Fiducials	35
Calibrated coil holder	12
Neuronavigation outside the MR room + marker on scalp/cap	16
Neuronavigation during fMRI	0

Hanlon et al., 2016; Hermiller et al., 2020; Kearney-Ramos et al., 2018; Oathes et al., 2021). Overall, sample sizes are highly variable, ranging from N = 1 to N = 49, but on average slightly increasing over the years. Roughly half of the studies (33x) used trains of TMS pulses, whereas the other half used short TMS-bursts (18x) or single-pulse TMS (18x). Notably, fMRI block designs were used to analyze the accumulated BOLD signal changes during TMS trains (19x) or groups of TMS bursts (41x), whereas event-related designs were used to analyze individual BOLD responses to single pulses or single bursts of TMS with sufficiently long stimulus onset asynchrony (SOA) (27x). See Table 2 for further details.

In the following review, we will first discuss the technical challenges and solutions regarding TMS and MR equipment, experimental setup, temporal interleaving, and image acquisition (section 2). We will then highlight the unique insights that can be gained by concurrent TMS-fMRI (section 3). We will describe key experimental confounds as well as countermeasures that can be taken to deal with these confounds, such as sham and active control conditions (section 4). Finally, we review the application of concurrent TMS-fMRI in clinical research and its value for developing and refining TMS treatments of psychiatric and neurological disorders (section 5), before we conclude with a brief outlook into the expected future advancements of concurrent TMS-fMRI (section 6).

2. Technical challenges and solutions for concurrent TMS-fMRI

The high methodological demands with respect to both stimulation equipment and data acquisition have for a long time limited the use of concurrent TMS-fMRI to a few specialized labs worldwide and prevented a more wide-spread adoption of the technique. The improved design of MR-compatible TMS coils, technical developments in multichannel MR-coils (Navarro de Lara et al., 2017; Navarro de Lara et al., 2015), and MR-compatible concurrent neuronavigation has revived the interest in concurrent TMS-fMRI. We therefore consider this a timely opportunity to review the technical challenges of this tool and the solutions identified to date, and to provide a concise summary of the methodological state-of-the-art for conducting concurrent TMS-fMRI studies. We will introduce the technical requirements regarding equipment and experimental setup, introduce the various TMS-related MR artifacts, and discuss strategies for the temporal interleaving of TMS and fMRI.

2.1. Equipment and experimental setup

The special situation of a TMS coil being located and discharged within an operating MR scanner poses multiple challenges with respect to both subject safety and imaging artifacts. A dedicated TMS-fMRI hardware setup is thus required to ensure optimal timing and minimization of artifacts (Fig. 1A).

2.1.1. MR-compatible TMS coils

TMS coils must not contain any ferromagnetic material, like any other equipment used in the MR environment. MR-compatible TMS coils must also be constructed in a way that they resist the heavy mechanical load resulting from the interaction of the strong static magnetic field (B_0) of the MR (up to 3 T) and the dynamic magnetic field of the TMS pulse (up to 3 T) via Lorenz forces. Non-MR-compatible TMS coils must not be used in the MR scanner, as they can move or break, posing a life-threatening danger for the subject. So far, exclusively biphasic pulse forms have been used, causing a lower mechanical load due to the balanced pulse shape compared to monophasic pulses. The stimulator itself must be placed outside the MR room or, if inside, within a dedicated shielded metal cabinet, and the TMS coil must be connected via a waveguide and an additional low-pass filter to remove external high-frequency noise (Bungert et al., 2012a). The required extra-long power cable (up to 5 m) and the low-pass filter result in significant power loss and thus reduce stimulation intensity by ~5 % and ~10 % respectively (i.e., a total of ~15 %) of the maximum stimulator output (MSO), for the setup provided by MagVenture (Farum, Denmark). Modifications of the electronics of the TMS device to suppress leakage currents (see 2.2.1) may further decrease stimulation intensity. Notably, also the static B_0 field of the MR has an effect of the magnitude of the magnetic field produced by the TMS coil during discharging, and significant variations in the effective field strength produced by TMS have been reported as a function of TMS coil position relative to the fringe field near the gantry. It is therefore recommended to perform TMS either inside of the bore, where the B_0 field is most stable, or outside at a distance > 70 cm from the gantry (Yau et al., 2014). Direct MR-based phase accumulation measurements in a phantom may help to empirically quantify the actual magnetic field produced by the TMS coil (Mandija et al., 2016). MR-compatible coils and low-pass filters are commercially available from MagVenture (Farum, Denmark) and MagStim (Whitland, UK), as well as a coil cooling option via compressed air flow (Magventure) to prevent overheating for rTMS protocols at higher intensities. There is, however, still room for improvement, e.g. with respect to the coil efficacy and its

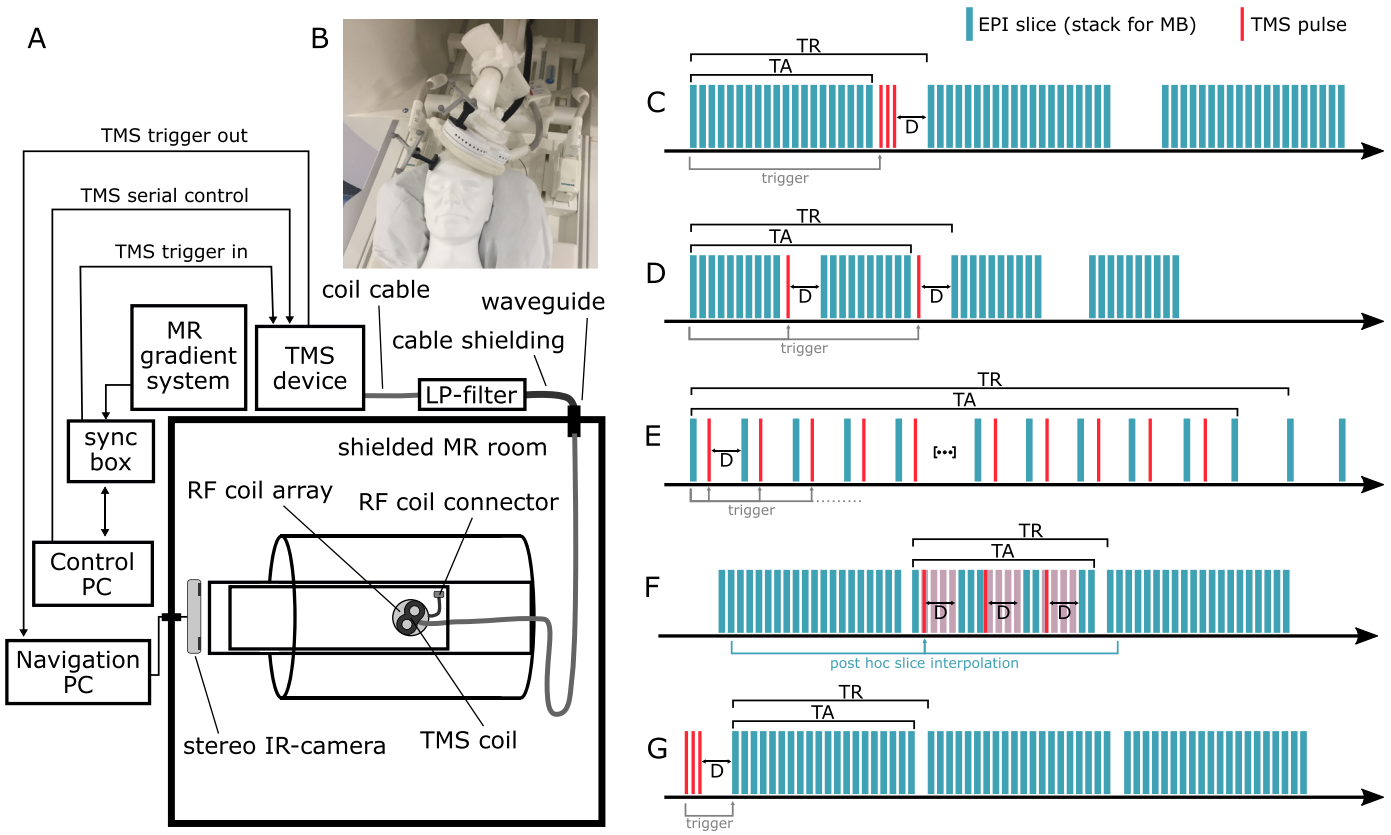

Fig. 1. Hardware setup and temporal interleaving for concurrent TMS-fMRI. Left: **(A)** Exemplary wiring diagram of hardware components required for concurrent TMS-fMRI. **(B)** Photograph displaying an example setup with coil holder, TMS-coil (MR-B91, MagVenture, Farum, Denmark), 2 × 7-channel RF-coil arrays (2nd located below vacuum pillow and thus not visible) (Navarro de Lara et al., 2015), trackers on coil and head for frameless stereotactic neuronavigation, and head stabilization via a vacuum pillow. **Right:** Schematic representation of the different strategies for temporal interleaving of TMS pulses (red) and EPI slice acquisition (blue), with grey arrows indicating which event is triggering the other. **(C)** Single-pulse or burst TMS in between volumes. **(D)** Single-pulse TMS applied both between volumes and within volumes between two slice packages. **(E)** TMS trains applied with single TMS pulses and single slices acquisition being interleaved alternatingly. **(F)** TMS burst applied during a volume causing interference with EPI acquisition and subsequent slice interpolation. **(G)** EPI acquisition of multiple volumes being triggered by TMS burst. Abbreviations: D = Delay between TMS pulse and the next MR imaging element, TA = Time of Acquisition, TR = Time of Repetition.

susceptibility to Lorentz forces (Cobos Sanchez et al., 2020). An interesting ongoing development is, for example, the combination of multiple MR-compatible 3-axis TMS coil arrays to steer the induced E-field within the brain without the need for coil relocation (Navarro de Lara et al., 2020).

2.1.2. *TMS-compatible MR radio frequency (RF) coils*

The most obvious limitation with respect to the MR radio frequency (RF) coils (aka “head-coils”, i.e., the antenna array via which the MR signals are received), is the constraint they impose on the positioning of the TMS coil. In modern helmet-like 32-, or 64-channel RF coils there is simply no space to fit in a TMS coil, which is why mainly large single-channel “birdcage” coils have been used, which provide a large opening at the back for the TMS coil and cable to be positioned (Bestmann et al., 2003b). While whole-brain imaging with good sensitivity for deep brain structures is possible with a single RF channel, TMS coil positioning is severely limited with these RF coils, and modern parallel multiband imaging sequences (Siemens’ SMS, GE’s HyperBand, and Philips’ Multi-band SENSE) require multiple spatially distributed receive coils. While some multi-band acceleration is already possible with large 8-channel receive-only head coils specifically designed for the use with TMS (Magnetica Ltd, Australia), the degrees of freedom for TMS coil positioning are still limited. Some labs therefore used one or multiple combined flexible multichannel surface RF coil arrays, which can be flexibly wrapped around head and TMS coil (Lu and Wang, 2018; Wang et al., 2017), e.g., 2x ”Siemens 4-Channel Flex coils” (de Graaf et al., 2018; Peters et al., 2020; Peters et al., 2013) or 2x “Philips FLEX-L MR receive coils” (de Weijer et al., 2014), or combined the posterior part (i.e., 6 channels) of a 12-channel Siemens “head matrix coil” with a 6-channel flexible “body matrix coil” (Oh et al., 2019). While these setups increase the flexibility of TMS positioning and allow the use of multiband sequences, signal-to-noise ratio (SNR) of the acquired images is still inherently limited by local field inhomogeneities and associated signal drop-out caused by the mere presence of the TMS coil between the subject’s brain and the RF coils (section 2.2.1). This may compromise the sensitivity particularly for signals from the targeted brain region itself. To overcome this limitation and to maximize SNR at the stimulation site while maintaining full flexibility in coil positioning, a novel thin MR-compatible 7-channel surface RF-coil array has been developed (and is commercially available via MagVenture), which is directly mounted to the bottom site of the TMS coil (Navarro de Lara et al., 2017; Navarro de Lara et al., 2015). The coil array adds an extra coil-scalp distance at the TMS coil hot-spot of 4.5 mm (according to Navarro de Lara et al., 2015) to 5.8 mm (according to our own measurements). This setup (Fig. 1B) has been reported to achieve 5-fold SNR for BOLD-signals at 3 cm depth underneath the TMS coil compared to birdcage coil setups and equal or better SNR in 42% of the brain volume (Navarro de Lara et al., 2015). However, the SNR at deeper brain regions is naturally limited for surface coil arrays of small diameters (here: 6 cm per coil). When used together with a second, supplementary 7-channel array, better whole brain coverage can be achieved, but the gradual loss of SNR towards the center of the brain still reduces the detection power for remote BOLD responses in some of the clinically relevant deep brain regions. An apparent lack

of activation may thus also result from low receive coil sensitivity in those regions, and it is advisable to estimate and provide the spatial sensitivity profile (or SNR maps) for the specific coil setup in use to critically guide the interpretation of the results. SNR maps can be produced by reconstructing raw images directly in SNR units (Kellman and McVeigh, 2005; Navarro de Lara et al., 2015), whereas the spatial sensitivity of receive coil arrays can simply be approached by estimating a relatively smooth bias field using standard tools (Ashburner and Friston, 2005; Zheng et al., 2009). Note that the latter is not directly related to sensitivity, but nonetheless provides an impression of the coil coverage. The spatial receive sensitivity may vary substantially if the positions of surface receive coils are not standardized across participants, which is sometimes difficult to achieve due to practical constraints, and in case of large variability this may need to be accounted for in group level analyses. A clear advantage of combining two multi-coil arrays is, however, that the resulting 14 channels enable the use of modern multiband imaging techniques (e.g., 4-fold acceleration, 60 slices at TR = 1 s and TE = 30 ms). The downside of mounting an MR coil array below the TMS coil is a further reduction of effective stimulation intensity in the range of ~15 % MSO (Navarro de Lara et al., 2015), resulting in an overall reduction (together with the 15 % owed to the long cable and lp-filter; section 2.1.1) of ~30 % MSO, which can make it difficult to achieve suprathreshold intensities in some participants with high thresholds.

2.1.3. MR-compatible TMS coil positioning and MR-guided neuronavigation

In addition to placing the TMS coil in the desired position, it is important to maintain this exact position throughout the entire fMRI recording. Stabilizing the coil at a fixed position can be achieved by customized MR-compatible coil holders made from non-ferromagnetic material. The coil holder has to be able to reach all desired coil positions and orientations (requiring at least 6 degrees of freedom) and stable enough to maintain the target position, withstanding head movements and Lorenz forces. These coil holders have successfully been developed by users for both MagStim (Bestmann et al., 2003b; Bohning et al., 2003a) and MagVenture setups (Bohning et al., 2003a; Moisa et al., 2009). The above discussed reductions in effective stimulation intensity emphasize the relevance of accurate coil positioning, which can be practically very challenging for some intended coil positions given the design constraints of the coil holders. The second challenge is to accurately navigate the TMS coil into the desired target position on the scalp once the actual target coordinates of the cortical stimulation have been identified. For motor cortex stimulation, MEP hot-spot search can be conducted immediately before moving the subject into the gantry, whereas for other brain regions the target needs to be determined beforehand. In principle, skull anatomy-based navigation methods (e.g., using the skull landmarks and EEG 10-20 system) can be used as outside the MR, but brain-anatomy MR-image guided navigation is more accurate and currently constitutes the gold standard in the field (Bergmann and Hartwigsen, 2021; Sack et al., 2009). Table 2 summarizes the methods used in TMS-fMRI studies so far.

For concurrent TMS-fMRI, two principal options exist for MR image-guided coil positioning. The first option is to use a customized calibrated coil-positioning systems to calculate the positioning parameters for its joints (in mm and degree angle) based on a fast structural image being acquired directly before the TMS experiment with the subject already positioned in the MR, which can then be adjusted manually while briefly moving the subject out of the MR (Bohning et al., 2003a; Moisa et al., 2009). This approach has been used in 12 studies so far (Table 2). The second option is to use a frameless stereotactic neuronavigation systems based on a co-registered structural MR image acquired anytime beforehand. This approach can either be implemented “offline” or “online”: For the offline approach, neuronavigation is used outside the MR to determine the exact coil position, which is then marked on the scalp or a swim cap with a felt pen, allowing the experimenter to roughly bring the coil in the same position once the subject has moved to the MR. Even though the control of coil rotation and tilt accuracy is rather limited with this approach, it has been used in 16 studies (Table 2). The online approach requires an MR-compatible frameless stereotactic neuronavigation system (e.g., TMS-Navigator, Localite GmbH, St. Augustin, Germany) with the stereo-infrared camera being positioned directly above the MR table. The system must be connected to a workstation outside the MR room via fiber optic cables and powered via a dedicated power cord with low-pass filters. While the calibrated coil holder and offline neuronavigation approaches can validate the TMS coil position only immediately before and after an fMRI run (if fiducials, such as fish oil/vitamin E capsules, are fixed at strategic positions on the coil; as done in 35 studies, Table 2), the online neuronavigation approach can monitor the coil position continuously throughout fMRI acquisition. However, given the limited space available between MR gantry opening and the subject’s body, in particular feet, knee, and chest may block the visibility of the two navigation trackers affixed to forehead and TMS coil, and their locations may need to be adjusted for a given coil position. Since the online neuronavigation solution became available only recently, no study using this approach has been published up to today.

2.1.4. Subject positioning

While a stable head positioning is already key for high quality fMRI recordings, it is even more so for concurrent application of TMS, since the application of TMS in the B_0 field of the MR results in enhanced sensory and auditory stimulation of the subject as compared to the TMS experience in the lab. Head motion can thus be triggered in response to (i) the constant pressure of the TMS coil, (ii) strong coil vibration during pulse delivery, (iii) in association with peripheral co-stimulation induced cranial/facial muscle twitches, or (iv) as a startle response when TMS pulses are delivered at longer inter-stimulus intervals. Solutions for stabilizing the subject’s head depend on the specific type of RF coil(s) used, but for surface coils, vacuum pillows are a flexible and effective means to comfortably stabilize the subjects head (and MR surface coil arrays) in the desired position. Additional adhesive tape, Velcro straps, and sandbags may be used to secure the TMS coil to the subject’s head, reducing movements and displacements. To minimize startle, it can help to familiarize the participants with the particular sensations related to TMS inside the MR scanner by providing several test pulses at the respective intensity before the beginning of the actual fMRI recording. To minimize drifts in head position away from the coil, one may also explicitly instruct the participants to actively maintain scalp pressure against the coil. Online motion detection software (Dosenbach et al., 2017) may help to identify overly strong head movements (independent of its position relative to the TMS coil) and extend or repeat a run after correcting head position. Beside the obligatory ear plugs, the subject should also be equipped with an emergency stop switch to terminate stimulation at any time. A TMS remote control located within the MR room (included with MagVenture MR-TMS coils) can help the experimenter to test the stimulation and adjust stimulation intensity in consultation with the subject before leaving the MR room.

2.2. TMS-related imaging artifacts

The application of TMS concurrent to fMRI acquisition can lead to significant image artifacts and distortions. In principle, one can distinguish between artifacts due to the mere presence of the TMS coil, affecting the static magnetic field of the MR scanner or its gradient fields, and artifacts that result from the actual discharging of the TMS coil (Bestmann et al., 2003a; Siebner et al., 2009). In this section, we will provide an overview of both artifact types as well as measures for avoiding or attenuating them.

2.2.1. Artifacts caused by the presence of the TMS coil

The mere presence of the TMS coil near the head, even though MR-compatible coils are free of ferromagnetic material, can affect the homogeneity of the static magnetic field of the scanner and by that

lead to geometric image distortions and signal drop out in functional (T2*-weighted) but much less so in structural (T1-weighted) MR images (Baudewig et al., 2000; Bestmann et al., 2003a). Any object in the scanner bore, including the human head, can change the static field of the MR scanner and introduce inhomogeneities, which can be reduced by automatic or manual shimming procedures before image acquisition. In addition, the time-varying MR gradient fields can induce eddy-currents in the copper windings of the TMS coil, which in turn temporarily and locally change the magnetic field of the scanner. Since the MR gradient fields depend on the MR imaging sequence, static shimming before image acquisition only helps to reduce inhomogeneities related to the presence of the TMS coil in the static field, but not the influence of MR gradients on these inhomogeneities. The latter can be effectively minimized by the choice of suitable wire types for the coil windings, as implemented for some of the available MR-compatible TMS coils.

Several strategies to reduce the remaining effects of the TMS coil on the MR images have been explored, and their usefulness and necessity depends on the coil type, the MR scanner model, and the stimulated brain area. Fortunately, the human scalp-cortex distance is in most cases sufficiently large to prevent substantial disruptions of echo planar imaging (EPI) data of the brain itself (Baudewig et al., 2000). The severity of distortions in EPI data depends also on the orientation of the TMS coil relative to the orientation of EPI slice acquisition and can be minimized by aligning them parallel to each other (Baudewig et al., 2000). However, optimizing the slice acquisition orientation to minimize image artifacts underneath the coil may in turn result in suboptimal orientations for brain regions strongly affected by susceptibility-related signal loss, such as the orbitofrontal cortices (Moisa et al., 2009). Oversampling in the phase-encoding direction has been recommended to shift ghosting artifacts outside of the brain image (Bestmann et al., 2008c; Ruff et al., 2008). Automated retraction of the TMS coil after each stimulus application and before image acquisition requires sophisticated coil-holding devices (Bohning et al., 2003a), is only feasible for low frequency stimulation and EPI acquisition with long TRs, and might induce additional vibration-related artifacts (see below). Also passive shimming with steel foil has been found effective (Bungert et al., 2012b). In addition, the TMS coil cable serves as antenna for high-frequency noise from outside the Faraday's cage of the MR room, which can effectively be removed by low-pass filters (Bungert et al., 2012a) to prevent interference with image acquisition. Also small leakage currents from the high-voltage capacitors of the TMS device can be transmitted to the coil via the coil cable and cause image artifacts via the resulting weak magnetic field (Weiskopf et al., 2009). These artifacts scale with TMS intensity and can affect the fMRI analysis when different stimulation intensities are compared to each other. While earlier actively controlled high-voltage relay-diode systems were used to electrically insulate the TMS coil from the stimulator until immediately before and then again directly after each TMS pulse (Weiskopf et al., 2009), nowadays, build-in leakage filters in the stimulator itself can avoid these type of artifacts. In summary, static artifacts can be sufficiently reduced by choice of dedicated equipment and do not pose a major challenge anymore.

2.2.2. Artifacts caused by TMS pulse

Another class of artifacts occurs only when the electromagnetic field induced by the discharge of the TMS coil interferes with EPI acquisition. When a TMS pulse is applied during the image readout part of an EPI sequence, the induced magnetic field acts as unintended spoiler gradient by dephasing the transverse magnetization, which results in loss of the T2*-weighted signal and image artifacts of very different spatial frequency, depending on when exactly the pulse was delivered during k-space sampling (Bestmann et al., 2003a). When a TMS pulse is applied sufficiently close to the excitation phase of an EPI sequence to interfere with the RF pulse, the image will be severely corrupted, and by disturbance of the steady-state longitudinal magnetization the subsequent volumes will still be affected, even though these disturbances may not result in immediately visible artifacts (Bestmann et al., 2003a). This effect corresponds to a modulation of the image intensity, which is time-locked to the TMS-pulse and can thereby cause false positive activations in the fMRI analysis.

But even when the TMS pulse is applied shortly before the RF pulse, image distortions can occur. The TMS coil experiences a torque when discharged, which results in mechanical vibration (also generating the characteristic click sound) and thus a movement within the B_0 field of the MR that is sufficient to create eddy currents in the coil wires via magnetoelectric induction (Bestmann et al., 2003a). These currents in turn create a magnetic field perpendicular to the coil, causing image distortions similar to (though much weaker than) the original TMS pulse itself, and the temporal and spatial association of these artifacts to the TMS-related neuronal effects can lead to false positive fMRI results. These artifacts caused by coil vibration can be observed for the entire duration of the coil movement, and intervals between TMS pulse and RF pulse of 100 ms (Bestmann et al., 2003a), 69 ms (Bestmann et al., 2004), and 50 ms (Navarro de Lara et al., 2017) have been introduced to avoid them. The precise interval required depends on the specific hardware setup (i.e., coil position, coil holder, stabilization procedures, et.) and may need to be determined initially via realistic phantom measurements that match the setup of the planned experiment as closely as possible, using procedures as outlined in Bestmann et al. (2003a). Finally, TMS-evoked head motion (due to transmitted coil vibration, cranial muscle twitches, or startle responses) can cause the typical head movement artifacts in close temporal correlation with TMS pulse delivery, possibly resulting in false positive activations or false negative results (if signal variance rather than consistent signal changes are induced). In summary, dynamic artifacts are the main challenge for concurrent TMS-fMRI and have to be avoided by precise timing of the two techniques, as detailed in section 2.3.

2.3. Temporal interleaving and implications for fMRI analyses

Over time many groups have evaluated the optimal temporal relationship between the delivery of the TMS pulse and the acquisition of the MRI data. TMS and image acquisition are usually not applied truly simultaneously but rather in a tightly interleaved fashion, meaning that TMS pulses are delivered during the gaps between volumes or between slices. This requires high temporal precision and usually customized technical solutions with one device being the main timing controller and the other one a satellite. One option is to assign the timing control to the MR scanner. This requires monitoring the volume triggers that are sent out by the MR gradient system. After the desired number of volumes (varied as a function of the inter-trial interval) has passed, a TTL trigger pulse is forwarded to the TMS machine as "satellite" with an additional delay (in Fig. 1A, this is done by the "sync box"). Another option is to externalize the timing control to a PC with parallel port or a microcontroller and actively trigger both the MRI scanner and TMS device as "satellites". In this case, the PC acts as controller triggering both MR image acquisitions and TMS pulses (with respective delays).

In principle, TMS can be applied as single pulses, short burst, or longer trains, and EPI sequences need to be modified with respect to time of repetition (TR), time of acquisition (TA), and echo time (TE). Temporal gaps can be deliberately inserted between volumes or slices for the delivery of TMS pulses. Depending on the specific TMS protocol and research question, researchers may employ either event-related or blocked designs. As for fMRI designs in general, the former is best suited to estimate the shape and other characteristics of the BOLD response to a single TMS pulse or short burst, whereas the latter has better detection power to identify the spatial location of TMS-related activations. Importantly, however, the optimal timing and repetition patterns of TMS pulses for inducing specific *online* or *offline* effects in neuronal activity may not always be easily reconciled with the optimal timing for fMRI acquisition to achieve maximal sensitivity or efficiency, and compromises need to be made.

There are several ways to interleave EPI acquisition with TMS. If one wishes to acquire all slices of a volume continuously and with minimal TR, the TMS pulses can only be applied in between volumes (Fig. 1C). Blocked fMRI designs can thus easily be realized when TMS pulses/bursts are repeatedly applied at a frequency of 1/TR, targeting every single gap in a series of volumes, followed by a respective rest period without concurrent TMS. For sufficiently short TRs (e.g., a TR of 1 s resulting in a max. TMS frequency of 1 Hz), the resulting superposition of BOLD responses provides a strong contrast between stimulation and rest periods (Bohning et al., 2003b; Navarro de Lara et al., 2017). Slice packaging also allows faster TMS frequencies at the cost of longer TRs and lower fMRI sampling rate (Fig. 1D). As an extreme case, Bestmann et al. (2004) applied TMS at 3.125 Hz, delivering TMS pulses after every other slice (i.e., every 320 ms) throughout an MR volume of 20 slices with a TR = 3320 ms, but principally TMS pulses and slices can also be continuously interleaved in an alternating fashion (Fig. 1E). For event-related designs, when targeting only gaps between volumes, stimulus onset asynchrony (SOA) cannot be randomly jittered, but has to be a multiple of the TR, and the BOLD response is thus always sampled at the same time points (a multiple of the TR) relative to the TMS pulse. This is problematic for longer TRs, but with multiband parallel imaging full brain coverage with ~60 slices per volume is easily possible with 1 s TR, nonetheless allowing a sufficiently dense sampling of the BOLD response. This procedure works fine for single-pulse TMS or short high-frequency bursts (e.g., 3 pulses at 40 Hz = 50 ms + ~50 ms safety interval = 100 ms). However, longer burst durations (e.g., 5 pulses at 5 Hz = 800 ms + ~50 ms safety interval = 850 ms) would increase the TR and significantly reduce the total number of volumes acquired. One solution for the latter case is to simply apply TMS during image acquisition and thus to sacrifice some slices or even the entire volume (Fig. 1F). In fact, the distorted volume can later be interpolated from neighboring volumes in the time series after spatial realignment to simplify subsequent fMRI analysis. For short TRs little information is lost, as the first second after an event is not crucial for robustly fitting a hemodynamic response function (HRF) to the BOLD response. For example, Bestmann et al. (2008c) applied 5 pulses at 11 Hz (i.e., a ~364 ms burst) with a TR of 1.8 s, thus sacrificing five successive slices in that volume (but different slices on each repetition). However, also in this approach TMS pulses should not be delivered in close temporal proximity to the RF excitation pulses to avoid disturbance of the steady-state longitudinal magnetization and resulting spin-history effects, which will be synchronized to the stimulation. Another, more sophisticated, option is to split the volume into multiple packages of slices with interleaved gaps of sufficient length and to apply TMS during a volume but yet in between slices. The advantage is that no volumes are lost and artifact-free images can continuously be obtained throughout longer bursts or even entire trains of repetitive TMS spanning multiple volumes in a row. On the downside, the TR is increased and fewer volumes can be acquired in total. Moreover, the different EPI sequences required for different stimulation parameters may not have the same sensitivity, complicating a direct comparison. For example, Jung et al. realized a 1 Hz repetition rate of TMS by splitting a volume with 2000 ms TR into two slice packets of 800 ms each and a 200 ms gap in between and applied TMS pulses 50 ms after each package (Jung et al., 2016, 2020). Hermiller et al. (2020) even orchestrated slice packages in a way to administer a standard intermittent theta burst stimulation (iTBS) protocol (i.e., 50 Hz triplets repeated at 5 Hz in trains of 2 s repeated every 10 s) during continuous fMRI acquisition as well as a respective 12.5 Hz "beta-burst" protocol as a frequency control. Finally, fMRI acquisition could in principle also be done in an event-triggered fashion, for which the occurrence of an event of interest (here the TMS pulse or burst) releases the acquisition of multiple volumes to exclusively assess the post-event BOLD signal (Fig. 1G). This approach would be maximally flexible, and principally even allow brain state-dependent (e.g., EEG-triggered) stimulation (Bergmann, 2018; Bergmann et al., 2016). However, the loss of steady-state longitudinal magnetization (achieved via continuous RF excitations and commonly guaranteed via dummy cycles already for the first acquired image) leading to spin-history effects, the psychological effects for the participant (loss of habituation, startle response, etc.), and the incompatibility with standard GLM analyses methods (requiring continuous time series) are disadvantages of this approach. In summary, different options of timing EPI acquisition and TMS are available, and one has to balance their pros and cons when designing a TMS-fMRI study, tweaking the timing to the scientific question.

2.4. Other functional measures

Beyond BOLD-fMRI using event-related or blocked EPI sequences, also arterial spin labeling (ASL) techniques have been used in combination with TMS to quantify TMS-related changes in regional cerebral blood flow (rCBF). Moisa et al. (2010), for example, used continuous ASL (CASL) to demonstrate TMS-evoked increases of perfusion in M1, which linearly increased with stimulation intensity for 2 Hz rTMS as well as with the number of 10 Hz trains per measurement block. In another study, they used CASL to map the effects of TMS at different intensities to the dorsal premotor cortex (dPMC) during a finger movement task (Moisa et al., 2012). For concurrent TMS-CASL, tagging pulses to label inflowing blood were applied via a separate RF-coil placed at the subject's neck followed by EPI readouts via a one-channel head coil. TMS pulses were applied during the tag delay, i.e., 100 ms before EPI readout or directly after EPI readout and before the next tagging pulse Moisa et al. (2010). CASL complements BOLD-fMRI by providing direct quantitative measures of perfusion, allowing the comparison of absolute values between sessions (e.g., in pre-post designs) and to control for the confounding effect of baseline perfusion changes in BOLD measures (e.g., after drug intake). TMS-CASL thus provides the possibility for assessing and contrasting both immediate online and subsequent offline of (r)TMS.

Another functional imaging technique, which can be concurrently combined with TMS and allows the assessment of rCBF, is positron emission tomography (PET). A review of TMS-PET studies would exceed the scope of this paper, and we will thus limit ourselves to highlighting a few illustrative examples. While PET is exposing the subject to radiation and therefore used conservatively in healthy participants, and even though its temporal resolution is rather limited as compared to BOLD fMRI or CASL, PET played an important role in the earlier times of combined TMS and neuroimaging. Its versatility and its ability to noninvasively assess brain metabolites and neurotransmitter systems render it now as before an important technique for studying the neuronal effects of TMS. In the first study of its kind Paus et al. (1997) used $H_2{}^{15}O$ PET concurrently with TMS and found the number of TMS pulses applied to the left frontal eye field (FEF) to correlate with rCBF not only locally in the FEF, but also remotely in connected visual and parietal regions. Later it was also shown that rCBF also increases in M1 during subthreshold rTMS, linearly scaling with stimulation frequency from 1 to 5 Hz (Siebner et al., 2001) and outlasting the stimulation period (Takano et al., 2004). Also 18-fluoro-2-deoxy-d-glucose (18FDG) PET has been used to measure glucose metabolism during 2 Hz rTMS, demonstrating for the first time an TMS click sound induced activation of the primary auditory cortex (Siebner et al., 1999b). While also ^{11}C raclopride PET has been used to show extracellular dopamine concentration in the caudate nucleus following 10 Hz rTMS (Strafella et al., 2001), no concurrent PET-TMS studies have been conducted with these kind of ligands up to date.

2.5. Future technical developments

The technical developments supporting the use of concurrent TMS-fMRI have not yet plateaued, and several constraints and limitations need to be overcome to unlock the full potential of the technique. Firstly, coil mounting and navigation needs to be facilitated. Available coil holders have been optimized to operate under the constraints of a birdcage head coil (Bohning et al., 2003a; Moisa et al., 2009), but do not take

advantage of the fundamentally increased spatial degrees of freedom achievable with modern coil RF-arrays mounted directly to the TMS coil (Navarro de Lara et al., 2017; Navarro de Lara et al., 2015), and currently a large percentage of the precious experimental time is spent on practical hassles of precise coil positioning. However, coil holders also need to be extremely stable to reduce vibration-related artifacts, which imposes certain constraints on their design. Secondly, the coil position needs to be monitored and maintained continuously, which is now possible by the use of frameless stereotactic neuronavigation while the participant is inside the bore. Providing real-time feedback of deviations from the target coil position, may allow the subject to self-correct their head-position accordingly (Woletz et al., 2020). Alternatively, future developments may involve MR-compatible actuators to remotely steer the coil position. This would not only compensate for small head movements, but also facilitate the mapping of multiple adjacent target sites within the same run or even implement automated hotspot hunting procedures when using real-time fMRI derived BOLD-responses as immediate feedback. Thirdly, the design of MR-compatible TMS-coils needs to be improved, to allow higher effective stimulation intensities, as currently the long cables and additional distance in case of sandwiched RF-coil arrays considerably reduce stimulation efficacy, and often participants need to be excluded because their high motor thresholds do not allow effective stimulation. The development of novel multi-coil setups (Koponen et al., 2018; Navarro de Lara et al., 2020) may solve this issue together with providing steerability of the E-field without a need to move the coil. And finally, more established TMS protocols need to be translated into the concurrent TMS-fMRI context. So far, neither single-coil paired-pulse nor dual-coil TMS protocols have been used with concurrent fMRI. They would provide insights into the intra- as well as inter-cortical circuits underlying local and remote BOLD-response to TMS. The ability to use two TMS coils simultaneously would also allow the intermingling of multiple targets as well as active and sham conditions within the same session.

3. Insights to be gained from concurrent TMS-fMRI

The “costs” imposed by the technical challenges of the concurrent combination of TMS and fMRI are more than outweighed by its scientific “benefits”. This section summarizes which scientific questions can be tackled with combined TMS-fMRI.

3.1. Mapping neuronal excitability and effective connectivity

TMS can be used to quantify neuronal excitability as the immediate response of the targeted brain circuit to its perturbation (Bergmann et al., 2016). Changes in the response amplitude for a fixed stimulation intensity reflect variations in the excitability of the involved neuron populations. For M1 and visual cortex, MEP amplitudes and phosphene perception provide well established read-outs, but for most other brain regions the regional responsiveness to TMS must be assessed via neuroimaging techniques. Following the same rationale as for MEPs, one could argue that with increasing excitability of the stimulated neurons, the same E-field would drive more neurons beyond their firing threshold, thus also resulting in more trans- and postsynaptic activity in intra-cortical circuits, larger energy consumption, and – thanks to neurovascular coupling – eventually in larger BOLD-responses. While in principle, the immediate BOLD response to TMS may thus be used as an index of cortical excitability, the situation is more complicated compared to the MEP. The main difference is that the MEP is a highly specific measure of the integrated net excitability of the corticomotor pathway (i.e., pyramidal corticospinal output neurons in M1 and spinal motoneurons). Although the MEP is modulated by the regional excitation-inhibition balance at the cortical and spinal level, the MEP amplitude is proportional to the number of corticospinal output neurons that are driven beyond firing threshold by the TMS pulse. The local BOLD response in M1 is rather driven by local peri- and postsynaptic processes in both inhibitory and excitatory local intra-cortical circuits (Logothetis, 2008) and thus not proportional to the neuronal output of the target region. The analogy between the TMS-evoked BOLD and MEP response is more appropriate, when considering remote BOLD responses arising in connected brain regions, which do eventually rely on the firing of local output neurons in the targeted cortex and may thus serve as an index of their excitability. Importantly, just like the MEP also depends on spinal excitability, remote BOLD responses are additionally influenced by the excitability of the receiving remote neurons, so that both measures are technically reflecting the excitability or responsiveness of entire networks, rather than single brain regions or neuron populations. Therefore, despite the discussed caveats and the need for cautious interpretation, both local and remote BOLD responses to TMS can thus provide valuable information about neural responsiveness and network excitability of non-motor circuits.

TMS does not only cause locally confined activations in the immediate intra-cortical circuits receiving suprathreshold E-field strengths, but the locally elicited neural activation spreads via cortico-cortical and other corticofugal projections and their synaptic connections to neighboring and distant parts of the brain. This spread of activation in the network may complicate the causal inference derived from TMS interference paradigms in cognitive neuroscience (Bergmann and Hartwigsen, 2021). Yet this spread of excitation within the stimulated brain network is not a shortcoming of TMS but reflects an inherent and defining feature of the brain that no single brain region can be manipulated in isolation. Therefore, the spread of excitation from the primary cortical target region along pre-existing neuronal connections constitutes an interesting property of TMS that opens several exciting avenues for causal brain mapping. This becomes immediately obvious when considering MEP and muscle twitch, observable at distant muscles following suprathreshold TMS of M1. The initial TMS-induced depolarization of axonal fibers in the targeted cortex results in a transsynaptic excitation of large corticospinal motor neurons. The orthodromic spread of excitation via the large corticospinal motor neurons and spinal motoneurons to the muscle causes the MEP, involving at least three synapses (Di Lazzaro et al., 2008). While the assessment of MEPs following single-pulse TMS of M1 is usually taken as measure of corticospinal excitability, it is also a measure of effective connectivity of the stimulated corticomotor projections. Likewise, dual-coil paired-pulse protocols, with a test-pulse applied to M1 (evoking an MEP) and a preceding (often subthreshold) conditioning pulse applied to a distant but connected brain region, such as premotor, supplementary motor, parietal cortex, or cerebellum (modulating that MEP) have repeatedly demonstrated that TMS-evoked action potentials also spread via long-range cortico-cortical projections (Koch, 2020; Lafleur et al., 2016). Such M1-centered dual-coil approaches allow researchers to assess cortical excitability and effective connectivity for the many cortico-cortical pathways converging on the motor cortex.

For cortical targets outside the extended motor system, however, TMS combined with neuroimaging can help establish effective connectivity. While measures of functional connectivity can be derived from observational fMRI data alone, they eventually rely in one form or the other on the correlation of BOLD time series between brain regions, and sophisticated methods have been invented in an attempt to infer causal influences from these data (Friston, 2011; Reid et al., 2019). In contrast, concurrent TMS-fMRI attempts to solve this problem with the so-called “perturb-and-measure” approach, that is by experimentally manipulating neuronal activity in a superficial target region via the magnetically induced E-field, while measuring directional effective connectivity originating from the target region via the evoked BOLD-responses throughout the entire brain (Fig. 2A). By now, many concurrent TMS-fMRI studies have indeed corroborated the spread of TMS-evoked activation in the brain at rest, which enables the mapping of causal inter-regional influences (for reviews see Bestmann and Feredoes, 2013; Bestmann et al., 2008a; Driver et al., 2010; Hallett et al., 2017; Reithler et al., 2011; Siebner et al., 2009). In principle, also dedicated fMRI connectivity anal-

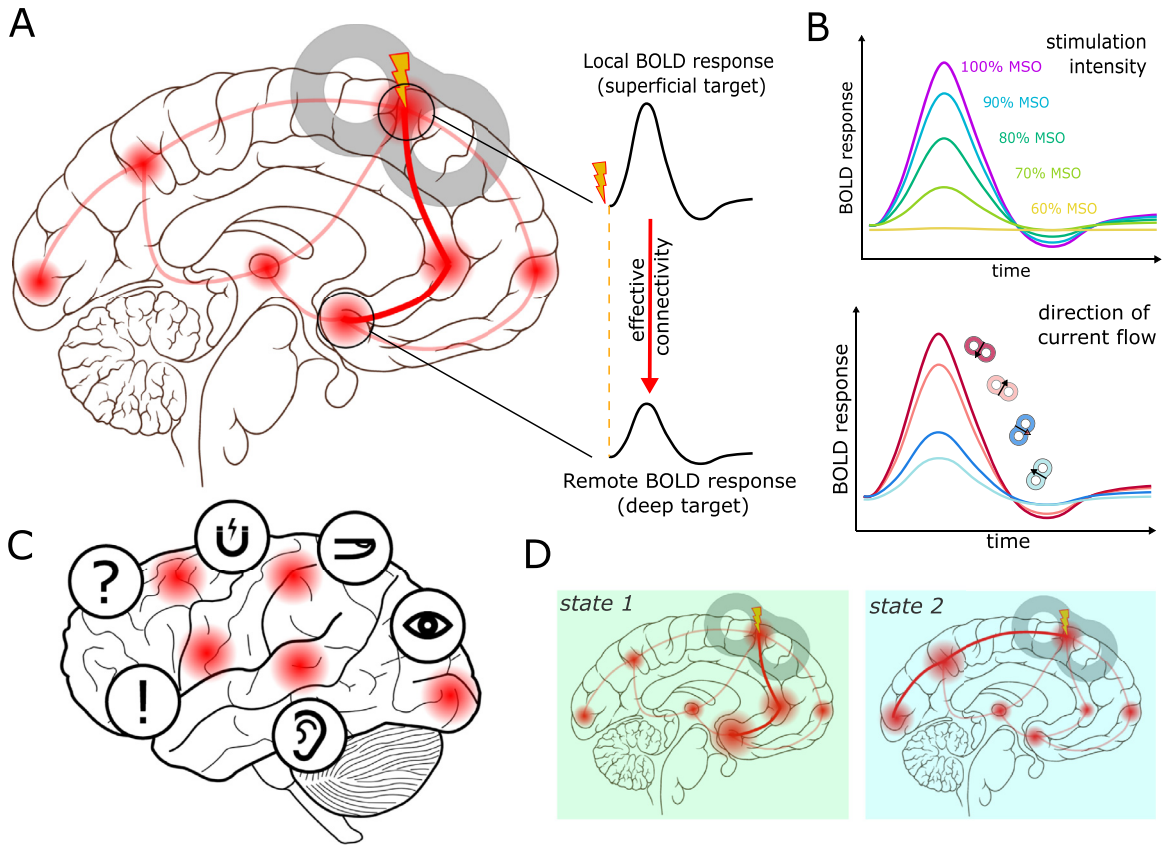

Fig. 2. Principles of TMS-fMRI research. **(A)** Schematic representation of TMS-evoked BOLD activity maps including local (directly stimulated) and remote brain regions (indirectly stimulated via network connections), providing proof of target engagement (section 3.2) as well as measures of neuronal excitability and effective connectivity between brain regions (section 3.1). **(B)** Schematic representation of TMS-evoked BOLD response amplitude as a function of stimulation intensity (left) or direction of current flow (right) for the optimization of stimulation parameters (section 3.3); note that these relationships may be non-linear in both cases. **(C)** Schematic representation of TMS-locked BOLD-responses unrelated to the local BOLD-response at the target site but caused by magnetic artifacts (section 4.1) peripheral co-stimulation (auditory cortex due to TMS click, sensory cortex due to cranial nerve stimulation and afferent feedback from muscle twitches, visual cortex due to eye blinks; section 4.2), orientation responses to the stimulation, or stimulation related expectations. **(D)** State-dependent activation maps with different (sub)networks being preferably activated depending on the current state of the brain at the time of stimulation (section 3.4).

yses can be conducted based on TMS-fMRI datasets, e.g., using the superficial TMS target site as seed region for functional connectivity metrics or dynamic causal modelling (DCM) to explicitly model TMS as external perturbation and evaluate the resulting changes in effective connectivity within the model system of interest (Bestmann et al., 2008b). The potential of such techniques has, however, hardly been exploited so far in combination with concurrent TMS-fMRI. Li et al. (2011) provide one of the rare examples, where DCM was used to investigate pharmacological effects on the circuit-specific effective connectivity between the TMS target region (either M1 or dlPFC) and connected structures of the respective networks. They found both lamotrigine and valproic acid to inhibit effective connectivity in motor circuits, but only lamotrigine to increase effective connectivity in prefrontal circuits.

Even though the attribution of cause and effect is much less ambiguous compared to merely observational data, a number of confounds have to be considered when inferring causality from TMS studies as well (Bergmann and Hartwigsen, 2021), such as the unintended co-activation of non-target brain regions either by direct co-stimulation of neighboring regions via an extended E-field or the associated auditory and somatosensory peripheral co-stimulation (section 4.2). Therefore, not any remote BOLD response time-locked to TMS can unambiguously be interpreted as the result of effective connectivity with the stimulation site, and specific control conditions are required to disambiguate these responses (section 4.3). Moreover, we know from invasive electrical stimulation studies in animals that electrical depolarization of axonal fibers also results in an antidromic spread of action potentials, which causes a retrograde trans-synaptic activation of brain regions upstream to the stimulation site via axon collaterals (Edgley et al., 1990). One may further argue that the effective connectivity estimated from TMS-evoked BOLD-response should additionally be constraint by structural connectivity, i.e., a priori knowledge about the existing anatomical connections. However, while the structural connectome undoubtably provides a solid framework for any functional interaction of brain regions, TMS-evoked activity can travel long distances via multiple synapses. While it is reasonable to assume that areas that are directly connected with the target region will show the strongest remote effects, we are cautioning against the a-priori exclusion of brain regions simply based on their structural proximity or the number of synapses that need to be overcome.

Remote activations in response to TMS of M1 have been revealed early on for regions of the extended motor network, including contralateral M1 as well as bilateral premotor cortex and supplementary motor areas (Baudewig et al., 2001; Bestmann et al., 2003b; Bohning et al., 1999; Bohning et al., 2000b; Hanakawa et al., 2009; Shitara et al., 2011). Also for the visual system, long-range top-down connections from the dorsal attention network, i.e., frontal eye field (FEF) and intra-parietal sulcus (IPS), have successfully been mapped using TMS-fMRI (Ruff et al., 2008; Ruff et al., 2006; Ruff et al., 2009a). TMS of the right FEF, for example, revealed an intensity-dependent modulation of retinotopic visual areas that, in line with the function of FEF in saccade control, increased

BOLD responses for peripheral but decreased them for foveal representations (Ruff et al., 2006). Importantly, as Ruff et al. (2009b) pointed out, the topographical specificity of TMS-evoked remote effects and their dependency on the initially targeted entry node even within the same network, indicates that TMS-evoked brain activity spreads via topographically specific anatomical tracts instead of diffusely spreading throughout the brain or network. Yet another set of studies, mapped the remote activations for TMS of the different subregions of the prefrontal cortex (PFC), a region considered highly relevant for therapeutic approaches based on its manifold connections to the deep brain structures of the basal ganglia and limbic system. Hanlon et al. (2013), for example mapped the connectivity of dlPFC (F3) vs. vmPFC (FP1) targets, with general remote effects in thalamus and striatum, but stronger effects on the ventral caudate nucleus for ventromedial TMS and in the hippocampus and dorsal caudate nucleus for dorsolateral TMS. In therapeutic settings, applying rTMS in treatment-resistant MDD, the left dlPFC is often stimulated 5 cm anterior to the M1 hotspot. Using this targeting approach, Vink et al. (2018) found remote activations in other connected prefrontal and cingulate regions, including in some participants also the sgACC, a region which is considered to be a key target region for MDD treatment with DBS (Hamani et al., 2011; Holtzheimer and Mayberg, 2011). However, inter-individual variability needs to be taken into account, and a direct comparison of resting-state functional connectivity and TMS-fMRI effective connectivity maps for the stimulation target (midpoint of F3 and F5) resulted in a good overlap on the group level but substantial variability across individuals (Hawco et al., 2018). The mapping of effective connectivity via TMS-fMRI therefore not only helps to understand functional brain networks in the healthy brain but may also improve the personalized targeting of therapeutic TMS approaches (section 5).

3.2. Proof of target engagement for local and remote regions

How do we know whether TMS has effectively stimulated the desired brain region? When targeting M1, the peripheral MEP provides direct proof that the corticospinal output neurons in the primary motor cortex must have at least indirectly been stimulated. Likewise, phosphene perception provides some immediate, even though subjectively reported, evidence for successful excitation of the early visual cortex. But for most other brain regions, either the behavioral consequences of TMS-induced interference with cognitive performance have to be taken as indirect evidence (Bergmann and Hartwigsen, 2021), or neuroimaging is required to demonstrate stimulation-related brain activity as immediate brain response (online) or as after-effect of an excitability modulating protocol (offline) (Bergmann et al., 2016). Since offline TMS effects are subject to considerable inter-individual variability, may also result from rapid network reorganization, and are directionally ambiguous (Hartwigsen, 2018), the immediate stimulation-induced brain response is a more direct proof of target engagement. A successful proof of immediate target engagement does not only retrospectively corroborate causal interpretations of the relation between regional brain activity and cognitive function (Bergmann and Hartwigsen, 2021), but can also be used prospectively to adjust and optimize stimulation parameters before conducting a TMS study (section 3.3).

The immediate BOLD response to TMS can prove functional engagement of the cortical patch that is directly stimulated by the induced electrical field. For the primary target of TMS, a local activation cluster in the cortical crown close to the center of the figure-of-eight coil would be expected. Such local activations in the primary target site have been reported by many studies, while others failed to reveal any activation in close proximity to the stimulation target (see Table 1 for an overview). For TMS of the sensorimotor cortex, local activations in the left M1 have only been found for suprathreshold TMS, while subthreshold TMS only caused remote activations in the motor network but not in the targeted M1 itself (Baudewig et al., 2001; Bestmann et al., 2003b, 2004, 2005; Bohning et al., 2000b; Denslow et al., 2005b), suggesting that local activation of the stimulated M1 was exclusively due to afferent feedback from the evoked peripheral muscle twitches. While Hanakawa et al. (2009) and Shitara et al. (2011) confirmed the particular activation of the stimulated M1 by supra- but not subthreshold TMS, these studies also assessed the BOLD response to electrical median nerve stimulation at the wrist, evoking either only sensory or also motor responses. Contrasting these with the suprathreshold TMS condition suggested that there is a TMS-related BOLD response in M1 that cannot be explained by reafferent feedback alone (Shitara et al., 2013). However, to fully disentangle the immediate and re-afferent effects on the M1 BOLD signal, the latter would need to be blocked experimentally. Notably, stimulation intensities above the motor threshold were also required to observe local activations in target regions not eliciting motor responses, such as the dorsal premotor cortex (Bestmann et al., 2005), pointing towards a more general dependency of local activations on stimulation intensity. On the other hand, it is possible for TMS to clearly evoke neuronal activity and associated conscious perception, e.g., a phosphene for V1 stimulation, without a corresponding BOLD signal being detectable on the single subject level (de Graaf et al., 2018).

Which factors determine whether or not focal TMS produces a regional change in BOLD signal in the directly stimulated patch of cortex? Several considerations are relevant and may account for a lack of local activation in the primary network target directly below the TMS coil. Firstly, the activation may be present but not where it is expected, because the coil position has not been validated by neuronavigation or fiducials and moved relative to the subject during the scanning session. Without realistic E-field simulations, it also remains unknown at which cortical location relative to the center of the TMS coil the largest stimulation effects should actually be expected (Gomez et al., 2020). As a rule of thumb, it can be stated that TMS always produces the strongest E-fields in the crown and not in the wall or fundus of the targeted cortical gyri and preferential targeting of “deep” locations is impossible without concurrent and more prominent stimulation of more superficial structures that are closer to the stimulation coil (see below for a more detailed discussion). Secondly, the stimulation might have failed to evoke neuronal activity in the target region because stimulation intensity or coil position/orientation were not appropriate. Given the difficulty to adjust stimulation intensities and coil orientation for non-motor/-visual regions, the induced E-field in the brain tissue may not have been sufficient for evoking neuronal activity in the cortex, rendering this a true negative finding. However, if the lack of local activation is accompanied nonetheless by plausible remote effects in the targeted network, a false negative activation is the more likely explanation. Thirdly, there may have been TMS-evoked neuronal activation but no neurovascular effect and thus no blood oxygenation changes. This may be the case when TMS-induced depolarization of neuronal membranes has evoked mainly action potential firing as output of the cortex below the coil, while the resulting postsynaptic potentials and the associated local field potential are rather found in connected regions receiving input from the stimulated site. Since BOLD-fMRI is mainly sensitive for the latter but not the former (Logothetis, 2002; Logothetis, 2008), the excitation of the directly stimulated regions may not be visible to fMRI. However, it is believed that TMS usually activates a cascade of intra-cortical circuits, only transsynaptically exciting cortico-cortical or cortico-spinal (in M1) output neurons (Di Lazzaro et al., 2008), therefore providing plenty of opportunities for peri- and post-synaptic activity and associated BOLD responses in the stimulated cortex. An important issue to consider here is that TMS-evoked neuronal firing is usually followed by an even longer lasting suppression of neuronal activity (Moliadze et al., 2003), which may compensate for the metabolic needs associated with the initial excitation, and the complex relationship between the TMS-induced shift in excitation-inhibition balance and the resulting BOLD response (Logothetis, 2008) may lead to a lack of neurovascular response. Electrophysiological recordings of single-pulse TMS evoked neuronal firing in monkeys suggest highly focal effects, albeit the recording window

could not capture the initial neuronal response before 10 ms post-TMS due to stimulation artifacts (Romero et al., 2019). This, nonetheless, raises the possibility that some TMS-evoked neural effects may be very focal and TMS may induce opposing effects in the BOLD signal in multiple spots within a voxel which may cancel each other out at the voxel level. A mixture of neuronal effects at the micro-millimeter level may not lead to a measurable BOLD response, because they are below the typical spatial resolution and sensitivity of fMRI sequences at 3T, even though previous work in monkeys combining fMRI and single-cell recordings did show that also very small clusters of active neurons can be associated with pronounced fMRI signals (Van Dromme et al., 2015). Fourthly, it is conceivable that the BOLD-response resulting from such a comparably artificial stimulus is not well explained by the typical shape and timing of the canonical hemodynamic response function (HRF). This may contribute to the higher sensitivity of block designs to detect TMS-evoked BOLD-signal changes compared to event-related designs. An atypical shape and timing of the HRF in the directly targeted brain region may partially explain why the indirect remote activations (with thus more physiological HRFs) are more likely to be detected by BOLD fMRI. It is also unclear whether only positive or also negative BOLD-responses should be expected in response to TMS given its complex effects on intra- and intercortical excitatory and inhibitory circuits (Di Lazzaro et al., 2008), the de-/synchronization of brain activity, which may again express opposite relations with the BOLD-signal (Scheeringa et al., 2011), and the complex relationship between neuronal excitation-inhibition balance and the BOLD signal (Logothetis, 2008). Finally, the remaining possibility is a lack of sensitivity or signal-to-noise ratio (SNR) to pick up the respective BOLD signal changes. This may be due to inhomogeneity artifacts resulting from the presence of the TMS coil in between brain and RF-coil of the MR, noise from TMS-related coil-vibration of subject movement, low trial numbers or less power full fMRI designs and thus insufficient statistical power, or other factors. In fact, novel ultrathin RF-coil arrays placed between TMS coil and head have been reported to improve the SNR for cortical activations directly under the coil by a factor of five (Navarro de Lara et al., 2017), while the SNR at deeper brain regions is naturally limited for surface coil arrays with small diameters. On the other hand, also false positive activations need to be considered. While less likely in case of a circumscribed and anatomically plausible activation directly under the coil, it is possible that the targeted area is also activated by peripheral co-stimulation (section 4.2) or that spurious BOLD signal changes due to TMS-related artifacts from coil vibration or subject movement are mistaken for a truly transcranial stimulation effect section 4.1).

Depending on the field-of-view covered by fMRI, the immediate BOLD response to TMS can also confirm successful functional engagement of remote brain areas that are indirectly activated by TMS via cortico-cortical or cortico-subcortical pathways. For these secondary network targets, a respective BOLD-response time-locked to the TMS pulse can only be considered proof of indirect engagement via the respective anatomical connections, if an indirect activation via co-stimulated sensory pathways or other TMS-related cognitive or behavioral events or artifacts can be excluded. Activations in areas involved in the processing of auditory or somatosensory stimuli, or orientation responses to infrequent stimuli (such as TMS pulses or bursts in a slow event-related design) but also arousal related effects on regional brain activity need to be considered as alternative explanation for remote BOLD-responses associated with TMS.

The possibility to obtain proof of remote target engagement via concurrent TMS-fMRI can facilitate and validate approaches that aim to primarily target deep brain structures transsynaptically via network connections. Such deep targets are otherwise inaccessible to TMS, which can reach only superficial cortical targets, preferably those located in the crown of cortical gyri (Bungert et al., 2017), and becomes unsafe at field strengths theoretically able to excite targets deeper than ~4 cm scalp-cortex distance (Deng et al., 2014). Therefore, many deeper cortical and all subcortical targets are out of reach. Simply increasing the effective E-field in deep targets by larger coils and higher stimulation intensities is not a viable solution, as it inevitably comes with reduced spatial precision and causes unsafe intensities in superficial structures when reaching targets at ~6 cm depth (Deng et al., 2014). Here, indirect connectivity-informed TMS of deep targets is a safe and promising alternative. For this approach, a primary superficial target is typically determined as entry point for the deep target or network perturbation based on fMRI functional connectivity analyses. The specific procedures differ largely, depending on whether (i) the seed is defined as single voxel, region of interest, or entire network, (ii) resting-state or task-related functional connectivity is assessed, (iii) the methods aim for estimating undirected or directed connectivity, (iv) global signal regression is employed (Murphy and Fox, 2017) and maximum correlation or anticorrelation values are determined, and whether (v) they are based on group data (incl. large publicly available connectome cohorts), individual recordings, or a mixture of both (Cash et al., 2020; Cash et al., 2019; Drysdale et al., 2017; Siddiqi et al., 2020; Weigand et al., 2018). However, eventually, any such approach lacks the ultimate proof that TMS-related neuronal activation has actually reached the remote target, even though behavioral effects or therapeutic success may suggest it did, and concurrent TMS-fMRI is required to verify this assumption.

The sgACC constitutes a clinically relevant deep target for therapeutic rTMS interventions, because its activity is altered in major depressive disorder (MDD) (Hamani et al., 2011), and the sgACC has been used as target for deep brain stimulation (Holtzheimer and Mayberg, 2011). There is indeed accumulating evidence that facilitatory rTMS of specific coordinates in the left dlPFC can ameliorate MDD symptoms (Lefaucheur et al., 2019; Lefaucheur et al., 2014), that treatment success strongly depends on the proximity of the stimulated MDD coordinates to the coordinates of maximal anti-correlation with the sgACC (Cash et al., 2019; Fox et al., 2013; Weigand et al., 2018), and that the target network is actually affected by such an rTMS treatment, even when applied in healthy subjects (Tik et al., 2017). Importantly, there is now also preliminary evidence from concurrent TMS-fMRI that TMS of the dlPFC at specific coordinates can produce an immediate BOLD-response in the sgACC (Oathes et al., 2021; Tik et al., 2020; Vink et al., 2018); see section 5 for a more detailed discussion of rTMS and TMS-fMRI in MDD. Another example is the targeting of an adjacent part of the ventromedial prefrontal cortex (vmPFC), involved in the extinction of fear memory and its consolidation (Gerlicher et al., 2018). Raij et al. (2018) used psycho-physiological interaction (PPI) analysis (Friston et al., 1997) to determine the maximally positive correlation with the vmPFC target coordinate during an extinction learning task from an independent group sample to identify the group coordinate in the superficial frontal cortex that would relate to successful fear extinction and then stimulated that coordinate (de-normalized to individual native space) in a separate study. While brief 20 Hz TMS bursts during extinction learning successfully augmented extinction memory, a proof of actual vmPFC target engagement based on concurrent TMS-fMRI is still lacking. Also the hippocampus and its connectivity with connected brain regions has successfully been targeted with rTMS to improve memory performance (Freedberg et al., 2019; Hermiller et al., 2019; Wang et al., 2014; Warren et al., 2019). The maximal positive correlation with the hippocampal network has been identified within the posterior parietal cortex based on each individual subject's resting-state fMRI scan to guide subsequent rTMS interventions (Hebscher and Voss, 2020). A recent well-controlled concurrent TMS-fMRI study showed indeed that short theta (but not beta frequency) bursts delivered to this specific coordinate (but not an out-of-network control coordinate) caused immediate increases in hippocampal activity during memory encoding (but not a numerical control task) and subsequently improved memory recollection (Hermiller et al., 2020). Together, these examples show that consensus is currently lacking as to how superficial target sites should be determined based on functional connectivity data. Here, concurrent

TMS-fMRI provides a viable means to validate and compare such approaches.

3.3. Systematic evaluation and optimization of stimulation parameters

For any TMS study it is important to exactly localize the superficial cortical region to directly target with TMS, regardless of whether it is the primary target of interest or merely serves as superficial entry point for connectivity-based indirect stimulation of a deep target of interest. However, the planning and personalization of TMS has to go beyond mere target localization, since other stimulation parameters, such as stimulation intensity, frequency, and coil orientation (i.e., direction of current flow in the brain tissue) have a major impact on the immediate response of the brain to the stimulation. Accordingly, TMS-evoked BOLD responses (and their underlying neuronal activations) may systematically differ as a function of these parameters, and whether or not positive proof of target engagement can be established via concurrent TMS-fMRI may depend on choices that are often not more than an educated guess if not based on systematic investigations (Fig. 2B). Notably, there may not only be effective vs. ineffective stimulation parameters, but rather continuous (though likely non-linear) quantitative changes as well as certain qualitative differences, when intensity, frequency, and orientation are varied.

The maybe most obvious parameter is stimulation intensity. MEPs can only be observed in the peripheral EMG following corticospinal spread of activity, if a certain TMS intensity is reached at the resting motor cortex, termed the resting motor threshold (RMT). However, already at much lower intensities certain intra-cortical and cortico-cortical connections are activated. This is not only evident from paired-pulse TMS protocols such as the short-interval intracortical inhibition (SICI), which demonstrates marked effects of conditioning intensities as low as 60 % RMT on GABA-ergic interneurons (Kujirai et al., 1993). Also concurrent TMS-fMRI has shown activation in remote regions of the extended motor network following subthreshold stimulation (90 % active motor threshold, AMT) of M1 in the absence of MEPs (Bestmann et al., 2003b). These examples raise a note of caution when using subthreshold stimuli above 50% of RMT as control conditions in concurrent TMS-fMRI studies targeting M1 (section 4.3). Given that RMT cannot be determined outside M1, and given the lack of correlation between RMT and indices of excitability for other cortical regions such as the phosphene threshold (Stewart et al., 2001), an adjustment of stimulation intensity to RMT (even if adjusted to scalp-cortex distance (Stokes et al., 2005)) appears problematic for non-motor regions. This highlights the need for a systematic evaluation of dose-response relationships using concurrent TMS-fMRI. While many studies have used sub- vs suprathreshold intensities in M1, so far only few studies have measured dose-response curves, with a larger number of intensities. Hanakawa et al. (2009), for example, measured BOLD-responses for single-pulse TMS-intensities from 30 to 100 % of MSO and reported significant BOLD responses in M1 only for intensities roughly exceeding the individual RMT. Also Navarro de Lara et al. (2017) reported increasing BOLD response amplitudes when varying the intensities of 1 Hz TMS trains of M1 (i.e., 80, 90, 100, 110 % AMT), only significant for 100% AMT and higher. However, the relationship between TMS intensity and the increase in MEP amplitude and motorcortical BOLD-response remains to be characterized while controlling for MEP-related afferent feedback. Outside M1, only Dowdle et al. (2018) have systematically varied intensity for stimulation at position F3 from 90 to 120 %, but did not observe a significant dose effect (possibly owed to the limited number of stimuli and associated lack of statistical power). Future studies need to establish well-powered dose-response curves for a larger range of intensities and regions, since those curves may be nonlinear and region-specific. Notably, while remote effects have been reported for subthreshold intensities (Bestmann et al., 2003b), the stimulation intensity required for a BOLD response in a specific remote region may diverge from that of the superficial target and depend on several factors, such as the particular thresholds for the superficial target's output neurons and the deep target's receiving input neurons. Thus, individual dose-response curves need to be established for each region of interest.

The second well established parameter is coil orientation, more precisely the direction of current flow in the brain tissue. While its massive impact on MEP threshold and amplitude is long known (Mills et al., 1992), no fixed standards have been established for non-motor regions, and many studies simply stick to previously published orientations (from M1 or other regions) without readjusting them to local/individual gyral anatomy. Realistic E-field modelling has suggested a current flow orthogonal to the target gyrus of interest to be a good heuristic (Thielscher et al., 2011), but it remains to be established how E-field distributions actually translate into spatial brain activity patterns. In fact, concurrent TMS-fMRI could provide a valuable means to validate E-field simulations, by investigating the spatial overlap between the maximal E-field and the location of the TMS-evoked BOLD response. But even without modelling, by systematically varying TMS coil orientation and monitoring the TMS-evoked BOLD response in the target region, coil orientation may be optimized empirically to engage a specific superficial cortical target. Given that different directions of current flow may maximally excite different neuronal subpopulations with different connectivity profiles within a region, also the compilation of remote effects may change. Jung et al. (2016) compared 0° and 180° orientations for vertex stimulation, and found different patterns of distributed deactivation, even though only biphasic stimuli are used for concurrent TMS-fMRI and opposite coil directions should be expected to have limited effects, whereas rotations by 90° should cause maximal differences. However, so far, no concurrent TMS-fMRI study has systematically investigated multiple step-wise coil rotations.

The third key parameter is stimulation frequency. On the one hand, the mere temporal summation of TMS-evoked neuronal activations may already be reflected by a respective increase in BOLD response amplitude, which is why the majority of concurrent TMS-fMRI studies have used trains of TMS pulses in fMRI block designs (e.g., Bestmann et al., 2004; Bohning et al., 1998; Leitao et al., 2012; Li et al., 2004a; Moisa et al., 2009; Navarro de Lara et al., 2017; Tik et al., 2017), but also short TMS bursts in fMRI event-related designs (Bestmann et al., 2008c; Leitao et al., 2015; Ruff et al., 2006; Sack et al., 2007). But also for event-related fMRI and suprathreshold single-pulse TMS, local activations could be observed in the primary motor hand area (e.g., Bestmann et al., 2003a; Bohning et al., 2000b; Hanakawa et al., 2009; Shitara et al., 2011) (but mind afferent feedback as potential confound for suprathreshold pulses) and the dlPFC (e.g., Dowdle et al., 2018; Hanlon et al., 2013; Hanlon et al., 2016; Hawco et al., 2018; Vink et al., 2018); see Table 1 for an overview. On the other hand, specific frequencies may also tap into different brain networks by resonating with and possibly entraining specific oscillatory activity (Thut et al., 2011a). Different brain regions many thus preferentially activate with specific stimulation frequencies, and also remote effects may differ as a function of frequency. A recent study for example, used concurrent TMS-fMRI to test the effects of theta vs. beta burst TMS of the parietal cortex as entry point for the hippocampal network (Hermiller et al., 2020). The found indeed theta (5 Hz) but not "beta" (12.5 Hz) TMS to activate the hippocampal network during memory encoding. Unfortunately, it may often be challenging to reconcile the constraints imposed by temporal interleaving and fMRI design requirements with the desired stimulation frequency (section 2.3 and Fig. 1C), and EPI sequences may need to be customized for each particular stimulation frequency (Hermiller et al., 2020), making it necessary to accept possible limitations in comparability between the BOLD effects to different stimulation frequencies.

In summary, the choice of stimulation intensity, orientation, and frequency is not trivial, and must be driven by the specific research question at hand. While for the sake of feasibility, not every concurrent TMS-fMRI study can afford to optimize all stimulation parameters, dedicated methodological studies are required that systematically investigate their impact for different target sites to inform future research.

The need for adjusting stimulation parameters actually pertains to TMS studies in general, and the concurrent application with fMRI provides at least a means for assessing the immediate effect of parameter choice, thus also informing other TMS studies performed without the help of neuroimaging.

3.4. Understanding the interaction of TMS with task-related brain activity and behavior

TMS is a well-established tool to transiently disrupt regional neuronal processing during task performance, and this "virtual lesion" approach has been widely used in cognitive neuroscience (Pascual-Leone et al., 2000; Walsh and Cowey, 2000). The possibility to interfere with task-related patterns of neuronal activity in a specific brain region and measure its impact on a specific cognitive function via behavioral assessment, principally allows conclusions about cause-effect relationships between brain activity and cognition - if all confounders are sufficiently controlled experimentally (Bergmann and Hartwigsen, 2021). The above discussed (section 3.1) spread of TMS-induced activation within the targeted network (and beyond), however, highlights that even with the most rigorous experimental controls for peripheral co-stimulation confounds (section 4.3), behavioral effects may not exclusively be attributable to neuronal activity in the initial target region, and the inevitable remote activations have to be considered as confounds offering alternative explanations for the observed effects (Bergmann and Hartwigsen, 2021). Concurrent TMS-fMRI offers a possibility to monitor both the task-related changes in neuronal activity and their TMS-related modulation. This makes it possible to examine the respective contributions of the involved regions to the behavioral outcome, e.g., via brain-behavior correlations across subjects (Sack et al., 2007). Remote effects may thus not categorically represent a potential confound but may rather reflect functionally relevant interactions between brain regions. Taking a network-centered (integration) rather than a module-centered perspective (segregation), the distributed network effects may help to study the network mechanisms mediating a specific cognitive function of interest. When combined with task performance, concurrent TMS-fMRI can reveal functionally relevant inter-regional interactions. Going beyond the mapping of neuronal excitability and effective connectivity at rest (section 3.1) task-based TMS-fMRI can reveal (i) how TMS of one region modulates the task-related activation of another region, (ii) how task-related activations of local and remote targets affect the spread of activation to connected brain regions in a state-dependent manner, and (iii) how connected regions in the target network mediate or instantaneously compensate for the interference effect of TMS on behavior. Yet, the interpretation of the observed brain activation patterns becomes more complicated when TMS is given during different behavioral (task-related) contexts. TMS-evoked BOLD responses as well as task-related BOLD responses occur both locally and remotely, and TMS-related and task-related activity patterns are not independent but result in reciprocal interactions. Accordingly, it may be necessary to assess not only the combination of TMS- and task-evoked BOLD effects, but also either one in isolation to disentangle their respective contributions and interactions.

The remote effects caused by TMS of a certain superficial cortical target may, for example, be exploited when investigating the function of long-range interactions between brain regions, such as the attentional top-down control of cortical excitability in sensory brain regions (and thus perception) via projections from frontal or parietal control regions (Driver et al., 2010; Ruff et al., 2009b). Beside the mere mapping of these pathways at rest (section 3.1), TMS may also be used to deliberately recruit these connections by stimulating the upstream control region (e.g., FEF or IPS) to send a top-down signal to the downstream sensory cortices and modulate local neuronal activity or ongoing stimulus processing.

Remote activations may also differ dramatically depending on the current brain state at the time of stimulation (Fig. 2D), for example on the neuronal context introduced by different conditions of a concurrently performed task (Bestmann et al., 2008b; Ruff et al., 2009b). The same anatomical projections can route neuronal information flow differently to its currently relevant nodes depending on the neuronal state that is expressed at the time of stimulation. Such a state-dependency of remote effects has been observed for the motor system, where TMS of the dPMC caused activity increases in contralateral M1 and dPMC during an active grip of the left hand, but decreased their activation during rest (Bestmann et al., 2008c). Cortical pre-activation seems to be a critical modulator of remote TMS effects also for sensory regions, here in form of the presence vs. absence of specific sensory input at the time of stimulation. The above mentioned TMS of the IPS, for example, resulted in remote activation of motion-sensitive visual area MT/V5 only when moving stimuli were presented, but activated visual areas V1-V4 in the absence of visual stimulation (Ruff et al., 2008). In another study, TMS of IPS caused deactivations the visual cortex in the absence of stimulation as well as under auditory stimulation, but facilitated visual cortex activations in response to visual stimulation (Leitao et al., 2012). Likewise, TMS of the right parietal cortex facilitated activity in the left primary somatosensory cortex (S1) in the presence of sensory input to the right wrist but did rather inhibit it in its absence (Blankenburg et al., 2008). Another key modulator is probably attention. TMS of the right posterior parietal cortex (pPC) during a covert spatial attention task, for example, revealed that the BOLD response to TMS in visual cortices depended on the currently attended hemifield (Blankenburg et al., 2010). Similarly, feature-based attention interacted with TMS of the right FEF, insofar as TMS-evoked BOLD-response in either MT/V5 or the fusiform face area (FFA) were facilitated when shifting attention between moving dots and faces, respectively (Heinen et al., 2014). Importantly, state-dependency has also been reported for the activation of deep brain targets and higher-order functions such as memory encoding, as theta burst TMS of the parietal cortex with concurrent fMRI revealed TMS-evoked BOLD-response in hippocampus and medial temporal lobe (MTL) during scene encoding but not during a numerical control task (Hermiller et al., 2020).

What underpins the state-dependency of remote activations evoked by TMS? Assuming the conductive properties of the connecting axons to remain largely stable, any modulation of (non-spurious) indirect remote activations must be explained by (i) a change of neuronal excitability in the stimulated region, (ii) changes in neuronal excitability in the remote regions, and/or (iii) a change in the synaptic efficacy by which the signal is transmitted from the former to the latter. A discussion of the potential neuronal mechanism mediating these changes, such as the phase and local or cross-regional synchronization of neuronal oscillations, is beyond the scope of this paper: However, changes in synaptic function presumably operate on slower timescales than the comparably fast task-dependent switches in remote activation patterns, which makes state-dependent network dynamics and resulting transient excitability changes more plausible. In any case, while remote changes in BOLD-response amplitude cannot easily be attributed to a single cause, concurrent TMS-fMRI can capture state-dependent changes in regional neural responsiveness and inter-regional effective connectivity as an important aspect of brain function.

Eventually, concurrent TMS-fMRI can also guide the researcher in locating the neuronal origin of an observed disruptive effect of TMS on behavioral task performance. Sack et al. (2007) found that TMS of the right (but not left) superior parietal lobe (SPL) interfered with a spatial judgement task but not with a color judgment task. While this may have led to the straight-forward conclusion that the right SPL is causally responsible for spatial judgement, concurrent fMRI revealed several TMS-evoked remote activations in the right medial frontal gyrus (MFG). Importantly, task-related deactivations in both right SPL and right MFG correlated with the behavioral disruption resulting from TMS. While a mere epiphenomenal spread of activation from SPL to MFG (proportional to the strength of the initial SPL activation) is still conceivable, this findings also support the interpretation that the disruptive effects

of TMS were mediated either by the MFG alone or, more likely, a joint effect of TMS on activity in both regions, affecting the functional interaction between the MFG and SPL.

4. Confounds and control conditions for concurrent TMS-fMRI

There are two main confounding sources, which undermine interpretability of the TMS-evoked BOLD response in concurrent TMS-fMRI studies. On the one hand, spurious BOLD signal changes may result from TMS-related distortions of the MR images, i.e., artifacts. On the other hand, non-transcranial peripheral co-stimulation and other cognitive processes related to the experimental situation may give rise to true BOLD-signal changes, reflecting regional neuronal processing that is associated with TMS but neither directly nor indirectly evoked via a transcranial mechanism.

4.1. Confounds resulting from technical artifacts

As discussed in section 2.2.2, artifacts related to the discharging of the TMS coil in close vicinity of the head can cause spurious signal changes. These spurious BOLD signal changes may result for example from coil vibration related field inhomogeneities or head movement related transient signal jumps. Since both these signal changes are time-locked to the TMS pulse, the general linear model used for fMRI analysis will not easily separate them from the actual BOLD response following neurovascular coupling. A possibility for slow event related designs (but not block designs) is to model such artifacts via a nuisance regressor indicating the onsets of the first volume following each TMS pulse but not convolved with the hemodynamic response function, so it would only explain signal changes limited to the short-lived signal inhomogeneities. Such a regressor often reveals considerable "activation" in close vicinity of the TMS coil, which is usually not limited to the brain but extends into CSF, skull, and scalp (if no brain mask is applied). Head movement related signals may also be observed far away from the stimulation site, typically at tissue boarders were movement results in brief and transient tissue shifts across voxel borders. While theoretically, for short TRs (e.g., 1 s), this first volume conveys negligible information for the subsequent BOLD response, in practice, such a regressor may still reduce the explanatory power of the convolved TMS pulse regressor of interest and hence reduce the sensitivity for the true TMS-evoked BOLD response, possible leading to false negatives. Given the difficulty to remove such confounds post-hoc, it is desirable to minimize them as much as possible during data acquisition by carefully stabilizing both TMS-coil and participant (section 2.1.4). Coil vibration related artifacts partially depend on the stability of the coil holder, and coil position may be supported further by straps and other fixation materials. Likewise, head motion related artifacts, may be reduced by proper head fixation via vacuum cushions and possibly tape. However, neither one of them can be completely avoided without causing considerable discomfort to the subject. Head motion that does result from cranial muscle twitches may only be reduced by changing coil position, a measure not applicable for many studies with a fixed target. Head movement resulting from startle response is yet another issue. It is less pronounced for block designs and sufficiently fast and regular event-related designs, when TMS pulses can be anticipated and habituate, whereas TMS pulses in slower and strongly jittered event-related designs can cause considerable startle responses. Unfortunately, a reduction of startle by a warning cue (e.g., an auditory stimulus or very low intensity TMS pulse) also makes stimuli expected and temporally predictable, leading to anticipatory brain and motor activity when the subject braces for the (often unpleasant) TMS pulse, another confound usually tried to avoid in TMS studies.

4.2. Confounds resulting from peripheral co-stimulation

TMS also evokes true BOLD-responses in the brain via non-transcranial, peripheral pathways, causing low-level sensory input and eventually recruiting high-level (e.g., attentional) functions (Fig. 2C). The TMS-induced E-field reaches peripheral nerves innervating scalp and cranial muscles, or entire branches of cranial nerves, such as trigeminal or facial nerve, even at lower intensities as needed to excite the much deeper cortical tissues (Schmid et al., 1995; Siebner et al., 1999a). The depolarization of peripheral axons either causes direct sensory input via afferent pathways or muscle responses in face, yaw, or neck via efferent pathways, which again results in re-afferent somatosensory feedback. In addition, the vibration of the discharging coil results not only in tactile sensations due to the activation of mechanoreceptors in the skin. The associated TMS click sound also activates auditory pathways via both airborne sound waves and bone conduction (Nikouline et al., 1999). The impact of these sensory co-stimulation effects has been discussed extensively for the case of concurrent TMS-EEG (Belardinelli et al., 2019; Conde et al., 2019; Siebner et al., 2019), since the waveform of TMS-evoked EEG potentials (TEPs) can be severely confounded with auditory and somatosensory evoked potentials (Conde et al., 2019). While the spatial unmixing of transcranially and peripherally evoked brain responses is much easier for the case of concurrent TMS-fMRI, in principle, the same potential confounders need to be considered. One may argue that for most stimulation sites, TMS-evoked BOLD response patterns can be separated sufficiently well from the peripherally induced activations in auditory and somatosensory cortices, and sometimes this may be the case. However, even visual cortex activation can be spurious when evoked by eye blinks (Guipponi et al., 2015) resulting from either startle response or direct facial nerve stimulation, and Guller et al. (2012) administered white noise via pneumatic headphones to reduce startle responses. Yet, also the exposure to loud white noise may exert its own state-dependent effects on the brain network of interest for instance by modulating the TMS-evoked BOLD response. Modulatory effects on brain networks due to continuous noise exposure may differ between experimental conditions and may thus complicate the interpretation of state-dependent effect of TMS. BOLD responses to TMS-evoked peripheral stimulation will also not remain confined to the initial sensory cortices, but – as any other sensory stimulus – also cause cross-modal activations (Leitao et al., 2012) or recruit higher-order supra-modal cortical regions, involved in its conscious perception, the attribution of saliency, orienting of attention, encoding into memory, etc., possibly in a state-dependent fashion. Since TMS during fMRI can be unpleasant and annoying, these stimuli have considerable saliency and are likely to grab reflexive attention. Dedicated questionnaires and rating scales as well as peripheral physiological measures, such as heart rate or respiration, may help to assess the subjective level of discomfort and annoyance per experimental condition and to detect possible confounds.

4.3. Control via sham stimulation and active control sites

Therefore, experimental control of peripheral co-stimulation effects is mandatory to allow valid conclusions regarding the causal relationship between applied transcranial brain stimulation and observed BOLD response. Importantly, both auditory and tactile co-stimulation are considerably augmented in the MRI due to the interaction of TMS-induced and MR B_0 magnetic fields, leading to larger coil vibrations and louder clicks. Perceptual masking, which is already challenging for TMS-EEG, may be impossible for TMS-fMRI. A confounder that cannot be eliminated needs to be controlled via the comparison with respective control conditions to rule out its causal impact on the outcome measure of interest. In TMS-research, this means that for most research questions, either a realistic sham condition (producing equal peripheral but no transcranial brain stimulation) or an active control site (producing equal peripheral and different transcranial brain stimulation) needs to be introduced. Alternatively, TMS of the same site and with identical parameters may be studied under different task or contextual factors to reveal state-dependency of the TMS-evoked response, although it needs

to be considered for each specific case, whether also the processing of sensory co-activations may vary in a state-dependent fashion.

Sham stimulation, a standard approach in conventional TMS outside the MR, is so far hardly used for concurrent TMS-fMRI, and no dedicated sham coils or even combined active/sham coil (able to blind both subject and experimenter) are commercially available at the moment. The majority of studies have compared low- and high-intensity TMS, often not to study dose-response relationships, but with the intention that the low-intensity pulse would be weak enough not to stimulate the brain effectively but still provide comparable auditory and somatosensory input to serve as control condition. Since stimulation intensity and loudness as well as sensory sensations are strongly correlated, the validity of this control condition is questionable. An alternative would be to rotate the coil to a less or even non-effective orientation, e.g., parallel instead of orthogonal to the target gyrus, as effective for M1 (Mills et al., 1992) and also recommended for other regions (Thielscher et al., 2011; Thut et al., 2011b). However, while this may produce very similar auditory inputs, the somatosensory sensations can strongly differ depending on how well the direction of current flow excites peripheral nerves bundles, and its inefficacy would need to be established first.

Dowdle et al. (2018) introduced a sham condition for TMS of the left dlPFC by inserting a 3 cm of firmly compressed open-cell reticulated foam padding between scalp and TMS coil, which increased coil-brain distance and resulted in a ~66 % reduction of the magnetic field in the brain tissue. According to the participants' subjective ratings, this procedure largely preserved sensory aspects of the stimulation, as pain, unpleasantness, intensity, and loudness were not reported differently for real and sham TMS. Leitao and colleagues fixed 2 cm of rigid plastic plates between TMS-coil and scalp to effectively control for both auditory noise and tactile sensations of coil vibration (Leitao et al., 2017b; Leitao et al., 2015). They slightly increased stimulation intensities for the sham condition to match the subjective perception of loudness and found no difference between real and sham TMS in terms of auditory cortex activations (Leitao et al., 2017b). Guller et al. (2012) attached a 4 cm hollow plastic block to TMS coil and administered white noise via pneumatic headphones to reduce startle responses. However, while such distance-based sham conditions can effectively control for auditory confounds, they remain imperfect regarding somatosensory co-stimulation, since some target sites and coil positions are inevitably associated with the peripheral excitation of cranial nerves and muscles, and these side-effects are inevitably reduced when weakening the induced E-field in these structures by increasing the distance to the TMS-coil.

Active control sites are thus often considered the gold standard for behavioral TMS studies (Bergmann and Hartwigsen, 2021), as both auditory (including bone-conduction) and somatosensory co-stimulation can be matched more effectively, even though ratings of unpleasantness and annoyance vary for different target sites as systematically investigated by Meteyard and Holmes (2018). The suitability of the most commonly used control site, the scalp vertex, has recently been actively investigated using concurrent TMS-fMRI (Jung et al., 2016). It is commonly assumed that TMS over the vertex has little effects on most cognitive tasks, as the underlying cortex is not only particularly distant from the scalp and mainly located in the central fissure, but also contains mainly the sensorimotor representations of the legs. Accordingly, Jung et al. (2016) found that low-frequency rTMS bursts at the vertex at suprathreshold intensity did indeed not cause any BOLD activations, neither locally at the stimulation site nor remotely elsewhere in the brain, but instead resulted in widespread deactivations, particularly in regions of the default mode network. On the one hand, such a pattern, reminiscent of non-specific task-related deactivations, can be considered particularly advantageous for an active control site, as no activations in task-positive networks are evoked. On the other hand, this interpretation also implicitly assumes that all other target sites would produce a comparable deactivation pattern, and a subtraction of target and vertex control conditions only remove those common deactivations. This may, however, not be the case. The actual deactivation pattern in response to TMS of M1 in the same study is not reported (only contrasted against vertex TMS), and it is simply unknown for many other possible target sites. The risk therefore remains that a direct contrast between a particular target site of interest and a vertex control site may result in spurious activation patterns, resulting from the subtraction of deactivations, which may then erroneously be interpreted as target TMS related activations. This is not a vertex specific problem, and direct statistical contrasts of activation maps between experimental and active control sites should be interpreted very cautiously. Moreover, since many TMS targets are clearly lateralized, also the control site should be, to avoid confounds in e.g., spatial reorienting of attention. An intriguing idea is to choose nearby "out-of-network" control sites with a comparable peripheral co-stimulation profile, but different functional connectivity profile (Hebscher and Voss, 2020), an approach that has been used both for concurrent TMS-fMRI (Hermiller et al., 2020) as well as fMRI connectivity-informed TMS outside the MR (Raij et al., 2018). However, whether this approach is feasible depends on the specific superficial target under investigation as well as the functional specialization of its immediately neighboring regions.

It should also be noted that effective control conditions – active or sham – may control for false positive findings, but not for false negative ones. Areas strongly influenced by the peripheral side-effects of the stimulation (such as the auditory cortex) may as a result show reduced sensitivity of their neural responsiveness and associated BOLD-response to the actual immediate or remote transcranial effect of the stimulation.

5. Clinical applications of concurrent TMS-fMRI

Since its invention, there have been many attempts to induce therapeutic changes in cortical and subcortical activity using TMS in patients with a variety of psychiatric and neurologic disorders. Although this has led to a few treatment protocols, which have been embraced internationally, finding effective TMS protocols for many other conditions has been elusive. Two international consensus papers have concluded that certain rTMS protocols are "definitely effective" (A-level evidence) for the treatment of neuropathic pain, motor recovery after stroke, and major depressive disorder (MDD), while others were considered "probably effective" (B-Level evidence) in ameliorating certain symptoms of fibromyalgia, Parkinson's disease, multiple sclerosis, post-stroke non-fluent aphasia, and post-traumatic stress disorder (PTSD) (Lefaucheur et al., 2019; Lefaucheur et al., 2014). In the United States, rTMS (in various forms, with various coil configurations) is currently FDA-approved for use as a therapeutic tool in treatment-resistant MDD (Avery et al., 2008; O'Reardon et al., 2007), obsessive compulsive disorder (OCD) (Carmi et al., 2019), and smoking cessation. There is also emerging evidence that various TMS protocols may be effective in curbing alcohol and substance abuse, as described in a recent international consensus paper (Ekhtiari et al., 2019). Despite the widespread evaluation of TMS for a variety of patients (with a variety of symptoms and in a variety of settings), however, the TMS parameters chosen are largely uniform. The vast majority of published studies targets the same limited selection of brain regions (e.g., dlPFC and motor cortex) with the same limited parameters (i.e., 1 Hz, 10 Hz, theta burst stimulation). It has become clear that meaningful innovation is needed in TMS target identification, parameter selection, and timing of the TMS pulses with respect to endogenous neural rhythms, brain states, or task-engagement.

Concurrent TMS-fMRI may serve as a necessary catalyst for the innovation of rTMS interventions. Specifically, through this multimodal approach, clinical researchers can gain unique insights into target selection and establish proof of engagement – a critical step towards developing high fidelity, evidence-based therapeutics. By applying single pulses of TMS to a given cortical location involved in the disease of interest, it may be possible to determine how rTMS might affect downstream neural targets when delivered in a therapeutic manner (section 3.1). For example, in order to determine if the dlPFC or the mPFC was a better strategy for modulating the caudate and putamen, Hanlon and col-

leagues (2016) performed a parametric assessment of the TMS-evoked BOLD signal in both healthy controls and substance dependent individuals (with known deficits in these cortical-subcortical circuits). The results of this "target identification" study, were subsequently applied to a small proof-of-principle clinical trial for rTMS to the mPFC in cocaine users (Hanlon et al., 2017). This randomized, sham-controlled "target engagement" study with TMS-fMRI then led to more clinically relevant evaluations of the effect of rTMS on drug and alcohol cue-reactivity. This translational discovery pipeline opens exciting avenues for the targeted stimulation and therapeutic modulation of deep brain circuits otherwise accessible only to invasive brain stimulation techniques (Horn and Fox, 2020). However, no study has so far tested explicitly whether pre-interventional TMS-fMRI BOLD responses can predict subsequent outcomes of an rTMS intervention in the same individual. Moreover, it is unclear whether single-pulses or bursts necessarily engage the same networks compared to the typical rTMS treatment protocols the effects of which are aimed to be predicted. While several studies have used 1 Hz rTMS trains and short 10 Hz bursts in healthy volunteers (Table 1), and even theta burst stimulation has been combined with concurrent fMRI (Hermiller et al., 2020), only few studies have applied these to patient populations, e.g., 1 Hz trains to the left dlPFC in MDD (Li et al., 2004a) or 10 Hz burst in schizophrenia (Webler et al., 2020), and the immediate network effects during the application of longer clinical protocols have yet to be investigated.

As described above, TMS-evoked BOLD responses can provide proof of target engagement (section 3.2). This is an important feature for therapeutic modulation of both cortical and subcortical brain regions which are directly or indirectly modulated by the TMS pulses. While E-field modeling can be used to estimate the strength of the E-field individually for each patient, empirically derived TMS-evoked BOLD responses also take into account the respective threshold of cortical excitability, which may be reduced e.g., in patients on antiepileptic or antipsychotic drugs, or those with chronic demyelinating disease. This may also help to elucidate the phenomenon of non-responders, distinguishing those for whom the intervention did not successfully engage the target from those for whom it did but yet produced no therapeutic effect.

Another important use of TMS-fMRI for clinical therapeutic discovery lies in the systematic evaluation of various rTMS parameters on the desired TMS-evoked BOLD response pattern (section 3.3), such as the effects of coil orientation, pulse sequence, stimulation frequency, or intensity. This may inform the optimization – and potentially the personalization – of interventional TMS protocols before investing in a long and expensive clinical trial.

Finally, TMS-evoked BOLD response patterns appear to be state-dependent (section 3.4), which suggests that the current brain state should be considered when administering therapeutic rTMS interventions. This notion is of particular relevance as many psychiatric conditions, such as addiction, PTSD, and OCD, are also subject to state-dependent influences (e.g., from medication, recall of traumatic experiences, or stimulus cue-reactivity). This state-dependent nature of brain disorders and their TMS-based treatments has recently been exploited in a study combining 10 Hz rTMS of the left dlPFC with simultaneous craving cue-exposure to support smoking cessation (Li et al., 2020b), and future studies may be able to evaluate such interactions of disorder-related brain state and TMS effects with concurrent TMS-fMRI designs.

Despite of its enormous potential, so far, only twelve concurrent TMS-fMRI studies have been conducted in patients suffering from stroke (Bestmann et al., 2010), limb amputation (Bestmann et al., 2006), and dystonia (de Vries et al., 2012) as well as addiction (Hanlon et al., 2015; Hanlon et al., 2017; Hanlon et al., 2016; Kearney-Ramos et al., 2018), MDD (Eshel et al., 2020; Li et al., 2004a; Li et al., 2003), PTSD (Fonzo et al., 2017), and schizophrenia (Guller et al., 2012; Webler et al., 2020). While studies into motor-related neurological syndromes have focused on accessible superficial targets in M1 following limb amputation (Bestmann et al., 2006), premotor cortex following stroke (Bestmann et al., 2010), and parietal cortex in dystonia (de Vries et al., 2012), many studies into psychiatric disorders are eventually interested in targeting deep brain structures indirectly via superficial targets.

For the case of MDD, accumulating evidence suggests that the sgACC and left dlPFC are hyper- and hypoactive, respectively (Drevets, 2000; Drevets et al., 1997; Mayberg et al., 1999). Accordingly, invasive DBS for treatment of MDD has targeted the sgACC directly using inhibitory stimulation (Mayberg et al., 2005), while rTMS interventions started to target the more accessible superficial dlPFC with facilitatory protocols (George et al., 1995). Fox et al. (2014) argued that resting-state functional connectivity may generally serve to link invasive (usually deep subcortical) and non-invasive (usually superficial cortical) therapeutic brain stimulation targets in neurological and psychiatric disease, as they may simply represent different (often antagonistic) nodes of the same dysfunctional symptom-related brain network. Note that such antagonistic nodes in symptom-relevant networks do not necessarily need a direct monosynaptic connection to interact and may at the same time be part of larger antagonistic resting networks, such as the dorsal attention network (DAN), the salience network (SN), and central executive network (CEN), including the dlPFC, and the default mode network (DAN), including the sgACC. A concurrent TMS-fMRI study by Chen et al. (2013) demonstrated that TMS of a CEN node induced negative connectivity of the DMN with CEN and SN, corroborating the notion of CEN/SN negatively regulating the DMN, and demonstrating that specific network interactions can be engaged by TMS of a single node. Liston et al. (2014) found rTMS treatment of the dlPFC to normalize the abnormally elevated DMN functional connectivity (especially of the sgACC) in MDD patients but not their reduced CEN connectivity, with pre-treatment sgACC connectivity predicting clinical improvement. Philip et al. (2018) also found negative pre-treatment sgACC-DMN connectivity to predict rTMS treatment effects and a reduction of that connectivity to be associated with symptom reduction.

Fox et al. (2014) further suggested that functional connectivity analyses may help to identify therapeutic targets across stimulation techniques, and that the sign of the observed correlation may even indicate whether excitatory or inhibitory stimulation of the respective node would be successful in ameliorating symptoms. Recent research supports the notion that the degree of anticorrelation in functional connectivity between the stimulated dlPFC coordinate and the sgACC strongly predicts treatment outcome of rTMS in MDD (Cash et al., 2020; Cash et al., 2019; Fox et al., 2012; Li et al., 2020a; Weigand et al., 2018), and recent accelerated rTMS treatment studies, using functional connectivity-guided targeting, have produced highly promising results (Cole et al., 2020; Williams et al., 2018).

While these relationships at the network level are interesting and may help to personalize the therapeutic use of focal TMS, it is yet unknown how exactly the targeting of different nodes produces similar effects on the symptoms, and several, not mutually exclusive, mechanisms of action have been discussed that may contribute to different degrees in different diseases (Fox et al., 2014): (i) activity evoked at the primary network target may spread within the network and exert its effect in the remote secondary network target; (ii) symptoms may be caused by an imbalance between antagonistic nodes within the symptom-related network (or possibly between entire antagonistic brain networks), and weakening or strengthening of the respective node/network may rebalance the network(s); (iii) symptoms may be related to abnormal (too high or too low) connectivity between the nodes, and stimulation of these pathways may re-normalize such connectivity; and (iv) stimulation of either node may break dysfunctional oscillatory activity in the network. While the particular mechanism underlying the therapeutic effects of targeting dlPFC and sgACC in MDD is yet unclear, concurrent TMS-fMRI can help to identify promising dlPFC coordinates to remotely affect the sgACC, to assess functional dlPFC-sgACC connectivity, and to measure immediate re-balancing effects within and between brain networks caused by rTMS.

Concurrent TMS-fMRI already revealed that the standard clinical approach of targeting an area 5 cm anterior to M1 is a very crude approx-

imation, as in only four out of nine healthy participants stimulation at this coordinate actually activated the sgACC (Vink et al., 2018). Based on this finding, the authors argued that the propagation of TMS-evoked activity from dlPFC to sgACC could in fact be used as biomarker for rTMS efficacy. Accordingly, the a priori choice of a target coordinate optimized with respect to the relevant dlPFC-sgACC anti-correlation pattern (Fox et al., 2012) did indeed result in remote activation of the sgACC also in healthy participants (Tik et al., 2020), even though these preliminary results yet require confirmation. In a very recent study, Oathes et al. (2021) applied functional connectivity-guided TMS with concurrent fMRI to multiple target sites in the left dlPFC that expressed either strong positive or negative functional connectivity with the sgACC (or the amygdala) and found negative BOLD responses in the sgACC regardless of the direction of correlation.

Surprisingly, few studies have been published that applyied concurrent TMS-fMRI in MDD patients. Li et al. (2004a) found that 1 Hz TMS of the left dlPFC increased BOLD signal in frontal-subcortical circuits and simultaneously led to a decrease in the left vmPFC. Eshel et al. (2020) demonstrated that single pulses of TMS, delivered to a functional connectivity-based target in the dlPFC, deactivated the amygdala in healthy controls but failed to do so in patients with MDD. Along the same lines, also those PTSD patients who respond better to treatment are the ones who show a stronger right dlPFC TMS-evoked inhibition of the left amygdala at baseline (Fonzo et al., 2017).

For schizophrenia, Guller and colleagues (2012) demonstrated that TMS of the precentral gyrus evoked a similar BOLD response in patients and matched controls in the vicinity of the cortical target, but patients showed reduced TMS-evoked activity in the thalamus and medial prefrontal cortex. A lack of remote TMS effects in schizophrenia patients was also reported by Webler et al. (2020). This group applied TMS to the left dlPFC and found that patients showed lower contralateral but higher ipsilateral dlPFC activity than controls – suggesting a blunted spreading of the TMS effects in these individuals.

A pipeline of target identification and therapeutic discovery studies have also been carried out with TMS-fMRI in patients with cocaine addiction (Hanlon et al., 2015; Hanlon et al., 2016; Kearney-Ramos et al., 2018). In an initial attempt to determine whether the dlPFC or the mPFC would be a more fruitful therapeutic target for TMS in cocaine users (based on their known frontal-striatal connectivity deficits) Hanlon et al. (2015) applied concurrent TMS-fMRI to two cortical targets (left dlPFC and left frontal pole) in healthy individuals and cocaine users. They demonstrated that the frontal pole-striatal circuitry was more strongly disrupted in patients than in controls (compared to dlPFC connectivity) and therefore chose this site for their next therapeutic study. In this second study, they used concurrent TMS-fMRI to evaluate the after-effects resulting from a session of continuous theta burst stimulation (cTBS) to the frontal pole on TMS-evoked mPFC-striatum connectivity (Hanlon et al., 2016). They found that cTBS to the frontal pole caused a specific decrease in TMS-evoked BOLD signal in the orbitofrontal cortex, caudate and nucleus accumbens. The ability of TMS to modulate activity in the deeper striatal regions, however, was dependent on gray matter density in the vicinity of the coil and white matter integrity of the mPFC-striatum pathway (Kearney-Ramos et al 2018). In summary, these three studies paved the way for a Phase 1/2 clinical trial of cTBS as therapeutic tool for decreasing relapse among treatment seeking cocaine users. Despite the above discussed differences in the brain's response to TMS for patients with MDD, schizophrenia, PTSD, and substance abuse, relative to healthy controls, the diagnostic potential of concurrent TMS-fMRI for identifying certain neurological and psychiatric disease in individual patients has yet to be studied explicitly in prospective trials with a larger sample size.

Another interesting application of concurrent TMS-fMRI in clinical research is the evaluation of pharmacological agents with respect to their modulation of neuronal excitability and effective connectivity. Accordingly, pharmaco-TMS-fMRI has been used to study the effects of lamotrigine (Li et al., 2011; Li et al., 2010; Li et al., 2004b) and valproic acid (Li et al., 2011; Li et al., 2010) in healthy participants, revealing reduced cortical responsiveness to TMS of M1 for both drugs, but increased responses in limbic regions when targeting the PFC only for lamotrigine. This approach can not only provide interesting insights into the excitability and effective connectivity changes caused by these drugs but may also help to understand the neuronal mechanisms modulating TMS-evoked BOLD responses and thus inform the interpretation of other TMS-fMRI studies.

6. Future advancements of concurrent TMS-fMRI

Concurrent TMS-fMRI has been a sophisticated niche method for highly specialized labs for the last two decades, but it has now reached a state of technical maturation that attracts a growing number of new users, and the respective investments to implement the technique in more labs. Its benefits outweigh its costs, as the capability to map effective connectivity, provide proof of target engagement, empirically optimize stimulation parameters, and investigate the state-dependent interaction of TMS with task-related brain activity and behavior, provides important solutions for the application of TMS in both cognitive neuroscience and clinical research. A wider availability of concurrent TMS-fMRI setups in the near future will also produce a growing number of studies taking advantage of these possibilities to tackle a wide range of different research questions and develop or refine therapeutic applications. We consider the following points key technical and conceptual challenges that will markedly improve the benefits of concurrent TMS-fMRI in the future.

1) Technical developments and refinements in several areas are required to improve practicability and flexibility of concurrent TMS-fMRI setups, such as facilitated coil mounting and navigation solutions, remote robotic positioning of the TMS-coil in the MR scanner, increased intensity and focality of MR-compatible TMS-coils, as well as the implementation of paired-pulse and dual-coil protocols.
2) Experimental designs need to be optimized further to control for confounds resulting from technical artifacts and peripheral co-stimulation. On the one hand, proper sham conditions need to be developed (Dowdle et al., 2018; Leitao et al., 2017b), at best mimicking both auditory and somatosensory co-stimulation as good as possible via dedicated MR-compatible sham-coils, to provide a robust low-level baseline. On the other hand, also high-level active control conditions using different stimulation frequencies, coil orientations, and well matched alternative "off-network" control sites provide very strong controls (Hebscher and Voss, 2020; Hermiller et al., 2020; Raij et al., 2018), even though the respective BOLD-responses resulting from these active control stimulations do not allow direct contrasting with the main experimental condition of interest anymore as often done with sham conditions.
3) An empirically validated theoretical framework is needed for successfully planning the stimulation of remote deep brain structures via the targeting of connected superficial cortical targets. While such approaches have repeatedly been employed, it is yet unclear (i) whether to use only functional or also structural connectivity, (ii) whether to focus on data from large cohorts or estimate connectivity individually, and (iii) whether to target positive or negative correlations with the deep target seed (voxel or network). Concurrent TMS-fMRI will be absolutely instrumental in validating these approaches (Tik et al., 2020).
4) Further personalization of the stimulation via the individual optimization of stimulation intensity, frequency, and coil orientation will be important to make concurrent TMS-fMRI approaches as effective as possible. This may involve empirical titration of stimulation parameters as well as the modelling of E-field using realistic head models (Weise et al., 2019) and the simulation of network responses to the stimulation based on individual virtual brains estimated from multimodal imaging data (Schirner et al., 2018).

In summary, we believe that concurrent TMS-fMRI is a technique that has matured significantly over the last two decades, but has not yet reached its peak, thus leaving exciting developments and new applications ahead of us. We predict that the number of publications involving concurrent TMS-fMRI will increase more steeply over the next few years, and we encourage other researchers to employ concurrent TMS-fMRI to make use of its manifold benefits, which we hope to have shown outweigh the efforts of its implementation.

Data and code availability statement

This is a review paper, and there is no data or code that could be made available.

Declaration of Competing Interest

Hartwig R. Siebner has received honoraria as speaker from Sanofi Genzyme, Denmark and Novartis, Denmark, as consultant from Sanofi Genzyme, Denmark, Lophora, Denmark, and Lundbeck AS, Denmark, and as editor-in-chief (Neuroimage Clinical) and senior editor (NeuroImage) from Elsevier Publishers, Amsterdam, The Netherlands. He has received royalties as book editor from Springer Publishers, Stuttgart, Germany and from Gyldendal Publishers, Copenhagen, Denmark. Til Ole Bergmann has received honoraria as handling editor (NeuroImage) from Elsevier Publishers, Amsterdam, The Netherlands.

Credit authorship contribution statement

Til Ole Bergmann: Conceptualization, Writing – original draft, Writing – review & editing, Visualization. **Rathiga Varatheeswaran:** Investigation, Data curtion, Writing – review & editing. **Colleen A. Hanlon:** Conceptualization, Writing – review & editing. **Kristoffer H. Madsen:** Writing – review & editing. **Axel Thielscher:** Writing – review & editing. **Hartwig Roman Siebner:** Conceptualization, Writing – review & editing.

Acknowledgements

T.O.B. and R.V. were supported by the Boehringer Ingelheim Foundation. A.T. received support by the Lundbeck foundation (grant R244-2017-196 and R313-2019-622). Hartwig R. Siebner holds a 5-year professorship in precision medicine at the Faculty of Health Sciences and Medicine, University of Copenhagen which is sponsored by the Lundbeck Foundation (Grant Nr. R186-2015-2138).

References

Antal, A., Boros, K., Poreisz, C., Chaieb, L., Terney, D., Paulus, W., 2008. Comparatively weak after-effects of transcranial alternating current stimulation (tACS) on cortical excitability in humans. Brain Stimul. 1, 97–105. doi:10.1016/j.brs.2007.10.001.

Ashburner, J., Friston, K.J., 2005. Unified segmentation. Neuroimage 26, 839–851. doi:10.1016/j.neuroimage.2005.02.018.

Avery, D.H., Isenberg, K.E., Sampson, S.M., Janicak, P.G., Lisanby, S.H., Maixner, D.F., Loo, C., Thase, M.E., Demitrack, M.A., George, M.S., 2008. Transcranial magnetic stimulation in the acute treatment of major depressive disorder: clinical response in an open-label extension trial. J. Clin. Psychiatry 69, 441–451. doi:10.4088/jcp.v69n0315.

Barker, A.T., Jalinous, R., Freeston, I.L., 1985. Non-invasive magnetic stimulation of human motor cortex. Lancet 1, 1106–1107.

Baudewig, J., Paulus, W., Frahm, J., 2000. Artifacts caused by transcranial magnetic stimulation coils and EEG electrodes in T(2)*-weighted echo-planar imaging. Magn. Reson. Imaging 18, 479–484. doi:10.1016/s0730-725x(00)00122-3.

Baudewig, J., Siebner, H.R., Bestmann, S., Tergau, F., Tings, T., Paulus, W., Frahm, J., 2001. Functional MRI of cortical activations induced by transcranial magnetic stimulation (TMS). Neuroreport 12, 3543–3548. doi:10.1097/00001756-200111160-00034.

Belardinelli, P., Biabani, M., Blumberger, D.M., Bortoletto, M., Casarotto, S., David, O., Desideri, D., Etkin, A., Ferrarelli, F., Fitzgerald, P.B., Fornito, A., Gordon, P.C., Gosseries, O., Harquel, S., Julkunen, P., Keller, C.J., Kimiskidis, V.K., Lioumis, P., Miniussi, C., Rosanova, M., Rossi, S., Sarasso, S., Wu, W., Zrenner, C., Daskalakis, Z.J., Rogasch, N.C., Massimini, M., Ziemann, U., Ilmoniemi, R.J., 2019. Reproducibility in TMS-EEG studies: a call for data sharing, standard procedures and effective experimental control. Brain Stimul. 12, 787–790. doi:10.1016/j.brs.2019.01.010.

Bergmann, T.O., 2018. Brain state-dependent brain stimulation. Front. Psychol. 9, 2108. doi:10.3389/fpsyg.2018.02108.

Bergmann, T.O., Hartwigsen, G., 2021. Inferring causality from noninvasive brain stimulation in cognitive neuroscience. J. Cogn. Neurosci. 33, 195–225. doi:10.1162/jocn_a_01591.

Bergmann, T.O., Karabanov, A., Hartwigsen, G., Thielscher, A., Siebner, H.R., 2016. Combining non-invasive transcranial brain stimulation with neuroimaging and electrophysiology: current approaches and future perspectives. Neuroimage 140, 4–19. doi:10.1016/j.neuroimage.2016.02.012.

Bestmann, S., Baudewig, J., Frahm, J., 2003a. On the synchronization of transcranial magnetic stimulation and functional echo-planar imaging. J. Magn. Reson. Imaging 17, 309–316. doi:10.1002/jmri.10260.

Bestmann, S., Baudewig, J., Siebner, H.R., Rothwell, J.C., Frahm, J., 2003b. Subthreshold high-frequency TMS of human primary motor cortex modulates interconnected frontal motor areas as detected by interleaved fMRI-TMS. Neuroimage 20, 1685–1696. doi:10.1016/j.neuroimage.2003.07.028.

Bestmann, S., Baudewig, J., Siebner, H.R., Rothwell, J.C., Frahm, J., 2004. Functional MRI of the immediate impact of transcranial magnetic stimulation on cortical and subcortical motor circuits. Eur. J. Neurosci. 19, 1950–1962. doi:10.1111/j.1460-9568.2004.03277.x.

Bestmann, S., Baudewig, J., Siebner, H.R., Rothwell, J.C., Frahm, J., 2005. BOLD MRI responses to repetitive TMS over human dorsal premotor cortex. Neuroimage 28, 22–29. doi:10.1016/j.neuroimage.2005.05.027.

Bestmann, S., Feredoes, E., 2013. Combined neurostimulation and neuroimaging in cognitive neuroscience: past, present, and future. Ann. N. Y. Acad. Sci. 1296, 11–30. doi:10.1111/nyas.12110.

Bestmann, S., Oliviero, A., Voss, M., Dechent, P., Lopez-Dolado, E., Driver, J., Baudewig, J., 2006. Cortical correlates of TMS-induced phantom hand movements revealed with concurrent TMS-fMRI. Neuropsychologia 44, 2959–2971.

Bestmann, S., Ruff, C.C., Blankenburg, F., Weiskopf, N., Driver, J., Rothwell, J.C., 2008a. Mapping causal interregional influences with concurrent TMS-fMRI. Exp. Brain Res. 191, 383–402. doi:10.1007/s00221-008-1601-8.

Bestmann, S., Ruff, C.C., Blankenburg, F., Weiskopf, N., Driver, J., Rothwell, J.C., 2008b. Mapping causal interregional influences with concurrent TMS-fMRI. Exp. Brain Res. 191, 383–402. doi:10.1007/s00221-008-1601-8.

Bestmann, S., Swayne, O., Blankenburg, F., Ruff, C.C., Haggard, P., Weiskopf, N., Josephs, O., Driver, J., Rothwell, J.C., Ward, N.S., 2008c. Dorsal premotor cortex exerts state-dependent causal influences on activity in contralateral primary motor and dorsal premotor cortex. Cereb. Cortex 18, 1281–1291. doi:10.1093/cercor/bhm159.

Bestmann, S., Swayne, O., Blankenburg, F., Ruff, C.C., Teo, J., Weiskopf, N., Driver, J., Rothwell, J.C., Ward, N.S., 2010. The role of contralesional dorsal premotor cortex after stroke as studied with concurrent TMS-fMRI. J. Neurosci. 30, 11926–11937. doi:10.1523/JNEUROSCI.5642-09.2010.

Blankenburg, F., Ruff, C.C., Bestmann, S., Bjoertomt, O., Eshel, N., Josephs, O., Weiskopf, N., Driver, J., 2008. Interhemispheric effect of parietal TMS on somatosensory response confirmed directly with concurrent TMS-fMRI. J. Neurosci. 28, 13202–13208. doi:10.1523/JNEUROSCI.3043-08.2008.

Blankenburg, F., Ruff, C.C., Bestmann, S., Bjoertomt, O., Josephs, O., Deichmann, R., Driver, J., 2010. Studying the role of human parietal cortex in visuospatial attention with concurrent TMS-fMRI. Cereb. Cortex 20, 2702–2711. doi:10.1093/cercor/bhq015.

Bohning, D.E., Denslow, S., Bohning, P.A., Walker, J.A., George, M.S., 2003a. A TMS coil positioning/holding system for MR image-guided TMS interleaved with fMRI. Clin. Neurophysiol. 114, 2210–2219. doi:10.1016/s1388-2457(03)00232-3.

Bohning, D.E., Shastri, A., Lomarev, M.P., Lorberbaum, J.P., Nahas, Z., George, M.S., 2003b. BOLD-fMRI response vs. transcranial magnetic stimulation (TMS) pulse-train length: testing for linearity. J. Magn. Reson. Imaging 17, 279–290. doi:10.1002/jmri.10271.

Bohning, D.E., Shastri, A., McConnell, K.A., Nahas, Z., Lorberbaum, J.P., Roberts, D.R., Teneback, C., Vincent, D.J., George, M.S., 1999. A combined TMS/fMRI study of intensity-dependent TMS over motor cortex. Biol. Psychiatry 45, 385–394 https://doi.org/S0006322398003680 [pii].

Bohning, D.E., Shastri, A., McGavin, L., McConnell, K.A., Nahas, Z., Lorberbaum, J.P., Roberts, D.R., George, M.S., 2000a. Motor cortex brain activity induced by 1-Hz transcranial magnetic stimulation is similar in location and level to that for volitional movement. Invest. Radiol. 35, 676–683. doi:10.1097/00004424-200011000-00005.

Bohning, D.E., Shastri, A., Nahas, Z., Lorberbaum, J.P., Andersen, S.W., Dannels, W.R., Haxthausen, E.U., Vincent, D.J., George, M.S., 1998. Echoplanar BOLD fMRI of brain activation induced by concurrent transcranial magnetic stimulation. Invest. Radiol. 33, 336–340. doi:10.1097/00004424-199806000-00004.

Bohning, D.E., Shastri, A., Wassermann, E.M., Ziemann, U., Lorberbaum, J.P., Nahas, Z., Lomarev, M.P., George, M.S., 2000b. BOLD-f MRI response to single-pulse transcranial magnetic stimulation (TMS). J. Magn. Reson. Imaging 11, 569–574. doi:10.1002/1522-2586(200006)11:6<569::aid-jmri1>3.0.co;2-3.

Bortoletto, M., Veniero, D., Thut, G., Miniussi, C. , 2015. The contribution of TMS-EEG coregistration in the exploration of the human cortical connectome. Neurosci. Biobehav. Rev. 49, 114–124. doi:10.1016/j.neubiorev.2014.12.014.

Bungert, A., Antunes, A., Espenhahn, S., Thielscher, A., 2017. Where does TMS stimulate the motor cortex? combining electrophysiological measurements and realistic field estimates to reveal the affected cortex position. Cereb. Cortex 27, 5083–5094. doi:10.1093/cercor/bhw292.

Bungert, A., Chambers, C.D., Long, E., Evans, C.J., 2012a. On the importance of specialized radiofrequency filtering for concurrent TMS/MRI. J. Neurosci. Methods 210, 202–205. doi:10.1016/j.jneumeth.2012.07.023.

Bungert, A., Chambers, C.D., Phillips, M., Evans, C.J., 2012b. Reducing image artefacts in concurrent TMS/fMRI by passive shimming. Neuroimage 59, 2167–2174. doi:10.1016/j.neuroimage.2011.10.013.

Buzsaki, G., Anastassiou, C.A., Koch, C., 2012. The origin of extracellular fields and currents–EEG, ECoG, LFP and spikes. Nat. Rev. Neurosci. 13, 407–420. doi:10.1038/nrn3241.

Caparelli, E.C., Backus, W., Telang, F., Wang, G.J., Maloney, T., Goldstein, R.Z., Anschel, D., Henn, F., 2010. Simultaneous TMS-fMRI of the visual cortex reveals functional network, even in absence of phosphene sensation. Open Neuroimag. J. 4, 100–110. doi:10.2174/1874440001004010100, TONIJ-4-100 [pii].

Carmi, L., Tendler, A., Bystritsky, A., Hollander, E., Blumberger, D.M., Daskalakis, J., Ward, H., Lapidus, K., Goodman, W., Casuto, L., Feifel, D., Barnea-Ygael, N., Roth, Y., Zangen, A., Zohar, J., 2019. Efficacy and safety of deep transcranial magnetic stimulation for obsessive-compulsive disorder: a prospective multicenter randomized double-blind placebo-controlled trial. Am. J. Psychiatry 176, 931–938. doi:10.1176/appi.ajp.2019.18101180.

Cash, R.F.H., Weigand, A., Zalesky, A., Siddiqi, S.H., Downar, J., Fitzgerald, P.B., Fox, M.D., 2020. Using brain imaging to improve spatial targeting of transcranial magnetic stimulation for depression. Biol. Psychiatry doi:10.1016/j.biopsych.2020.05.033.

Cash, R.F.H., Zalesky, A., Thomson, R.H., Tian, Y., Cocchi, L., Fitzgerald, P.B., 2019. Subgenual functional connectivity predicts antidepressant treatment response to transcranial magnetic stimulation: independent validation and evaluation of personalization. Biol. Psychiatry 86, e5–e7. doi:10.1016/j.biopsych.2018.12.002.

Chen, A.C., Oathes, D.J., Chang, C., Bradley, T., Zhou, Z.W., Williams, L.M., Glover, G.H., Deisseroth, K., Etkin, A., 2013. Causal interactions between fronto-parietal central executive and default-mode networks in humans. Proc. Natl. Acad. Sci. U. S. A. 110, 19944–19949. doi:10.1073/pnas.1311772110.

Cobos Sanchez, C., Cabello, M.R., Olozabal, A.Q., Pantoja, M.F., 2020. Design of TMS coils with reduced Lorentz forces: application to concurrent TMS-fMRI. J. Neural Eng. 17, 016056. doi:10.1088/1741-2552/ab4ba2.

Cohen, M.X., 2017. Where does EEG come from and what does it mean? Trends Neurosci. 40, 208–218. doi:10.1016/j.tins.2017.02.004.

Cole, E.J., Stimpson, K.H., Bentzley, B.S., Gulser, M., Cherian, K., Tischler, C., Nejad, R., Pankow, H., Choi, E., Aaron, H., Espil, F.M., Pannu, J., Xiao, X., Duvio, D., Solvason, H.B., Hawkins, J., Guerra, A., Jo, B., Raj, K.S., Phillips, A.L., Barmak, F., Bishop, J.H., Coetzee, J.P., DeBattista, C., Keller, J., Schatzberg, A.F., Sudheimer, K.D., Williams, N.R., 2020. Stanford accelerated intelligent neuromodulation therapy for treatment-resistant depression. Am. J. Psychiatry doi:10.1176/appi.ajp.2019.19070720, appiajp201919070720.

Conde, V., Tomasevic, L., Akopian, I., Stanek, K., Saturnino, G.B., Thielscher, A., Bergmann, T.O., Siebner, H.R., 2019. The non-transcranial TMS-evoked potential is an inherent source of ambiguity in TMS-EEG studies. Neuroimage 185, 300–312. doi:10.1016/j.neuroimage.2018.10.052.

de Graaf, T.A., van den Hurk, J., Duecker, F., Sack, A.T., 2018. Where are the fMRI correlates of phosphene perception? Front Neurosci 12, 883. doi:10.3389/fnins.2018.00883.

de Vries, P.M., de Jong, B.M., Bohning, D.E., Hinson, V.K., George, M.S., Leenders, K.L., 2012. Reduced parietal activation in cervical dystonia after parietal TMS interleaved with fMRI. Clin. Neurol. Neurosurg. 114, 914–921. doi:10.1016/j.clineuro.2012.02.006.

de Vries, P.M., de Jong, B.M., Bohning, D.E., Walker, J.A., George, M.S., Leenders, K.L., 2009. Changes in cerebral activations during movement execution and imagery after parietal cortex TMS interleaved with 3T MRI. Brain Res. 1285, 58–68. doi:10.1016/j.brainres.2009.06.006.

de Weijer, A.D., Sommer, I.E., Bakker, E.J., Bloemendaal, M., Bakker, C.J., Klomp, D.W., Bestmann, S., Neggers, S.F., 2014. A setup for administering TMS to medial and lateral cortical areas during whole-brain FMRI recording. J. Clin. Neurophysiol. 31, 474–487. doi:10.1097/WNP.0000000000000075.

Deng, Z.D., Lisanby, S.H., Peterchev, A.V., 2014. Coil design considerations for deep transcranial magnetic stimulation. Clin. Neurophysiol. 125, 1202–1212. doi:10.1016/j.clinph.2013.11.038.

Denslow, S., Bohning, D.E., Bohning, P.A., Lomarev, M.P., George, M.S., 2005a. An increased precision comparison of TMS-induced motor cortex BOLD fMRI response for image-guided versus function-guided coil placement. Cogn. Behav. Neurol. 18, 119–126. doi:10.1097/01.wnn.0000160821.15459.68.

Denslow, S., Lomarev, M., Bohning, D.E., Mu, Q., George, M.S., 2004. A high resolution assessment of the repeatability of relative location and intensity of transcranial magnetic stimulation-induced and volitionally induced blood oxygen level-dependent response in the motor cortex. Cogn. Behav. Neurol. 17, 163–173. doi:10.1097/01.wnn.0000117864.42205.6d.

Denslow, S., Lomarev, M., George, M.S., Bohning, D.E., 2005b. Cortical and subcortical brain effects of transcranial magnetic stimulation (TMS)-induced movement: an interleaved TMS/functional magnetic resonance imaging study. Biol. Psychiatry 57, 752–760.

Di Lazzaro, V., Ziemann, U., Lemon, R.N., 2008. State of the art: physiology of transcranial motor cortex stimulation. Brain Stimul. 1, 345–362. doi:10.1016/j.brs.2008.07.004.

Dosenbach, N.U.F., Koller, J.M., Earl, E.A., Miranda-Dominguez, O., Klein, R.L., Van, A.N., Snyder, A.Z., Nagel, B.J., Nigg, J.T., Nguyen, A.L., Wesevich, V., Greene, D.J., Fair, D.A., 2017. Real-time motion analytics during brain MRI improve data quality and reduce costs. Neuroimage 161, 80–93. doi:10.1016/j.neuroimage.2017.08.025.

Dowdle, L.T., Brown, T.R., George, M.S., Hanlon, C.A., 2018. Single pulse TMS to the DLPFC, compared to a matched sham control, induces a direct, causal increase in caudate, cingulate, and thalamic BOLD signal. Brain Stimul 11, 789–796. doi:10.1016/j.brs.2018.02.014.

Drevets, W.C. , 2000. Neuroimaging studies of mood disorders. Biol. Psychiatry 48, 813–829. doi:10.1016/s0006-3223(00)01020-9.

Drevets, W.C., Price, J.L., Simpson Jr., J.R., Todd, R.D., Reich, T., Vannier, M., Raichle, M.E., 1997. Subgenual prefrontal cortex abnormalities in mood disorders. Nature 386, 824–827. doi:10.1038/386824a0.

Driver, J., Blankenburg, F., Bestmann, S., Ruff, C.C., 2010. New approaches to the study of human brain networks underlying spatial attention and related processes. Exp. Brain Res. 206, 153–162. doi:10.1007/s00221-010-2205-7.

Drysdale, A.T., Grosenick, L., Downar, J., Dunlop, K., Mansouri, F., Meng, Y., Fetcho, R.N., Zebley, B., Oathes, D.J., Etkin, A., Schatzberg, A.F., Sudheimer, K., Keller, J., Mayberg, H.S., Gunning, F.M., Alexopoulos, G.S., Fox, M.D., Pascual-Leone, A., Voss, H.U., Casey, B.J., Dubin, M.J., Liston, C., 2017. Resting-state connectivity biomarkers define neurophysiological subtypes of depression. Nat. Med. 23, 28–38. doi:10.1038/nm.4246.

Edgley, S.A., Eyre, J.A., Lemon, R.N., Miller, S., 1990. Excitation of the corticospinal tract by electromagnetic and electrical stimulation of the scalp in the macaque monkey. J. Physiol. 425, 301–320. doi:10.1113/jphysiol.1990.sp018104.

Ekhtiari, H., Tavakoli, H., Addolorato, G., Baeken, C., Bonci, A., Campanella, S., Castelo-Branco, L., Challet-Bouju, G., Clark, V.P., Claus, E., Dannon, P.N., Del Felice, A., den Uyl, T., Diana, M., di Giannantonio, M., Fedota, J.R., Fitzgerald, P., Gallimberti, L., Grall-Bronnec, M., Herremans, S.C., Herrmann, M.J., Jamil, A., Khedr, E., Kouimtsidis, C., Kozak, K., Krupitsky, E., Lamm, C., Lechner, W.V., Madeo, G., Malmir, N., Martinotti, G., McDonald, W.M., Montemitro, C., Nakamura-Palacios, E.M., Nasehi, M., Noel, X., Nosratabadi, M., Paulus, M., Pettorruso, M., Pradhan, B., Praharaj, S.K., Rafferty, H., Sahlem, G., Salmeron, B.J., Sauvaget, A., Schluter, R.S., Sergiou, C., Shahbabaie, A., Sheffer, C., Spagnolo, P.A., Steele, V.R., Yuan, T.F., van Dongen, J.D.M., Van Waes, V., Venkatasubramanian, G., Verdejo-Garcia, A., Verveer, I., Welsh, J.W., Wesley, M.J., Witkiewitz, K., Yavari, F., Zarrindast, M.R., Zawertailo, L., Zhang, X., Cha, Y.H., George, T.P., Frohlich, F., Goudriaan, A.E., Fecteau, S., Daughters, S.B., Stein, E.A., Fregni, F., Nitsche, M.A., Zangen, A., Bikson, M., Hanlon, C.A., 2019. Transcranial electrical and magnetic stimulation (tES and TMS) for addiction medicine: a consensus paper on the present state of the science and the road ahead. Neurosci. Biobehav. Rev. 104, 118–140. doi:10.1016/j.neubiorev.2019.06.007.

Eshel, N., Keller, C.J., Wu, W., Jiang, J., Mills-Finnerty, C., Huemer, J., Wright, R., Fonzo, G.A., Ichikawa, N., Carreon, D., Wong, M., Yee, A., Shpigel, E., Guo, Y., McTeague, L., Maron-Katz, A., Etkin, A., 2020. Global connectivity and local excitability changes underlie antidepressant effects of repetitive transcranial magnetic stimulation. Neuropsychopharmacology doi:10.1038/s41386-020-0633-z.

Ferreri, F., Rossini, P.M., 2013. TMS and TMS-EEG techniques in the study of the excitability, connectivity, and plasticity of the human motor cortex. Rev. Neurosci. 24, 431–442. doi:10.1515/revneuro-2013-0019.

Fomenko, A., Neudorfer, C., Dallapiazza, R.F., Kalia, S.K., Lozano, A.M., 2018. Low-intensity ultrasound neuromodulation: an overview of mechanisms and emerging human applications. Brain Stimul. 11, 1209–1217. doi:10.1016/j.brs.2018.08.013.

Fonzo, G.A., Goodkind, M.S., Oathes, D.J., Zaiko, Y.V., Harvey, M., Peng, K.K., Weiss, M.E., Thompson, A.L., Zack, S.E., Lindley, S.E., Arnow, B.A., Jo, B., Gross, J.J., Rothbaum, B.O., Etkin, A., 2017. PTSD psychotherapy outcome predicted by brain activation during emotional reactivity and regulation. Am. J. Psychiatry 174, 1163–1174. doi:10.1176/appi.ajp.2017.16091072.

Fox, M.D., Buckner, R.L., Liu, H., Chakravarty, M.M., Lozano, A.M., Pascual-Leone, A., 2014. Resting-state networks link invasive and noninvasive brain stimulation across diverse psychiatric and neurological diseases. Proc. Natl. Acad. Sci. U. S. A. 111, E4367–E4375. doi:10.1073/pnas.1405003111.

Fox, M.D., Buckner, R.L., White, M.P., Greicius, M.D., Pascual-Leone, A., 2012. Efficacy of transcranial magnetic stimulation targets for depression is related to intrinsic functional connectivity with the subgenual cingulate. Biol. Psychiatry 72, 595–603. doi:10.1016/j.biopsych.2012.04.028.

Fox, M.D., Liu, H., Pascual-Leone, A., 2013. Identification of reproducible individualized targets for treatment of depression with TMS based on intrinsic connectivity. Neuroimage 66, 151–160. doi:10.1016/j.neuroimage.2012.10.082.

Freedberg, M., Reeves, J.A., Toader, A.C., Hermiller, M.S., Voss, J.L., Wassermann, E.M., 2019. Persistent enhancement of hippocampal network connectivity by parietal rTMS is reproducible. eNeuro 6. doi:10.1523/ENEURO.0129-19.2019.

Friston, K.J., Buechel, C., Fink, G.R., Morris, J., Rolls, E., Dolan, R.J., 1997. Psychophysiological and modulatory interactions in neuroimaging. Neuroimage 6, 218–229.

George, M.S., Wassermann, E.M., Williams, W.A., Callahan, A., Ketter, T.A., Basser, P., Hallett, M., Post, R.M., 1995. Daily repetitive transcranial magnetic stimulation (rTMS) improves mood in depression. Neuroreport 6, 1853–1856.

Gerlicher, A.M.V., Tuscher, O., Kalisch, R., 2018. Dopamine-dependent prefrontal reactivations explain long-term benefit of fear extinction. Nat. Commun. 9, 4294. doi:10.1038/s41467-018-06785-y.

Gomez, L.J., Dannhauer, M., Peterchev, A.V., 2020. Fast computational optimization of TMS coil placement for individualized electric field targeting. bioRxiv 2020.2005.2027.120022 doi:10.1101/2020.05.27.120022.

Guipponi, O., Odouard, S., Pinede, S., Wardak, C., Ben Hamed, S., 2015. fMRI cortical correlates of spontaneous eye blinks in the nonhuman primate. Cereb. Cortex 25, 2333–2345. doi:10.1093/cercor/bhu038.

Guller, Y., Ferrarelli, F., Shackman, A.J., Sarasso, S., Peterson, M.J., Langheim, F.J., Meyerand, M.E., Tononi, G., Postle, B.R., 2012. Probing thalamic integrity in schizophrenia using concurrent transcranial magnetic stimulation and functional magnetic resonance imaging. Arch. Gen. Psychiatry doi:10.1001/archgenpsychiatry.2012.23, https://doi.org/archgenpsychiatry.2012.23 [pii].

Hallett, M., Di Iorio, R., Rossini, P.M., Park, J.E., Chen, R., Celnik, P., Strafella, A.P., Matsumoto, H., Ugawa, Y., 2017. Contribution of transcranial magnetic stimulation to assessment of brain connectivity and networks. Clin. Neurophysiol. 128, 2125–2139. doi:10.1016/j.clinph.2017.08.007.

Hamani, C., Mayberg, H., Stone, S., Laxton, A., Haber, S., Lozano, A.M. , 2011. The subcallosal cingulate gyrus in the context of major depression. Biol. Psychiatry 69, 301–308. doi:10.1016/j.biopsych.2010.09.034.

Hanakawa, T., Mima, T., Matsumoto, R., Abe, M., Inouchi, M., Urayama, S., Anami, K., Honda, M., Fukuyama, H., 2009. Stimulus-response profile during single-pulse tran-

scranial magnetic stimulation to the primary motor cortex. Cereb. Cortex 19, 2605–2615. doi:10.1093/cercor/bhp013.
Hanlon, C.A., Canterberry, M., Taylor, J.J., DeVries, W., Li, X., Brown, T.R., George, M.S., 2013. Probing the frontostriatal loops involved in executive and limbic processing via interleaved TMS and functional MRI at two prefrontal locations: a pilot study. PLoS One 8, e67917. doi:10.1371/journal.pone.0067917.
Hanlon, C.A., Dowdle, L.T., Austelle, C.W., DeVries, W., Mithoefer, O., Badran, B.W., George, M.S., 2015. What goes up, can come down: novel brain stimulation paradigms may attenuate craving and craving-related neural circuitry in substance dependent individuals. Brain Res. doi:10.1016/j.brainres.2015.02.053.
Hanlon, C.A., Dowdle, L.T., Correia, B., Mithoefer, O., Kearney-Ramos, T., Lench, D., Griffin, M., Anton, R.F., George, M.S., 2017. Left frontal pole theta burst stimulation decreases orbitofrontal and insula activity in cocaine users and alcohol users. Drug Alcohol Depend. 178, 310–317. doi:10.1016/j.drugalcdep.2017.03.039.
Hanlon, C.A., Dowdle, L.T., Moss, H., Canterberry, M., George, M.S., 2016. Mobilization of medial and lateral frontal-striatal circuits in cocaine users and controls: an interleaved TMS/BOLD functional connectivity study. Neuropsychopharmacology 41, 3032–3041. doi:10.1038/npp.2016.114.
Hartwigsen, G., 2018. Flexible redistribution in cognitive networks. Trends Cogn. Sci. 22, 687–698. doi:10.1016/j.tics.2018.05.008.
Hawco, C., Armony, J.L., Daskalakis, Z.J., Berlim, M.T., Chakravarty, M.M., Pike, G.B., Lepage, M., 2017. Differing time of onset of concurrent TMS-fMRI during associative memory encoding: a measure of dynamic connectivity. Front. Hum. Neurosci. 11, 404. doi:10.3389/fnhum.2017.00404.
Hawco, C., Voineskos, A.N., Steeves, J.K.E., Dickie, E.W., Viviano, J.D., Downar, J., Blumberger, D.M., Daskalakis, Z.J., 2018. Spread of activity following TMS is related to intrinsic resting connectivity to the salience network: a concurrent TMS-fMRI study. Cortex 108, 160–172. doi:10.1016/j.cortex.2018.07.010.
Hebscher, M., Voss, J.L., 2020. Testing network properties of episodic memory using non-invasive brain stimulation. Curr. Opin. Behav. Sci. 32, 35–42. doi:10.1016/j.cobeha.2020.01.012.
Heinen, K., Feredoes, E., Weiskopf, N., Ruff, C.C., Driver, J., 2014. Direct evidence for attention-dependent influences of the frontal eye-fields on feature-responsive visual cortex. Cereb. Cortex 24, 2815–2821. doi:10.1093/cercor/bht157.
Heinen, K., Ruff, C.C., Bjoertomt, O., Schenkluhn, B., Bestmann, S., Blankenburg, F., Driver, J., Chambers, C.D., 2011. Concurrent TMS-fMRI reveals dynamic interhemispheric influences of the right parietal cortex during exogenously cued visuospatial attention. Eur. J. Neurosci. 33, 991–1000. doi:10.1111/j.1460-9568.2010.07580.x.
Hermiller, M.S., Chen, Y.F., Parrish, T.B., Voss, J.L., 2020. Evidence for immediate enhancement of hippocampal memory encoding by network-targeted theta-burst stimulation during concurrent fMRI. J. Neurosci. doi:10.1523/JNEUROSCI.0486-20.2020.
Hermiller, M.S., VanHaerents, S., Raij, T., Voss, J.L., 2019. Frequency-specific noninvasive modulation of memory retrieval and its relationship with hippocampal network connectivity. Hippocampus 29, 595–609. doi:10.1002/hipo.23054.
Holtzheimer, P.E., Mayberg, H.S., 2011. Deep brain stimulation for psychiatric disorders. Annu. Rev. Neurosci. 34, 289–307. doi:10.1146/annurev-neuro-061010-113638.
Horn, A., Fox, M.D., 2020. Opportunities of connectomic neuromodulation. Neuroimage, 117180 doi:10.1016/j.neuroimage.2020.117180.
Huang, Y.Z., Lu, M.K., Antal, A., Classen, J., Nitsche, M., Ziemann, U., Ridding, M., Hamada, M., Ugawa, Y., Jaberzadeh, S., Suppa, A., Paulus, W., Rothwell, J., 2017. Plasticity induced by non-invasive transcranial brain stimulation: a position paper. Clin. Neurophysiol. 128, 2318–2329. doi:10.1016/j.clinph.2017.09.007.
Ilmoniemi, R.J., Kicic, D., 2010. Methodology for combined TMS and EEG. Brain Topogr. 22, 233–248. doi:10.1007/s10548-009-0123-4.
Jung, J., Bungert, A., Bowtell, R., Jackson, S.R., 2016. Vertex stimulation as a control site for transcranial magnetic stimulation: a concurrent TMS/fMRI study. Brain Stimul. 9, 58–64. doi:10.1016/j.brs.2015.09.008.
Jung, J., Bungert, A., Bowtell, R., Jackson, S.R., 2020. Modulating brain networks with transcranial magnetic stimulation over the primary motor cortex: a concurrent TMS/fMRI study. Front. Hum. Neurosci. 14, 31. doi:10.3389/fnhum.2020.00031.
Kearney-Ramos, T.E., Lench, D.H., Hoffman, M., Correia, B., Dowdle, L.T., Hanlon, C.A., 2018. Gray and white matter integrity influence TMS signal propagation: a multimodal evaluation in cocaine-dependent individuals. Sci. Rep. 8, 3253. doi:10.1038/s41598-018-21634-0.
Kellman, P., McVeigh, E.R., 2005. Image reconstruction in SNR units: a general method for SNR measurement. Magn. Reson. Med. 54, 1439–1447. doi:10.1002/mrm.20713.
Koch, G., 2020. Cortico-cortical connectivity: the road from basic neurophysiological interactions to therapeutic applications. Exp. Brain Res. doi:10.1007/s00221-020-05844-5.
Koponen, L.M., Nieminen, J.O., Ilmoniemi, R.J., 2018. Multi-locus transcranial magnetic stimulation-theory and implementation. Brain Stimul. 11, 849–855. doi:10.1016/j.brs.2018.03.014.
Kujirai, T., Caramia, M.D., Rothwell, J.C., Day, B.L., Thompson, P.D., Ferbert, A., Wroe, S., Asselman, P., Marsden, C.D., 1993. Corticocortical inhibition in human motor cortex. J. Physiol. 471, 501–519.
Lafleur, L.P., Tremblay, S., Whittingstall, K., Lepage, J.F., 2016. Assessment of effective connectivity and plasticity with dual-coil transcranial magnetic stimulation. Brain Stimul. 9, 347–355. doi:10.1016/j.brs.2016.02.010.
Lefaucheur, J.P., Aleman, A., Baeken, C., Benninger, D.H., Brunelin, J., Di Lazzaro, V., Filipovic, S.R., Grefkes, C., Hasan, A., Hummel, F.C., Jaaskelainen, S.K., Langguth, B., Leocani, L., Londero, A., Nardone, R., Nguyen, J.P., Nyffeler, T., Oliveira-Maia, A.J., Oliviero, A., Padberg, F., Palm, U., Paulus, W., Poulet, E., Quartarone, A., Rachid, F., Rektorova, I., Rossi, S., Sahlsten, H., Schecklmann, M., Szekely, D., Ziemann, U., 2019. Evidence-based guidelines on the therapeutic use of repetitive transcranial magnetic stimulation (rTMS): an update (2014-2018). Clin. Neurophysiol. doi:10.1016/j.clinph.2019.11.002.
Lefaucheur, J.P., Andre-Obadia, N., Antal, A., Ayache, S.S., Baeken, C., Benninger, D.H., Cantello, R.M., Cincotta, M., de Carvalho, M., De Ridder, D., Devanne, H., Di Lazzaro, V., Filipovic, S.R., Hummel, F.C., Jaaskelainen, S.K., Kimiskidis, V.K., Koch, G., Langguth, B., Nyffeler, T., Oliviero, A., Padberg, F., Poulet, E., Rossi, S., Rossini, P.M., Rothwell, J.C., Schonfeldt-Lecuona, C., Siebner, H.R., Slotema, C.W., Stagg, C.J., Valls-Sole, J., Ziemann, U., Paulus, W., Garcia-Larrea, L., 2014. Evidence-based guidelines on the therapeutic use of repetitive transcranial magnetic stimulation (rTMS). Clin. Neurophysiol. 125, 2150–2206. doi:10.1016/j.clinph.2014.05.021.
Leitao, J., Thielscher, A., Lee, H., Tuennerhoff, J., Noppeney, U., 2017a. Transcranial magnetic stimulation of right inferior parietal cortex causally influences prefrontal activation for visual detection. Eur. J. Neurosci. 46, 2807–2816. doi:10.1111/ejn.13743.
Leitao, J., Thielscher, A., Tuennerhoff, J., Noppeney, U., 2017b. Comparing TMS perturbations to occipital and parietal cortices in concurrent TMS-fMRI studies-Methodological considerations. PLoS One 12, e0181438. doi:10.1371/journal.pone.0181438.
Leitao, J., Thielscher, A., Tunnerhoff, J., Noppeney, U., 2015. Concurrent TMS-fMRI reveals interactions between dorsal and ventral attentional systems. J. Neurosci. 35, 11445–11457. doi:10.1523/JNEUROSCI.0939-15.2015.
Leitao, J., Thielscher, A., Werner, S., Pohmann, R., Noppeney, U., 2012. Effects of parietal TMS on visual and auditory processing at the primary cortical level - a concurrent TMS-fMRI study. Cereb. Cortex doi:10.1093/cercor/bhs078, https://doi.org/bhs078 [pii].
Li, M., Dahmani, L., Wang, D., Ren, J., Stocklein, S., Lin, Y., Luan, G., Zhang, Z., Lu, G., Galie, F., Han, Y., Pascual-Leone, A., Wang, M., Fox, M.D., Liu, H., 2020a. Co-activation patterns across multiple tasks reveal robust anti-correlated functional networks. Neuroimage 227, 117680. doi:10.1016/j.neuroimage.2020.117680.
Li, X., Hartwell, K.J., Henderson, S., Badran, B.W., Brady, K.T., George, M.S., 2020b. Two weeks of image-guided left dorsolateral prefrontal cortex repetitive transcranial magnetic stimulation improves smoking cessation: a double-blind, sham-controlled, randomized clinical trial. Brain Stimul. 13, 1271–1279. doi:10.1016/j.brs.2020.06.007.
Li, X., Large, C.H., Ricci, R., Taylor, J.J., Nahas, Z., Bohning, D.E., Morgan, P., George, M.S., 2011. Using interleaved transcranial magnetic stimulation/functional magnetic resonance imaging (fMRI) and dynamic causal modeling to understand the discrete circuit specific changes of medications: lamotrigine and valproic acid changes in motor or prefrontal effective connectivity. Psychiatry Res. 194, 141–148. doi:10.1016/j.pscychresns.2011.04.012.
Li, X., Nahas, Z., Kozel, F.A., Anderson, B., Bohning, D.E., George, M.S., 2004a. Acute left prefrontal transcranial magnetic stimulation in depressed patients is associated with immediately increased activity in prefrontal cortical as well as subcortical regions. Biol. Psychiatry 55, 882–890. doi:10.1016/j.biopsych.2004.01.017.
Li, X., Nahas, Z., Lomarev, M., Denslow, S., Shastri, A., Bohning, D.E., George, M.S., 2003. Prefrontal cortex transcranial magnetic stimulation does not change local diffusion: a magnetic resonance imaging study in patients with depression. Cogn. Behav. Neurol. 16, 128–135. doi:10.1097/00146965-200306000-00006.
Li, X., Ricci, R., Large, C.H., Anderson, B., Nahas, Z., Bohning, D.E., George, M.S., 2010. Interleaved transcranial magnetic stimulation and fMRI suggests that lamotrigine and valproic acid have different effects on corticolimbic activity. Psychopharmacology (Berl.) 209, 233–244. doi:10.1007/s00213-010-1786-y.
Li, X., Teneback, C.C., Nahas, Z., Kozel, F.A., Large, C., Cohn, J., Bohning, D.E., George, M.S., 2004b. Interleaved transcranial magnetic stimulation/functional MRI confirms that lamotrigine inhibits cortical excitability in healthy young men. Neuropsychopharmacology 29, 1395–1407. doi:10.1038/sj.npp.13004521300452, [pii].
Liston, C., Chen, A.C., Zebley, B.D., Drysdale, A.T., Gordon, R., Leuchter, B., Voss, H.U., Casey, B.J., Etkin, A., Dubin, M.J., 2014. Default mode network mechanisms of transcranial magnetic stimulation in depression. Biol. Psychiatry 76, 517–526. doi:10.1016/j.biopsych.2014.01.023.
Logothetis, N.K., 2002. The neural basis of the blood-oxygen-level-dependent functional magnetic resonance imaging signal. Philos. Trans. R. Soc. Lond. B Biol. Sci. 357, 1003–1037.
Logothetis, N.K., 2008. What we can do and what we cannot do with fMRI. Nature 453, 869–878. doi:10.1038/nature06976.
Logothetis, N.K., Pauls, J., Augath, M., Trinath, T., Oeltermann, A., 2001. Neurophysiological investigation of the basis of the fMRI signal. Nature 412, 150–157. doi:10.1038/35084005.
Lu, H., Wang, S., 2018. A 2-in-1 single-element coil design for transcranial magnetic stimulation and magnetic resonance imaging. Magn. Reson. Med. 79, 582–587. doi:10.1002/mrm.26640.
Mandija, S., Petrov, P.I., Neggers, S.F., Luijten, P.R., van den Berg, C.A., 2016. MR-based measurements and simulations of the magnetic field created by a realistic transcranial magnetic stimulation (TMS) coil and stimulator. NMR Biomed. 29, 1590–1600. doi:10.1002/nbm.3618.
Mason, R.A., Prat, C.S., Just, M.A., 2014. Neurocognitive brain response to transient impairment of Wernicke's area. Cereb. Cortex 24, 1474–1484. doi:10.1093/cercor/bhs423.
Mayberg, H.S., Liotti, M., Brannan, S.K., McGinnis, S., Mahurin, R.K., Jerabek, P.A., Silva, J.A., Tekell, J.L., Martin, C.C., Lancaster, J.L., Fox, P.T., 1999. Reciprocal limbic-cortical function and negative mood: converging PET findings in depression and normal sadness. Am. J. Psychiatry 156, 675–682. doi:10.1176/ajp.156.5.675.
Mayberg, H.S., Lozano, A.M., Voon, V., McNeely, H.E., Seminowicz, D., Hamani, C., Schwalb, J.M., Kennedy, S.H., 2005. Deep brain stimulation for treatment-resistant depression. Neuron 45, 651–660. doi:10.1016/j.neuron.2005.02.014.
McConnell, K.A., Bohning, D.E., Nahas, Z., Shastri, A., Teneback, C., Lorberbaum, J.P., Lomarev, M.P., Vincent, D.J., George, M.S., 2003. BOLD fMRI response to direct stimulation (transcranial magnetic stimulation) of the motor cortex shows no decline with age. J Neural Transm (Vienna) 110, 495–507. doi:10.1007/s00702-002-0804-6.

Merton, P.A., Morton, H.B., 1980. Stimulation of the cerebral cortex in the intact human subject. Nature 285, 227.
Meteyard, L., Holmes, N.P., 2018. TMS SMART - Scalp mapping of annoyance ratings and twitches caused by Transcranial Magnetic Stimulation. J. Neurosci. Methods 299, 34–44. doi:10.1016/j.jneumeth.2018.02.008.
Mills, K.R., Boniface, S.J., Schubert, M., 1992. Magnetic brain stimulation with a double coil: the importance of coil orientation. Electroencephalogr. Clin. Neurophysiol. 85, 17–21.
Moisa, M., Pohmann, R., Ewald, L., Thielscher, A., 2009. New coil positioning method for interleaved transcranial magnetic stimulation (TMS)/functional MRI (fMRI) and its validation in a motor cortex study. J. Magn. Reson. Imaging 29, 189–197. doi:10.1002/jmri.21611.
Moisa, M., Pohmann, R., Uludag, K., Thielscher, A., 2010. Interleaved TMS/CASL: Comparison of different rTMS protocols. Neuroimage 49, 612–620. doi:10.1016/j.neuroimage.2009.07.010.
Moisa, M., Siebner, H.R., Pohmann, R., Thielscher, A., 2012. Uncovering a context-specific connectional fingerprint of human dorsal premotor cortex. J. Neurosci. 32, 7244–7252. doi:10.1523/JNEUROSCI.2757-11.2012.
Moliadze, V., Zhao, Y., Eysel, U., Funke, K., 2003. Effect of transcranial magnetic stimulation on single-unit activity in the cat primary visual cortex. J. Physiol. 553, 665–679. doi:10.1113/jphysiol.2003.050153jphysiol.2003.050153, [pii].
Murphy, K., Fox, M.D., 2017. Towards a consensus regarding global signal regression for resting state functional connectivity MRI. Neuroimage 154, 169–173. doi:10.1016/j.neuroimage.2016.11.052.
Nahas, Z., Lomarev, M., Roberts, D.R., Shastri, A., Lorberbaum, J.P., Teneback, C., McConnell, K., Vincent, D.J., Li, X., George, M.S., Bohning, D.E., 2001. Unilateral left prefrontal transcranial magnetic stimulation (TMS) produces intensity-dependent bilateral effects as measured by interleaved BOLD fMRI. Biol. Psychiatry 50, 712–720. doi:10.1016/s0006-3223(01)01199-4.
Navarro de Lara, L.I., Golestanirad, L., Makarov, S.N., Stockmann, J.P., Wald, L.L., Nummenmaa, A., 2020. Evaluation of RF interactions between a 3T birdcage transmit coil and transcranial magnetic stimulation coils using a realistically shaped head phantom. Magn. Reson. Med. 84, 1061–1075. doi:10.1002/mrm.28162.
Navarro de Lara, L.I., Tik, M., Woletz, M., Frass-Kriegl, R., Moser, E., Laistler, E., Windischberger, C., 2017. High-sensitivity TMS/fMRI of the human motor cortex using a dedicated multichannel MR coil. Neuroimage 150, 262–269. doi:10.1016/j.neuroimage.2017.02.062.
Navarro de Lara, L.I., Windischberger, C., Kuehne, A., Woletz, M., Sieg, J., Bestmann, S., Weiskopf, N., Strasser, B., Moser, E., Laistler, E., 2015. A novel coil array for combined TMS/fMRI experiments at 3 T. Magn. Reson. Med. 74, 1492–1501. doi:10.1002/mrm.25535.
Nikouline, V., Ruohonen, J., Ilmoniemi, R.J., 1999. The role of the coil click in TMS assessed with simultaneous EEG. Clin. Neurophysiol. 110, 1325–1328.
Nitsche, M.A., Paulus, W., 2000. Excitability changes induced in the human motor cortex by weak transcranial direct current stimulation. J. Physiol. 527 (Pt 3), 633–639.
O'Reardon, J.P., Solvason, H.B., Janicak, P.G., Sampson, S., Isenberg, K.E., Nahas, Z., McDonald, W.M., Avery, D., Fitzgerald, P.B., Loo, C., Demitrack, M.A., George, M.S., Sackeim, H.A., 2007. Efficacy and safety of transcranial magnetic stimulation in the acute treatment of major depression: a multisite randomized controlled trial. Biol. Psychiatry 62, 1208–1216. doi:10.1016/j.biopsych.2007.01.018.
Oathes, D.J., Zimmerman, J.P., Duprat, R., Japp, S.S., Scully, M., Rosenberg, B.M., Flounders, M.W., Long, H., Deluisi, J.A., Elliott, M., Shandler, G., Shinohara, R.T., Linn, K.A., 2021. Resting fMRI-guided TMS results in subcortical and brain network modulation indexed by interleaved TMS/fMRI. Exp. Brain Res. doi:10.1007/s00221-021-06036-5.
Oh, H., Kim, J.H., Yau, J.M., 2019. EPI distortion correction for concurrent human brain stimulation and imaging at 3T. J. Neurosci. Methods 327, 108400. doi:10.1016/j.jneumeth.2019.108400.
Oliviero, A., Mordillo-Mateos, L., Arias, P., Panyavin, I., Foffani, G., Aguilar, J., 2011. Transcranial static magnetic field stimulation of the human motor cortex. J. Physiol. 589, 4949–4958. doi:10.1113/jphysiol.2011.211953.
Pascual-Leone, A., Walsh, V., Rothwell, J., 2000. Transcranial magnetic stimulation in cognitive neuroscience–virtual lesion, chronometry, and functional connectivity. Curr. Opin. Neurobiol. 10, 232–237 https://doi.org/S0959-4388(00)00081-7 [pii].
Pasquinelli, C., Hanson, L.G., Siebner, H.R., Lee, H.J., Thielscher, A., 2019. Safety of transcranial focused ultrasound stimulation: a systematic review of the state of knowledge from both human and animal studies. Brain Stimul. doi:10.1016/j.brs.2019.07.024.
Paus, T., Jech, R., Thompson, C.J., Comeau, R., Peters, T., Evans, A.C., 1997. Transcranial magnetic stimulation during positron emission tomography: a new method for studying connectivity of the human cerebral cortex. J. Neurosci. 17, 3178–3184.
Peters, J.C., Reithler, J., Graaf, T.A., Schuhmann, T., Goebel, R., Sack, A.T., 2020. Concurrent human TMS-EEG-fMRI enables monitoring of oscillatory brain state-dependent gating of cortico-subcortical network activity. Commun. Biol. 3, 40. doi:10.1038/s42003-020-0764-0.
Peters, J.C., Reithler, J., Schuhmann, T., de Graaf, T., Uludag, K., Goebel, R., Sack, A.T. , 2013. On the feasibility of concurrent human TMS-EEG-fMRI measurements. J. Neurophysiol. 109, 1214–1227. doi:10.1152/jn.00071.2012.
Philip, N.S., Barredo, J., van 't Wout-Frank, M., Tyrka, A.R., Price, L.H., Carpenter, L.L., 2018. Network mechanisms of clinical response to transcranial magnetic stimulation in posttraumatic stress disorder and major depressive disorder. Biol. Psychiatry 83, 263–272. doi:10.1016/j.biopsych.2017.07.021.
Raij, T., Nummenmaa, A., Marin, M.F., Porter, D., Furtak, S., Setsompop, K., Milad, M.R., 2018. Prefrontal cortex stimulation enhances fear extinction memory in humans. Biol. Psychiatry 84, 129–137. doi:10.1016/j.biopsych.2017.10.022.
Reithler, J., Peters, J.C., Sack, A.T., 2011. Multimodal transcranial magnetic stimulation: Using concurrent neuroimaging to reveal the neural network dynamics of non-invasive brain stimulation. Prog. Neurobiol. doi:10.1016/j.pneurobio.2011.04.004, https://doi.org/S0301-0082(11)00055-4 [pii].
Ricci, R., Salatino, A., Li, X., Funk, A.P., Logan, S.L., Mu, Q., Johnson, K.A., Bohning, D.E., George, M.S., 2012. Imaging the neural mechanisms of TMS neglect-like bias in healthy volunteers with the interleaved TMS/fMRI technique: preliminary evidence. Front. Hum. Neurosci. 6, 326. doi:10.3389/fnhum.2012.00326.
Ritter, P., Villringer, A., 2006. Simultaneous EEG-fMRI. Neurosci. Biobehav. Rev. 30, 823–838. doi:10.1016/j.neubiorev.2006.06.008, https://doi.org/S0149-7634(06)00053-4 [pii].
Rogasch, N.C., Sullivan, C., Thomson, R.H., Rose, N.S., Bailey, N.W., Fitzgerald, P.B., Farzan, F., Hernandez-Pavon, J.C., 2017. Analysing concurrent transcranial magnetic stimulation and electroencephalographic data: a review and introduction to the open-source TESA software. Neuroimage 147, 934–951. doi:10.1016/j.neuroimage.2016.10.031.
Romero, M.C., Davare, M., Armendariz, M., Janssen, P., 2019. Neural effects of transcranial magnetic stimulation at the single-cell level. Nat. Commun. 10, 2642. doi:10.1038/s41467-019-10638-7.
Ruff, C.C., Bestmann, S., Blankenburg, F., Bjoertomt, O., Josephs, O., Weiskopf, N., Deichmann, R., Driver, J., 2008. Distinct causal influences of parietal versus frontal areas on human visual cortex: evidence from concurrent TMS-fMRI. Cereb. Cortex 18, 817–827.
Ruff, C.C., Blankenburg, F., Bjoertomt, O., Bestmann, S., Freeman, E., Haynes, J.D., Rees, G., Josephs, O., Deichmann, R., Driver, J., 2006. Concurrent TMS-fMRI and psychophysics reveal frontal influences on human retinotopic visual cortex. Curr. Biol. 16, 1479–1488.
Ruff, C.C., Blankenburg, F., Bjoertomt, O., Bestmann, S., Weiskopf, N., Driver, J., 2009a. Hemispheric differences in frontal and parietal influences on human occipital cortex: direct confirmation with concurrent TMS-fMRI. J. Cogn. Neurosci. 21, 1146–1161. doi:10.1162/jocn.2009.21097.
Ruff, C.C., Driver, J., Bestmann, S., 2009b. Combining TMS and fMRI: from 'virtual lesions' to functional-network accounts of cognition. Cortex 45, 1043–1049. doi:10.1016/j.cortex.2008.10.012.
Sack, A.T., Cohen Kadosh, R., Schuhmann, T., Moerel, M., Walsh, V., Goebel, R., 2009. Optimizing functional accuracy of TMS in cognitive studies: a comparison of methods. J. Cogn. Neurosci. 21, 207–221. doi:10.1162/jocn.2009.21126.
Sack, A.T., Kohler, A., Bestmann, S., Linden, D.E., Dechent, P., Goebel, R., Baudewig, J., 2007. Imaging the brain activity changes underlying impaired visuospatial judgments: simultaneous FMRI, TMS, and behavioral studies. Cereb. Cortex 17, 2841–2852.
Sarasso, S., Rosanova, M., Casali, A.G., Casarotto, S., Fecchio, M., Boly, M., Gosseries, O., Tononi, G., Laureys, S., Massimini, M., 2014. Quantifying cortical EEG responses to TMS in (un)consciousness. Clin. EEG Neurosci. 45, 40–49. doi:10.1177/1550059413513723.
Scheeringa, R., Fries, P., Petersson, K.M., Oostenveld, R., Grothe, I., Norris, D.G., Hagoort, P., Bastiaansen, M.C., 2011. Neuronal dynamics underlying high- and low-frequency EEG oscillations contribute independently to the human BOLD signal. Neuron 69, 572–583. doi:10.1016/j.neuron.2010.11.044, https://doi.org/S0896-6273(10)01081-0 [pii].
Schirner, M., McIntosh, A.R., Jirsa, V., Deco, G., Ritter, P., 2018. Inferring multi-scale neural mechanisms with brain network modelling. Elife 7. doi:10.7554/eLife.28927.
Schmid, U.D., Moller, A.R., Schmid, J., 1995. Transcranial magnetic stimulation of the trigeminal nerve: intraoperative study on stimulation characteristics in man. Muscle Nerve 18, 487–494. doi:10.1002/mus.880180503.
Shitara, H., Shinozaki, T., Takagishi, K., Honda, M., Hanakawa, T., 2011. Time course and spatial distribution of fMRI signal changes during single-pulse transcranial magnetic stimulation to the primary motor cortex. Neuroimage 56, 1469–1479. doi:10.1016/j.neuroimage.2011.03.011.
Shitara, H., Shinozaki, T., Takagishi, K., Honda, M., Hanakawa, T., 2013. Movement and afferent representations in human motor areas: a simultaneous neuroimaging and transcranial magnetic/peripheral nerve-stimulation study. Front. Hum. Neurosci. 7, 554. doi:10.3389/fnhum.2013.00554.
Siddiqi, S.H., Taylor, S.F., Cooke, D., Pascual-Leone, A., George, M.S., Fox, M.D., 2020. Distinct symptom-specific treatment targets for circuit-based neuromodulation. Am. J. Psychiatry doi:10.1176/appi.ajp.2019.19090915, appiajp201919090915.
Siebner, H.R., Auer, C., Roeck, R., Conrad, B., 1999a. Trigeminal sensory input elicited by electric or magnetic stimulation interferes with the central motor drive to the intrinsic hand muscles. Clin. Neurophysiol. 110, 1090–1099. doi:10.1016/s1388-2457(98)00053-4.
Siebner, H.R., Bergmann, T.O., Bestmann, S., Massimini, M., Johansen-Berg, H., Mochizuki, H., Bohning, D.E., Boorman, E.D., Groppa, S., Miniussi, C., Pascual-Leone, A., Huber, R., Taylor, P.C., Ilmoniemi, R.J., De Gennaro, L., Strafella, A.P., Kähkönen, S., Klöppel, S., Frisoni, G.B., George, M.S., Hallett, M., Brandt, S.A., Rushworth, M.F., Ziemann, U., Rothwell, J.C., Ward, N., Cohen, L.G., Baudewig, J., Paus, T., Ugawa, Y., Rossini, P.M., 2009. Consensus paper: Combining transcranial stimulation with neuroimaging. Brain Stimul. 2, 58–80.
Siebner, H.R., Conde, V., Tomasevic, L., Thielscher, A., Bergmann, T.O., 2019. Distilling the essence of TMS-evoked EEG potentials (TEPs): a call for securing mechanistic specificity and experimental rigor. Brain Stimul. 12, 1051–1054. doi:10.1016/j.brs.2019.03.076.
Siebner, H.R., Peller, M., Willoch, F., Auer, C., Bartenstein, P., Drzezga, A., Schwaiger, M., Conrad, B., 1999b. Imaging functional activation of the auditory cortex during focal repetitive transcranial magnetic stimulation of the primary motor cortex in normal subjects. Neurosci. Lett. 270, 37–40.
Siebner, H.R., Takano, B., Peinemann, A., Schwaiger, M., Conrad, B., Drzezga, A., 2001. Continuous transcranial magnetic stimulation during positron emission tomography: a suitable tool for imaging regional excitability of the human cortex. Neuroimage 14, 883–890. doi:10.1006/nimg.2001.0889, S1053-8119(01)90889-4 [pii].

Stewart, L.M., Walsh, V., Rothwell, J.C., 2001. Motor and phosphene thresholds: a transcranial magnetic stimulation correlation study. Neuropsychologia 39, 415–419.

Stokes, M.G., Chambers, C.D., Gould, I.C., Henderson, T.R., Janko, N.E., Allen, N.B., Mattingley, J.B., 2005. Simple metric for scaling motor threshold based on scalp-cortex distance: application to studies using transcranial magnetic stimulation. J. Neurophysiol. 94, 4520–4527.

Strafella, A.P., Paus, T., Barrett, J., Dagher, A., 2001. Repetitive transcranial magnetic stimulation of the human prefrontal cortex induces dopamine release in the caudate nucleus. J. Neurosci. 21, RC157.

Takano, B., Drzezga, A., Peller, M., Sax, I., Schwaiger, M., Lee, L., Siebner, H.R., 2004. Short-term modulation of regional excitability and blood flow in human motor cortex following rapid-rate transcranial magnetic stimulation. Neuroimage 23, 849–859. doi:10.1016/j.neuroimage.2004.06.032.

Thielscher, A., Opitz, A., Windhoff, M., 2011. Impact of the gyral geometry on the electric field induced by transcranial magnetic stimulation. Neuroimage 54, 234–243. doi:10.1016/j.neuroimage.2010.07.061, https://doi.org/S1053-8119(10)01034-7 [pii].

Thut, G., Schyns, P.G., Gross, J., 2011a. Entrainment of perceptually relevant brain oscillations by non-invasive rhythmic stimulation of the human brain. Front. Psychol. 2, 170. doi:10.3389/fpsyg.2011.00170.

Thut, G., Veniero, D., Romei, V., Miniussi, C., Schyns, P., Gross, J., 2011b. Rhythmic TMS causes local entrainment of natural oscillatory signatures. Curr. Biol. 21, 1176–1185. doi:10.1016/j.cub.2011.05.049.

Tik, M., Hoffmann, A., Sladky, R., Tomova, L., Hummer, A., Navarro de Lara, L., Bukowski, H., Pripfl, J., Biswal, B., Lamm, C., Windischberger, C., 2017. Towards understanding rTMS mechanism of action: stimulation of the DLPFC causes network-specific increase in functional connectivity. Neuroimage 162, 289–296. doi:10.1016/j.neuroimage.2017.09.022.

Tik, M., Woletz, M., Schuler, A.L., Princic, M., Linhardt, D., Hummer, A., Windischberger, C., 2020. TMS/fMRI demonstrates sgACC target engagement. Clin. Neurophysiol. 131, e30–e31. doi:10.1016/j.clinph.2019.12.145.

Van Dromme, I.C., Vanduffel, W., Janssen, P., 2015. The relation between functional magnetic resonance imaging activations and single-cell selectivity in the macaque intraparietal sulcus. Neuroimage 113, 86–100. doi:10.1016/j.neuroimage.2015.03.023.

Verhagen, L., Gallea, C., Folloni, D., Constans, C., Jensen, D.E., Ahnine, H., Roumazeilles, L., Santin, M., Ahmed, B., Lehericy, S., Klein-Flugge, M.C., Krug, K., Mars, R.B., Rushworth, M.F., Pouget, P., Aubry, J.F., Sallet, J., 2019. Offline impact of transcranial focused ultrasound on cortical activation in primates. Elife 8. doi:10.7554/eLife.40541.

Vernet, M., Thut, G., 2014. Electroencephalography during transcranial magnetic stimulation: current modus operandi. In: Rotenberg, A., Horvath, J., Pascual-Leone, A. (Eds.), Transcranial Magnetic Stimulation. Humana Press, New York, pp. 197–232. doi:10.1007/978-1-4939-0879-0_11.

Vink, J.J.T., Mandija, S., Petrov, P.I., van den Berg, C.A.T., Sommer, I.E.C., Neggers, S.F.W., 2018. A novel concurrent TMS-fMRI method to reveal propagation patterns of prefrontal magnetic brain stimulation. Hum. Brain Mapp. 39, 4580–4592. doi:10.1002/hbm.24307.

Walsh, V., Cowey, A., 2000. Transcranial magnetic stimulation and cognitive neuroscience. Nat. Rev. Neurosci. 1, 73–79.

Wang, J.X., Rogers, L.M., Gross, E.Z., Ryals, A.J., Dokucu, M.E., Brandstatt, K.L., Hermiller, M.S., Voss, J.L., 2014. Targeted enhancement of cortical-hippocampal brain networks and associative memory. Science 345, 1054–1057. doi:10.1126/science.1252900.

Wang, W.T., Xu, B., Butman, J.A., 2017. Improved SNR for combined TMS-fMRI: a support device for commercially available body array coil. J. Neurosci. Methods 289, 1–7. doi:10.1016/j.jneumeth.2017.06.020.

Warren, K.N., Hermiller, M.S., Nilakantan, A.S., Voss, J.L., 2019. Stimulating the hippocampal posterior-medial network enhances task-dependent connectivity and memory. Elife 8. doi:10.7554/eLife.49458.

Webler, R.D., Hamady, C., Molnar, C., Johnson, K., Bonilha, L., Anderson, B.S., Bruin, C., Bohning, D.E., George, M.S., Nahas, Z., 2020. Decreased interhemispheric connectivity and increased cortical excitability in unmedicated schizophrenia: A prefrontal interleaved TMS fMRI study. Brain Stimul. 13, 1467–1475. doi:10.1016/j.brs.2020.06.017.

Weigand, A., Horn, A., Caballero, R., Cooke, D., Stern, A.P., Taylor, S.F., Press, D., Pascual-Leone, A., Fox, M.D., 2018. Prospective validation that subgenual connectivity predicts antidepressant efficacy of transcranial magnetic stimulation sites. Biol. Psychiatry 84, 28–37. doi:10.1016/j.biopsych.2017.10.028.

Weise, K., Numssen, O., Thielscher, A., Hartwigsen, G., Knosche, T.R., 2019. A novel approach to localize cortical TMS effects. Neuroimage, 116486 doi:10.1016/j.neuroimage.2019.116486.

Weiskopf, N., Josephs, O., Ruff, C.C., Blankenburg, F., Featherstone, E., Thomas, A., Bestmann, S., Driver, J., Deichmann, R., 2009. Image artifacts in concurrent transcranial magnetic stimulation (TMS) and fMRI caused by leakage currents: modeling and compensation. J. Magn. Reson. Imaging 29, 1211–1217. doi:10.1002/jmri.21749.

Williams, N.R., Sudheimer, K.D., Bentzley, B.S., Pannu, J., Stimpson, K.H., Duvio, D., Cherian, K., Hawkins, J., Scherrer, K.H., Vyssoki, B., DeSouza, D., Raj, K.S., Keller, J., Schatzberg, A.F., 2018. High-dose spaced theta-burst TMS as a rapid-acting antidepressant in highly refractory depression. Brain 141, e18. doi:10.1093/brain/awx379.

Woletz, M., Tik, M., Pratapa, N., Princic, M., Schuler, A.L., Windischberger, C., 2020. Real-time neuronavigation feedback in concurrent TMS-fMRI. Brain Stimul. 131, 574–575. doi:10.1016/j.brs.2018.12.904.

Xu, B., Sandrini, M., Wang, W.T., Smith, J.F., Sarlls, J.E., Awosika, O., Butman, J.A., Horwitz, B., Cohen, L.G., 2016. PreSMA stimulation changes task-free functional connectivity in the fronto-basal-ganglia that correlates with response inhibition efficiency. Hum. Brain Mapp. 37, 3236–3249. doi:10.1002/hbm.23236.

Yau, J.M., Hua, J., Liao, D.A., Desmond, J.E., 2013. Efficient and robust identification of cortical targets in concurrent TMS-fMRI experiments. Neuroimage 76, 134–144. doi:10.1016/j.neuroimage.2013.02.077.

Yau, J.M., Jalinous, R., Cantarero, G.L., Desmond, J.E., 2014. Static field influences on transcranial magnetic stimulation: considerations for TMS in the scanner environment. Brain Stimul. 7, 388–393. doi:10.1016/j.brs.2014.02.007.

Zheng, W., Chee, M.W., Zagorodnov, V., 2009. Improvement of brain segmentation accuracy by optimizing non-uniformity correction using N3. Neuroimage 48, 73–83. doi:10.1016/j.neuroimage.2009.06.039.